HEPATIC BIOTRANSFORMATION OF LITHOCHOLIC ACID:
ROLE OF CYTOCHROME P450 ENZYMES

by

ANAND K. DEO

B. Pharm., University of Pune, India, 2000
M. Pharm. Sci., University of Mumbai, 2002

A THESIS SUBMITTED IN PARTIAL FULFILLMENT OF

THE REQUIREMENTS FOR THE DEGREE OF

MASTER OF SCIENCE

in

THE FACULTY OF GRADUATE STUDIES

(PHARMACEUTICAL SCIENCES)

THE UNIVERSITY OF BRITISH COLUMBIA

July 2005

ABSTRACT

The purpose of the present study was to investigate the *in vitro* biotransformation of lithocholic acid (3α-hydroxy-5β-cholanoic acid, LCA). A validated and optimized method to analyze metabolite formation was developed using liquid chromatography-electrospray mass spectrometry (LC/MS). LCA (0.5–300 μM) was incubated with 0.5 mg/ml of hepatic microsomal protein (untreated male Wistar rats) for 30 min in a reaction mixture consisting of 1 mM NADPH and 46.5 mM potassium phosphate buffer at pH 7.4. LCA metabolites were resolved using a LC/MS and XTerra™ MS C_{18} (2.1 mm × 150 mm, 3.5 mm) column. The major metabolites were murideoxycholic acid (MDCA), isolithocholic acid (ILCA), and 3-ketocholanic acid (3KCA). Minor metabolites were β-muricholic acid (β-MCA), 6-ketolithocholic acid (6KLCA) and ursodeoxycholic acid (UDCA) and also included, M-1 to M-5, which were not identified. Recovery of all metabolite standards, except for 3KCA (60%), was between 80-100%. Metabolite formation was not observed in the absence of NADPH, with boiled microsomes, or following carbon monoxide treatment. Formation of MDCA, ILCA, UDCA and 6KLCA followed typical Michaelis-Menten kinetics. To identify the cytochrome P450 (CYP) enzymes involved in the formation of LCA metabolites, hepatic microsomes prepared from rats (Long Evans) treated with inducers including 3-methylcholanthrene (MC, 25 mg/kg bw/day × 4 days), phenobarbital (PB, 75 mg/kg bw/day × 4 days) and dexamethasone (DEX, 100 mg/kg bw/day × 4 days) were used. Formation of MDCA and ILCA was decreased with all three inducer treatments and formation of 3KCA was increased with DEX treatment suggesting that CYP3A is involved in formation of 3KCA, and non-inducible CYP enzymes catalyze formation of MDCA and ILCA. Metabolite formation was greater with male than female rat liver microsomes. Rabbit polyspecific anti-rat CYP2C IgG inhibited MDCA formation by 50% and polyspecific anti-rat CYP3A IgG inhibited 3KCA formation by 50%.

Anti-rat CYP3A IgG inhibited MDCA, ILCA and 6KLCA formation partially, but inhibited M-1 and M-3 formation completely. Monospecific anti-rat CYP2C11 IgG was not effective in inhibiting the formation of any metabolites. In summary, the results demonstrate the involvement of CYP2C and CYP3A enzymes in rat hepatic LCA biotransformation.

TABLE OF CONTENTS

1. INTRODUCTION

2. MATERIALS AND METHODS

3. RESULTS

4. DISCUSSION

LIST OF FIGURES

ABBREVIATIONS

α-MCA	alpha-muricholic acid
β-MCA	beta-muricholic acid
γ-MCA	gamma-muricholic acid
3KCA	3-ketocholanic acid
6KLCA	6-ketocholic acid
AhR	aryl hydrocarbon receptor
AIP	aryl hydrocarbon receptor-interacting protein
ANOVA	analysis of variance
Arnt	aryl hydrocarbon receptor nuclear translocator
ASBT	apical sodium-dependent bile salt transporter
AUC	area under curve
BSA	bovine serum albumin
BSEP	bile salt export protein
C.V.	coefficient of variation
CA	cholic acid
CAR	constitutive androstane receptor
CDCA	chenodeoxycholic acid
CMC	critical micellar concentration
CYP	cytochrome P450
DCA	deoxycholic acid
DEX	dexamethasone
DRE	direct response element
EST	expressed sequence tag
FIC1	familial intrahepatic cholestasis-1
FXR	farnesoid X receptor
GC/MS	gas chromatography mass spectrometry
GH	growth hormone
HCA	hyocholic acid
HDCA	hyodeoxycholic acid
HPLC	high performance liquid chromatography
Hsp90	heat shock protein 90
IgG	Immunoglobin G
ILCA	isolithocholic acid
IR-6	inverted response elements
IS	internal standard
ISBT	ileal sodium-dependent bile salt transporter
LCA	lithocholic acid
LC/MS/MS	liquid chromatography tandem mass spectrometry
LC-MS	liquid chromatography mass spectrometry
LOD	limit of detection
LST	liver specific transporter
LXR	liver X receptor
MC	3- methylcholanthrene
MDCA	murideoxycholic acid

(List of Abbreviations cont'd...)

MDR	multidrug resistance P-glycoprotein
MRP	multiple resistance associated protein
NADPH	reduced nicotinamide adenine dinucleotide phosphate
NOR	nuclear orphan receptor
NRE	nuclear response element
NTCP	sodium taurocholate cotransporting polypeptide
OATP	organic anion transporter protein
PAH	polyaromatic hydrocarbons
PAR	peak area ratio
PB	phenobarbital
PBRE	phenobarbital response elements
PCBs	polychlorinated biphenyls
PCN	pregnenolone 16α-carbonitrile
PPAR	peroxisome proliferator-activated receptor
PPRE	peroxisome proliferator responsive elements
PXR	pregnane X receptor
RXR	retinoid X receptor
s.c.	subcutaneous
SEM	standard error of mean
SNK	student neuman-keuls test
SPGP	sister of P-glycoprotein
SULT	sulfotransferase
SXR	steroid X receptor
T_3	triiodothyronine
T_4	thyroxine
TAO	triacetyloleandomycin
TCDCA	taurochenodeoxycholic acid
TCDD	tetrachlorodibenzo-p-dioxin
TCDF	tetrachlorodibenzofuran
THDCA	taurohyodeoxycholic acid
TLC	thin layer chromatography
TLCA	taurolithocholic acid
UDCA	ursodeoxycholic acid
UV	ultraviolet
VDR	vitamin D receptor
XRE	xenobiotic response elements

ACKNOWLEDGEMENTS

DEDICATED

TO

MY PARENTS

1. INTRODUCTION

The primary mechanism by which organisms prevent the accumulation of various lipophilic compounds is oxidative biotransformation. Lipophilic xenobiotics (Greek:- xenos = foreign) such as foreign chemicals or drugs enter the body and get absorbed. Lipophilic endobiotics (Greek:-endon = within, of the body) such as fatty acids, steroids and bile acids are produced as catalytic byproducts of various biochemical pathways within the body. The lipophilic nature of these compounds prevents them from being excreted easily. The elimination of lipophilic compounds from the body is usually initiated by the cytochrome P450 (CYP) enzymes, which catalyze the conversion of lipophilic substrates to water-soluble metabolites by the process of biotransformation (Nelson et al., 1996).

R.T. Williams proposed that biotransformation occurs in two distinct phases, namely, Phase I and Phase II (Williams, 1959). In Phase I biotransformation reactions, a polar functional group (e.g. -OH, -COOH, -NH$_2$ and –SH) is introduced, or unmasked if already present, to a lipid soluble substrate. These reactions are called functionalization reactions and involve hydrolysis, reduction and oxidation. The product formed in Phase I reactions may be susceptible to Phase II biotransformation (Guengerich, 1991). In Phase II biotransformation reactions, covalent attachment of an endogenous polar moiety such as glucuronic acid, sulfate or glycine to either unchanged drugs or Phase I products occurs. This leads to the formation of highly water-soluble conjugates that are excreted mainly through the kidneys. These reactions are also called conjugation reactions (Parkinson, 1996). The current project focuses on the Phase I biotransformation of a class of endobiotics, bile acids.

1.1 Cytochrome P450 enzymes

CYP enzymes were first recognized by Martin Klingenberg, while studying the spectrophotometric properties of pigments in microsomal fractions of rat liver. Klingenberg added sodium dithionite, a reducing agent, to diluted microsomes saturated with carbon monoxide. A unique spectral absorbance band with a maximum at approximately 450 nm appeared that was found to be unique among hemeproteins and served as the signature of CYP proteins. The name cytochrome P450 was derived from the ability of this pigment to absorb light with an absorbance band maximum at 450 nm (Klingenberg, 1958). Omura and Sato characterized the pigment as a hemeprotein (Omura and Sato, 1964a).
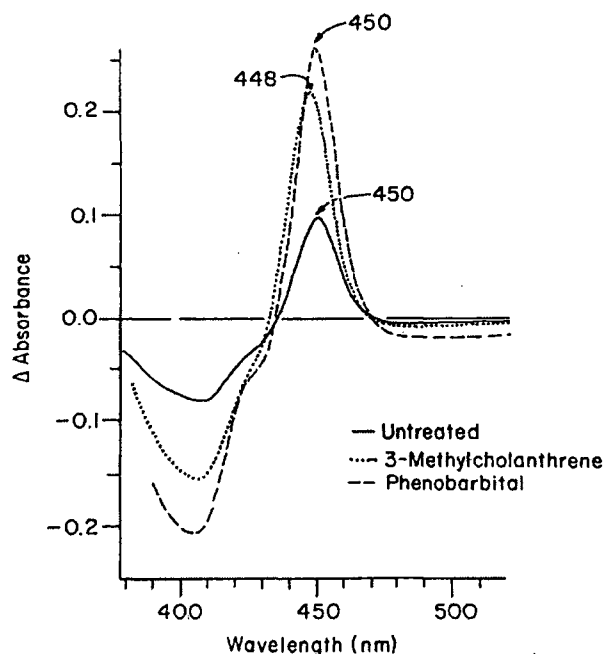
Fig. 1.1 Spectrophotometric identification of CYP enzymes.

Microsomes were prepared from livers of untreated rats, rats treated with phenobarbital, or 3-methylcholanthrene. Microsomes were diluted in 0.1 M potassium phosphate buffer to a concentration of 1 mg of protein per ml. The diluted samples were reduced with a small amount of sodium dithionite, divided equally into two spectrophotometer cuvettes and the contents of one cuvette gassed for 30 s with carbon monoxide. The difference spectrum was recorded using an Aminco-Chance DW2 spectrophotometer (Taken from Klingenberg, 1958).

CYP enzymes are widely distributed in nature with different CYP enzymes present in plants, insects, some bacteria, yeast, and mammals. CYP enzymes are present in all tissues of mammals, but are found in higher concentration in liver. Several research groups have provided evidence that CYP enzymes in liver microsomes play a central role in the metabolism of drugs and other xenobiotics. CYP enzymes are remarkable catalysts that show great diversity of action in many reactions. The number of substrates metabolized by CYP enzymes is enormous and is certainly greater than one thousand (Estabrook, 1999).

1.1.1 Hepatic CYP enzyme system

CYP enzymes belong to the class of enzymes called oxygenases. Specifically, they are monooxygenases or mixed function oxidases. All CYP enzymes contain a heme group with iron in the ferric state (Fe^{3+}). The CYP enzymes serve as the common interaction site for the chemical substrate to be oxidized, for electrons donated from reduced pyridine nucleotides (NADPH or NADH), for atmospheric oxygen, and for protons contributed by water so that reactions involving hydrogen abstraction, oxygen activation, and stereo- and regiospecific oxygenation can occur (Parkinson, 1996; Williams, 1999). CYP enzymes consist of a protoporphyrin IX heme moiety (prosthetic group) and a single polypeptide chain (apoprotein) of 45 to 55 kDa (Guengerich, 1990). The heme moiety is part of the catalytic active site of the enzyme. The iron ion associated with the heme group is coordinated to the center of the protoporphyrin ring. Four ligands of the heme iron are coordinated to the porphyrin ring. The fifth ligand is a thiolate anion from a cysteinyl residue of the apoprotein. The sixth ligand acts as the binding site for molecular oxygen (Guengerich, 1990).

In most instances, mammalian CYP enzymes catalyze oxidative reactions as per the equation illustrated in equation 1.

$$NADPH + O_2 + RH + H^+ \longrightarrow NADP^+ + ROH + H_2O \qquad (1)$$

Two electrons originating from NADPH are transferred to the heme ion by NADPH-CYP reductase in the presence of an organic chemical and molecular oxygen (See Fig. 1.2). In general, CYP enzymes undergo a cyclic series of reactions (Porter and Coon, 1991) where:

(a) the ferric form of the hemeprotein initially reacts with a substrate (RH) to form a complex-

$$Fe^{3+} + RH \longrightarrow Fe^{3+}\text{-}RH \qquad (1.1)$$

(b) the ferric CYP enzyme-substrate complex is reduced by an electron transported from NADPH to a ferrous state complex-

$$Fe^{3+} + RH \longrightarrow Fe^{2+}\text{-}RH \qquad (1.2)$$

(c) the ferrous-substrate complex reacts with molecular oxygen to form a ternary complex of ferrous CYP-substrate oxygen. Carbon monoxide can compete with molecular oxygen resulting in the formation of a carbon monoxide complex of ferrous CYP enzymes (which forms the characteristic absorbance pattern of CYP, see Fig. 1.1)

$$Fe^{2+}\text{-}RH + O_2 \longrightarrow Fe^{2+}\text{-}RH\text{-}O\text{-}O \qquad (1.3)$$
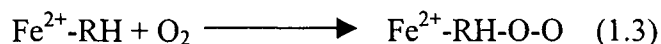
(d) the ternary complex of ferrous CYP-organic chemical substrate-molecular oxygen is further reduced by a second electron transferred from NADPH. This generates a two electron reduced intermediate where a molecular rearrangement occurs with the incorporation of oxygen into the substrate.

(e) the complex of ferric CYP and oxidized product dissociates regenerating the uncomplexed ferric CYP, which can participate in the metabolism of another molecule of chemical-

$$Fe^{2+}RH\text{-}O\text{-}O + e^- \longrightarrow Fe^{3+} + H_2O \qquad (1.4)$$

ROH   RH

(ROH)Fe^{3+} ← Fe^{3+} → (RH)Fe^{3+} [NADPH]
                                    e$^-$ CYP reductase

(R·)(Fe-OH)$^{3+}$ (RH)Fe^{2+}

2e$^-$, 2H$^+$ O$_2$

H$_2$O ← RH(Fe-O)$^{3+}$ (RH)Fe^{2+}(O$_2$)

H$_2$O

2H$^+$ (RH)Fe^{3+}(O$_2^=$)   (RH)Fe^{3+}(O$_2^-$)

2H$^+$

H$_2$O$_2$ e$^-$ O$_2^-$
        [NADPH]
        CYP reductase

Fig. 1.2 Representation of mechanism of a CYP monooxygenase reaction

The diagram represents the CYP catalytic cycle. Fe represents the heme iron of the CYP enzyme, RH represents the substrate, ROH the monooxygenation product (adapted from Porter and Coon 1991).

1.1.2 Nomenclature and classification of CYP enzymes

The human genome encodes fifty-seven CYP enzymes (Guengerich, 2003). A majority of these are involved in the metabolism of steroids, bile acids, fatty acids, eicosanoids, and fat-soluble vitamins (Guengerich, 2003). Molecular biology has provided techniques that permit identification and characterization of the large number of CYP enzymes. A major milestone in research on CYP enzymes was the first cloning of a CYP by Fujii-Kuriyama and his colleagues (Fujii-Kuriyama et al., 1982). Nebert et al. published a recommended nomenclature for the CYP gene superfamily in order to standardize the naming of new and existing CYP enzymes (Nebert

et al., 1987). The authors classified the CYP supergene family on the basis of structural relationships.

CYP enzymes are named using the root symbol 'CYP' followed by an Arabic numeral that denotes the family member, a letter denoting the subfamily and another Arabic numeral representing the individual gene (Nebert et al., 1987).

When a newly found CYP enzyme is identified, the primary amino acid sequence of the protein is aligned with a representative sequence from each family and subfamily, and by comparison of overlapping regions of the amino acid sequences, excluding the gaps and unmatched ends in overall length, the percentage of the sequence similarity is determined. A rule was created by Nebert and Gonzalez to name the CYP enzymes according to the homology of the amino acid sequence (Nebert and Gonzalez, 1987). The rules state that-

1. If the sequence of the new protein is less than 40% identical to all other sequences, the new protein constitutes the first member of a new family.

2. If the sequence is at least 40% identical to any other sequence, then the protein belongs in the same family.

3. If the sequence is from 40-68% identical to that of any subfamily in that family, the new protein will be the first member of a new subfamily.

4. If the sequence is at least 68% identical to other proteins in the same subfamily, the new protein is given the next available number in the group.

5. If the sequence is different by only a few (less than 3%) amino acids from a known sequence, it is given the same name and assumed to be the same protein unless it can be shown to be a product of a distinct CYP gene.

In humans, at least sixteen families of CYP enzymes are known to exist. More than nine families of human CYP enzymes are associated with cholesterol and steroid hormone metabolism. Four families of CYP enzymes are located within the mitochondria and use an electron transport chain containing adrenodoxin (an iron sulfur protein) and adrenodoxin reductase. The largest number of human CYP enzymes are in families CYP1 to CYP4 with the CYP2 family containing as many as eight subfamilies.
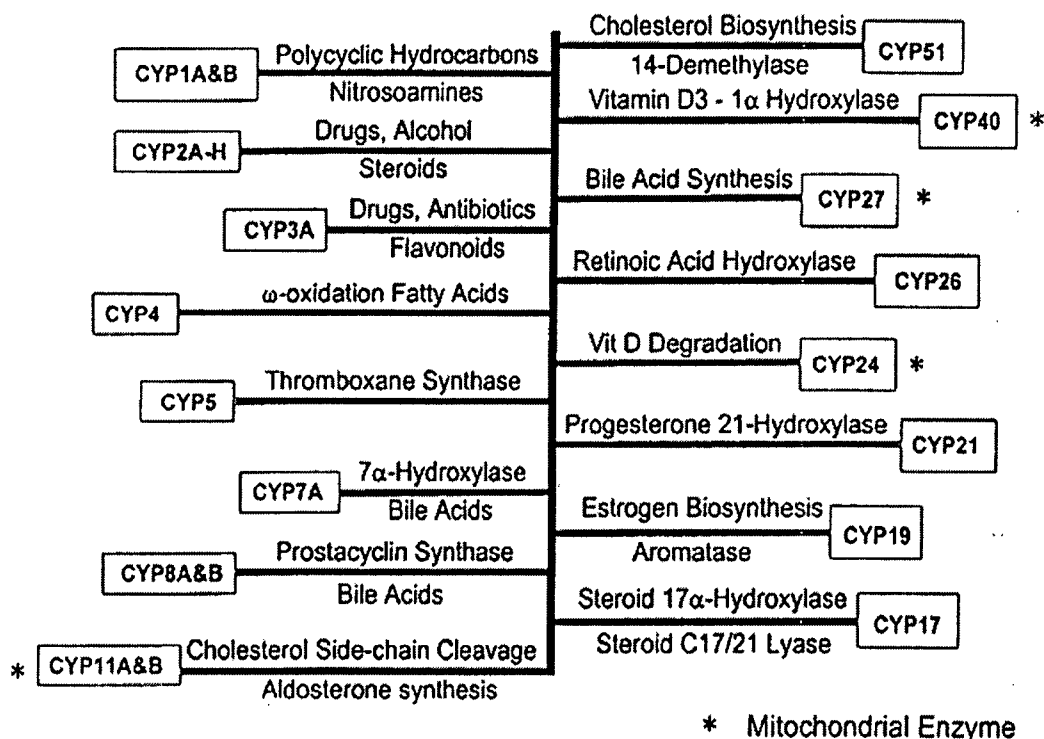
Fig. 1.3 Division of currently known 40 human CYPs into subfamilies (Estabrook, 1999).

Fig. 1.3 above shows the different human CYP enzymes that have been identified. The figure also indicates the primary substrates associated with a specific family or subfamily. Four families, CYP1, CYP2, CYP3 and CYP4, are mainly responsible for hepatic xenobiotic biotransformation in humans and other mammalian species (e.g. rodents such as rat). The levels of these enzymes in liver of various species may differ. A comparison of CYP enzyme levels in

human and rat is shown in Table 1.1. A discussion of rat CYP1A, CYP2A, CYP2B, CYP2C and

CYP3A enzymes and a brief comparison with human CYP enzymes follows.

Table 1.1
CYP enzyme levels in human and rat liver microsomes

Human CYP Enzyme	Specific Content (pmol/mg)	% of Total CYP	Rat CYP Enzyme	Specific Content (pmol/mg)	% of Total CYP
CYP1A (CYP1A1, 1A2)	1-65	7-18	CYP1A (1A1, 1A2)	5-20	1-3
CYP2A6	1-27	1-7	CYP2A (2A1, 2A2)	20-40	3-6
CYP2B6	0-3	0-0.5	CYP2B (2B1, 2B2)	5-20	1-3
CYP2C (CYP2C8, 2C9, 2C18, 2C19)	30-90	12-24	CYP2C (2C6, 2C7, 2C11, 2C12, 2C13)	380-650	40-65
CYP2D6	1-9	0.2-4	CYP2D1	not known	?
CYP2E1	10-34	4-10	CYP2E1	60-80	8-10
CYP3A (CYP3A4, 3A5, 3A7)	45-147	18-40	CYP3A (3A2, 3A9, 3A18, 3A23)	40-100	5-12
			CYP4A (4A1, 4A2, 4A3, 4A8)	not known	?

Adapted from Bandiera, 2001.

1.1.3 CYP subfamilies

a) CYP1A subfamily

The CYP1A subfamily found in rat consists of two enzymes, CYP1A1 and CYP1A2. These are immunochemically related and have a 68% similarity in amino acid sequence (Kawajiri et al., 1984; Yabusaki et al., 1984). Purified rat CYP1A1 has high catalytic activity towards O-deethylation of 7-ethoxyresorufin and hydroxylation of benzo[a]pyrene (BaP) (Burke and Mayer, 1974). CYP1A2 displays a lower activity toward oxidation of 7-ethoxyresorufin and BaP but it efficiently catalyzes melatonin 6-hydroxylation (Skene et al., 2001; Kobayashi et al., 2003) (See Table 1.2).

CYP1A enzymes are found in humans, rodents, fish, birds, insects, plants and bacteria and their associated monooxygenase activities are well conserved among different species. For example, CYP1A1-mediated BaP hydroxylase activity has been found in many organisms ranging from fungi to humans. CYP1A enzymes activate procarcinogens such as aromatic hydrocarbons (e.g. BaP) and heterocyclic amines (e.g. 2-amino-1methyl-6-phenylimidazo) and the expression of CYP1A1 has been correlated with development of polycyclic aromatic hydrocarbon related cancers in rodents (Nebert, 1989).

b) CYP2A subfamily

In rat, the CYP2A subfamily consists of three enzymes, CYP2A1, CYP2A2 and CYP2A3. A 93% sequence homology is observed in the CYP2A1 and CYP2A2 genes. CYP2A1 and CYP2A2 are found only in the liver (Ryan and Levin, 1990). CYP2A3 is found in the lung but not in the liver (Gonzalez, 1990). Purified CYP2A1 catalyzes the regioselective hydroxylation of testosterone predominantly at the 7α position and to a minor extent at the 6α position (Ryan and Levin, 1990). Testosterone 7α-hydroxylation is used as a marker for

CYP2A1 in hepatic microsomes (See Table 1.2). CYP2A1 is a female predominant enzyme that is regulated mainly by sex steroids and growth hormone (GH). It represents approximately 3% of total hepatic CYP in adult male and 6% of total hepatic CYP in female rats (Waxman et al., 1985). CYP2A2 hydroxylates testosterone predominantly at the 15α position (Gonzalez, 1990). CYP2A2 is constitutively expressed in male rats and is regulated by testosterone and GH (Waxman et al., 1988).

In humans, three enzymes in the CYP2A subfamily have been identified, CYP2A6, CYP2A7, and CYP2A13 (Nelson et al., 1996). CYP2A6 appears to be the only CYP2A enzyme expressed in human liver. It is not expressed in fetal liver or in tissues other than adult liver. CYP2A6 catalyzes coumarin 7-hydroxylation and this reaction is used as a specific marker for CYP2A6 as shown in Table 1.2 (Guengerich, 1995). CYP2A6 can activate nitrosamines to mutagenic and cytotoxic metabolites (Guengerich, 1995).

c) CYP2B subfamily

CYP2B1 and CYP2B2 are the main enzymes in the rat CYP2B subfamily. They share 97% sequence homology, are immunochemically cross-reactive and are highly inducible in liver by phenobarbital (PB) (Gonzalez, 1988). Purified CYP2B1 catalyzes demethylation of benzphetamine, demethylation of hexobarbital and hydroxylation of testosterone at the 16α and 16β positions (Gonzalez, 1988; Ryan and Levin, 1990). Hydroxylation of testosterone at the 16β position can be used as a marker for CYP2B1 in hepatic microsomes. CYP2B2 has a similar substrate profile but catalyzes the reactions at a 2- to 5-fold lower rate than CYP2B1 (Gonzalez, 1988). CYP2B3 is constitutively expressed at a low level in the liver of male and female rats. It is not inducible by PB and is 77% similar in its amino acid sequence to CYP2B1 and CYP2B2 (Gonzalez, 1988).

Human CYP2B6 shares approximately 76% sequence homology with rat CYP2B1. It is expressed constitutively in human liver at a level representing approximately 2% of total CYP content (Guengerich, 1995). Buproprion hydroxylation is considered to be a characteristic marker activity of the human CYP2B6 (Hesse et al., 2000). CYP2B6 can be induced in primary cultures of human hepatocytes with PB, dexamethasone (DEX) or rifampicin (Chang et al., 1997).

d)   CYP2C subfamily

CYP2C is a diverse subfamily of CYP enzymes. In rats, the CYP2C subfamily consists of CYP2C6, CYP2C7, CYP2C11, CYP2C12 and CYP2C13, which share 68% to 75% of sequence homology (Nelson et al., 1996). Most CYP2C enzymes are constitutively expressed. CYP2C6 and CYP2C7 are expressed in adult male and female rats whereas CYP2C11 and CYP2C13 are expressed in males only and CYP2C12 is expressed in females only (Ryan and Levin, 1993). Expression of CYP2C6, CYP2C7, CYP2C11, CYP2C12 and CYP2C13 is developmentally regulated (Ryan and Levin, 1990; Ryan and Levin, 1993). The hepatic content of CYP2C7 increases from less than 1% of total microsomal CYP in immature rat to 7% and 14% in mature female and male rats (Bandiera et al., 1986; Gonzalez et al., 1986). The expression level of CYP2C7 is approximately two times higher in liver of female rats compared to male rats. The expression of CYP2C6 does not exhibit any sex difference in rat liver (Gonzalez et al., 1986). Expression of CYP2C7, CYP2C11, CYP2C12 and CYP2C13 is regulated by growth hormone, estradiol and testosterone (MacGeoch et al., 1985; Morgan et al., 1985; Bandiera et al., 1986; Westin et al., 1990).

Purified CYP2C11 hydroxylates testosterone mainly at the 2α and 16α positions and catalyzes the metabolism of a number of drugs and xenobiotics (Ryan and Levin, 1990).

Hydroxylation of testosterone at the 2α position can be used as a marker for CYP2C11 in hepatic microsomes (See Table 1.2). CYP2C12 efficiently hydroxylates the steroid sulfate, 5α-androstane-3α,17β-diol-3,17-disulfate (Ryan et al. 1984).

The human CYP2C enzymes, CYP2C8, CYP2C9, CYP2C18 and CYP2C19, are not expressed in a sex specific manner and are more than 80% identical with each other (Guengerich, 1995). CYP2C enzymes metabolize a variety of clinically important drugs including hypoglycemic, anticonvulsant, antimalarial, anticoagulant, antiulcer and antidepressant drugs. CYP2C19 is of major clinical importance. CYP2C9 and CYP2C19 are inducible by rifampicin and barbiturates (Chen et al., 2004). 7-Hydroxylation of S-warfarin can be used as a marker for CYP2C9 in hepatic microsomes (Goldstein et al., 1994). CYP2C19 catalyzes 4'-hydroxylation of S-mephenytoin and exhibits a genetic polymorphism in the human population. Two to five percent of the Caucasian population and twenty percent of the Oriental population have been identified as poor metabolizers with respect to 4'-hydroxylation of S-mephenytoin (Goldstein and de Morais, 1994; Guengerich, 1995). CYP2C8 metabolizes taxol efficiently to 6-hydroxytaxol (Rahman et al., 1994). The characteristic marker activities of these CYP enzymes are compiled in Table 1.2.

e) CYP3A subfamily

The rat CYP3A subfamily consists of CYP3A1, CYP3A2, CYP3A9 and CYP3A18. CYP3A23 is considered to be an allelic variant of CYP3A1 (Mahnke et al., 1997). CYP3A1 and CYP3A2 are 89% similar in their amino acid sequences and are immunochemically cross-reactive but are differentially regulated (Gonzalez, 1990). CYP3A1 is undetectable in untreated male and female rats. CYP3A2 is expressed constitutively in immature and mature male rats and in immature but not mature female rats (Wrighton and Stevens, 1992; Cooper et al., 1993). DEX

and triacetyloleandomycin induce both CYP3A1 and CYP3A2, but rifampicin and PB induce CYP3A1 to a higher level than CYP3A2. 3-Methylcholanthrene (MC) induces CYP3A2 but has no effect on CYP3A1 (Cooper et al., 1993). Both CYP3A1 and CYP3A2 hydroxylate testosterone at the 2β and 6β positions. Hydroxylation of testosterone at the 6β position can be used as a marker for CYP3A in hepatic microsomes (Gonzalez, 1988).

In human liver, the CYP3A enzymes are the most abundant and consist of four closely related enzymes, CYP3A3, CYP3A4, CYP3A5 and CYP3A7. The contribution of CYP3A enzymes to total CYP content in human liver is 20-60% (Guengerich, 1995). CYP3A3 and CYP3A4 are the most abundant enzymes in adult liver and are responsible for the metabolism of many clinically important drugs such as corticosteroids, antifungal agents, macrolide antibiotics and neoplastic agents. CYP3A3 and CYP3A4 are 98% similar in their amino acid sequence and are also found in kidney and intestine (Gonzalez, 1990). CYP3A enzymes are inducible by steroid antagonists, endogenous and synthetic glucocortocoids, macrolide antibiotics, various antifungal agents, rifampicin, and PB (Handschin and Meyer, 2003). CYP3A5 is found in only 10-20% of adult and fetal livers examined. The substrate specificity of CYP3A5 is similar to that of CYP3A3 and CYP3A4, but its metabolic capacity is limited (Wrighton and Stevens, 1992). CYP3A7 is expressed in fetal liver only, where it constitutes 30-50% of the total hepatic CYP content. CYP3A7 is absent in adult liver. It catalyzes the 16α-hydroxylation of dehyroepiandrosterone 3-sulfate (Wrighton and Stevens, 1992).

f)   CYP4A subfamily

The CYP4 family consists of 11 subfamilies (CYP4A-CYP4M). CYP4A1 was isolated, cloned and sequenced in 1987 and its amino acid sequence was predicted to be less than 36% homologous to the CYP enzymes known at that time. Thus, CYP4A was designated as the first member of a new gene family (Hardwick et al., 1987; Nebert et al., 1987). The CYP4A1 gene is the most extensively studied member of this family and is expressed constitutively in rat liver and kidney. Expression of this enzyme is induced by clofibrate [2-(4-chlorophenoxy)-2methyl propionate]. Clofibrate is a hypolipidemic drug that lowers plasma triglyceride and cholesterol levels. CYP4A1 is also induced by other hypolipidemic agents, such as di(2-ethylhexyphthalate), 2,4,5-trichlorophenoxyacetic acid (a chlorophenoxy acetic acid herbicide), and tridiphane (a herbicide synergist) (Bacher and Gibson, 1988; Sharma et al., 1988). These compounds cause proliferation of peroxisomes in sensitive species, where they also appear to be nongenotoxic carcinogens, and are known as peroxisome proliferators. Steptozotocin-induced diabetes, a high fat diet, ibuprofen, and exposure to polychlorinated biphenyls (PCBs) have also been reported to induce CYP4A1 expression (Neat et al., 1981; Barnett et al., 1990; Diaz et al., 1993; Rekka et al., 1994). CYP4A1 exhibits high specificity for the hydroxylation of lauric acid, which is found in very small quantities in the hepatic renal endoplasmic reticulum.

The CYP4A subfamily is found in rats, rabbits, mice, and in humans. In humans, the only two known isoforms of CYP4A are CYP4A11 and CYP4A9. Both are present in kidney and liver (Nelson et al., 1993; Kawashima et al., 1994). CYP4A11-catalyzed lauric acid 12-hydroxylation is considered a characteristic marker activity for CYP4A11 (Crespi et al., 1998).

Table 1.2
Marker activities for human and rat CYP enzymes

Human CYP enzyme	Characteristic catalytic activity	Rat CYP enzyme	Characteristic catalytic activity
CYP1A1	7-ethoxyresorufin O-dealkylation	CYP1A1/2	7-ethoxyresorufin O-dealkylation
CYP2A6	coumarin 7-hydroxylation	CYP2A1	testosterone 7α-hydroxylation
CYP2B6	S-mephenytoin N-demethylation	CYP2B1/2	testosterone 16β-hydroxylation
CYP2C8	taxol 6α-hydroxylation	CYP2C6	progesterone 21-hydroxylation
CYP2C9	S-warfarin 7-hydroxylation	CYP2C11 (m)	testosterone 2α-hydroxylation
CYP2C19	S-mephenytoin 4'-hydroxylation	CYP2C12 (f)	5α-androstane-3α,17β-diol-3,17-disulfate hydroxylation
CYP2D6	dextromethorphan O-demethylation	CYP2D	MDMA demethylation
CYP2E1	chlorozoxazone 6-hydroxylation	CYP2E1	p-nitrophenol hydroxylation
CYP3A4	testosterone 6β-hydroxylation	CYP3A2 (m), 3A9, 3A18, 3A23	testosterone 6β-hydroxylation
CYP4A11	lauric acid 12-hydroxylation	CYP4A1	lauric acid 12-hydroxylation

m-male specific, f-female specific, MDMA-methylene dioxymethamphetamine. Compiled from (Ryan et al., 1984; Hasegawa et al., 1994; Lin et al., 1996; Parkinson, 1996; Chen et al., 1998; Lenart and Pikula, 1999; Bandiera, 2001; Skene et al., 2001; Huynh and Teel, 2002; Kobayashi et al., 2003; Richter et al., 2005)

1.1.4 CYP induction

The hepatic concentration of many CYP enzymes is increased or induced by exposure to xenobiotics. In many instances, the inducer is a substrate for the induced CYP enzyme, thereby providing a mechanism for enhancing the body's detoxification response during prolonged periods of chemical exposure. CYP enzyme levels return to normal on withdrawal of exposure to the chemical. Numerous clinically relevant drugs also induce various CYP enzymes. The induction of CYP enzymes, in turn, accelerates the metabolism of other medications. Thus, the need to understand the underlying mechanisms for CYP induction is necessary.

Members of CYP1A, CYP2B, and CYP4A gene subfamilies show low basal expression in the absence of substrate and highly elevated expression in the presence of their substrates or inducers. Recently, a series of nuclear orphan receptors (NORs) such as constitutive androstane receptor (CAR), human pregnane X receptor (PXR), and peroxisome proliferator-activated receptor (PPAR) have been found to be involved in the induction of CYP2B, CYP3A and CYP4A, respectively (See Table. 1.3). The mechanism of induction of CYP enzymes and the role of the NORs is discussed below.

Table 1.3
Inducers of CYP enzymes and mechanisms of induction

CYP inducer	CYP subfamily/ CYP isoform	Receptor/mechanism involved in induction
3-Methylcholanthrene	rCYP1A1/2, hCYP1A2	Aryl hydrocarbon receptor (AhR)
Phenobarbital	hCYP2B6, rCYP2B1, rCYP2B2	Constitutive androstane receptor (CAR) Pregnane X receptor (PXR)
Ethanol	CYP2E1	mRNA stabilization
Dexamethasone	hCYP3A4, CYP3A23	Pregnane X receptor (PXR)
Clofibrate	rCYP4A, hCYP4A	Peroxisome proliferator-activated receptor (PPAR)

Compiled from (Parkinson, 1996; Bandiera, 2001; Xie and Evans, 2001; Handschin and Meyer, 2003) r- rat, h-human.

a)   CYP1A induction

Hepatic expression of CYP1A1 and CYP1A2 enzymes is induced by exposure to MC or "MC-type" inducers. This class of inducers includes the polycyclic aromatic hydrocarbons (PAHs) and the halogenated hydrocarbons such as PCBs, 2,3,7,8-tetrachlorodibenzo-*p*-dioxin (TCDD) and 2,3,7,8-tetrachlorodibenzofuran (TCDF) (Knutson and Poland, 1982; Mason and Safe, 1986). The PAH group includes the prototype inducers, MC, BaP and β-napthoflavone (Conney, 1967). CYP1A1 induction is mediated by the aryl hydrocarbon receptor (AhR) (Knutson and Poland, 1982; Okey, 1990). The unliganded AhR resides in the cytoplasm in a complex with heat shock protein 90 (Hsp90) and AIP (Ah receptor-interacting protein), an immunophilin type of chaperone protein. TCDD and other inducers bind to the AhR and activate it. Activation of the AhR triggers the dissociation of AhR from Hsp90 and AIP complex, followed by the translocation of the AhR into the nucleus. The AhR dimerizes with Ah receptor nuclear translocator (Arnt). The AhR/Arnt dimer binds to the DNA response elements and activates the transactivation domains of the AhR leading to the increase in transcription of the CYP1A1 gene (Ma, 2001). Induction of CYP1A1 enhances the metabolism of PAHs, and therefore, represents an adaptive response to chemical exposure in mammalian cells.

b)   CYP2B induction

PB is an inducer of many CYP genes including CYP2A, CYP2B, CYP2C, CYP2H, and CYP3A (Sueyoshi and Negishi, 2001). Of these genes, the CYP2B genes have been studied most intensively because they are induced to the greatest extent by PB. PB activates CYP2B gene transcription through a DNA-response-element module that is located in the 5' flanking

17

sequence of the PB-responsive genes (Waxman, 1999; Sueyoshi and Negishi, 2001). The mechanism of CYP induction by PB has not been fully elucidated. However, PB is known to stimulate both the nuclear translocation and nuclear activation of CAR (Sueyoshi and Negishi, 2001). CAR was purified from hepatocytes as a factor that was associated with the PB-responsive CYP2B regulatory element, and was subsequently shown to bind to a promoter as a heterodimer with RXR (Honkakoski et al., 1998). Interestingly, endogenous CAR resides in the cytoplasm of hepatocytes where it is unable to affect gene transcription. On exposure to PB, CAR is translocated from the cytoplasm to the nucleus by a phosphorylation-dependent mechanism (Sueyoshi and Negishi, 2001; Zelko et al., 2001). Although there is no evidence that PB binds directly to CAR, the PB-induced translocation of the CAR receptor leads to an increase in CYP2B gene transcription in the cell nucleus. The generation of CAR knockout mice provided definitive proof of the role of CAR in the regulation of CYP2B expression *in vivo*. CAR knockout mice were unable to induce CYP2B gene expression on exposure to PB-type inducers (Wei et al., 2000).

c) Induction of CYP3A

The rat CYP3A enzymes are inducible by an array of chemically unrelated compounds, including steroids such as pregnenolone 16α-carbonitrile (PCN), DEX, betamethasone, hydrocortisone, α-methylprednisolone, mifepristone and spirinolactone, macrolide antibiotics such as triacetyloleandomycin (TAO), rifampicin and antifungal agents such as clotrimazole, and antidiabetic agents such as troglitazone. PCN was first described by Hans Seyle and colleagues as one of the most potent catatoxic steroids (Selye, 1971). This steroid was identified as the first prototype inducer for the CYP3A subfamily in the liver, and confers resistance to various toxins or intoxicants by accelerating their metabolism (Lu et al., 1972). It was later

shown that PCN induces transcription of CYP3A23 and CYP3A2 genes in rodents by acting through DNA response elements conserved in the promoter region of these genes (Quattrochi and Guzelian, 2001). However, the expression of the human CYP3A4 gene is not stimulated by PCN but is stimulated by various other xenobiotics. These findings suggested important pharmacological differences in the regulation of CYP3A gene expression between species. PXR was identified as a new NOR in 1997 from a fragment that was found in the Washington University Mouse Expressed Sequence Tag (EST) Database (Kliewer et al., 1998). PXR was later cloned from a wide variety of species including mammals, birds and fish. It was observed that PXR functions as a heterodimer with the retinoid X receptor (RXR) and is activated by the naturally occurring progesterone metabolite, 5β-pregnane-3, 20-dione. Many compounds that activate PXR have also been reported to increase CYP3A activity *in vivo* or in primary cultures of hepatocytes (Kocarek et al., 1995; Michalets, 1998). PXR ligands were identified as activators of CYP3A as well. The PXR ligand binds to the PXR and induces expression of CYP3A enzyme accelerating the metabolism of drugs (e.g warfarin, tamoxifen, doxorubicin, cyclosporin, atorvastatin, erythromycin, etc.) that are substrates of CYP3A (Willson and Kliewer, 2002). PXR knockout mice had increased basal levels of CYP3A mRNA that were not increased on exposure of the animals to PCN or DEX (Xie et al., 2000a; Staudinger et al., 2001). Presently, PXR is widely accepted as the main transcriptional regulator of CYP3A induction.

d) CYP4A induction

The induction of CYP4A enzymes by peroxisome proliferators and fatty acids is mediated by the PPAR-α. It has been proposed that PPAR forms heterodimers with RXR and binds to DNA sequences, peroxisome proliferator responsive elements (PPRE) in the 5' flanking

sequence of those genes, that are regulated by peroxisome proliferators. The PPREs contain the binding motif, which consists of a direct repeat of the hexanucleotide TGA(A/C/T)CT, separated by a single nucleotide. This arrangement is typical of other receptor elements including those for the thyroid hormone, vitamin D or RXR. Similar to the mechanism of other nuclear receptors, the PPAR is activated by binding of the peroxisome proliferator that binds to the PPRE located upstream of the peroxisome proliferator target gene leading to an increase in the transcription rate of the CYP4A1 gene.

In rats and mice, exposure to peroxisome proliferators stimulates the proliferation of peroxisomes, increases mitogenesis and produces hepatocellular carcinomas. Inactivation of the PPAR-α gene in mice not only blocks the induction of CYP4A enzymes and the peroxisomal enzymes catalyzing fatty acid β-oxidation, (Lee et al., 1995) but also prevents carcinogenesis induced by the peroxisome proliferator, WY14643 (Peters et al., 1997). PPAR-α null mice express relatively normal levels of microsomal fatty acid β-hydroxylation and peroxisomal β-oxidation activities as well as normal numbers of peroxisomes. However, depressed levels of several mitochondrial enzymes that participate in ketogenesis and fatty acid β-oxidation are evident (Aoyama et al., 1998), and fasting PPAR-α knockout animals exhibit severe hypoglycemia and reduced ketogenesis (Leone et al., 1999; Kersten et al., 1999; LeMaya et al., 2000). These results are consistent with a physiologic role for PPAR-α in regulating fatty acid metabolism and maintaining energy homeostasis.

e)   CYP2E induction

The induction of CYP2E is not nuclear receptor mediated. CYP2E1 is inducible by ethanol, the anti-tubercular drug, isoniazid and other volatile compounds such as acetone and pyrazole. The CYP2E1 gene is transcriptionally activated in rat liver from a dormant state

within a few hours after birth (Gonzalez et al., 1991; Lieber, 1997). It is also induced during fasting (Tu et al., 1983) and diabetic conditions (Bellward et al., 1988). Ethanol affects CYP2E1 at a post-translational level by stabilization of the mRNA encoding the enzyme. Thus, CYP2E induction does not seem to be nuclear receptor mediated.

Increasing evidence suggests that the nuclear receptors PXR, CAR, and RXR along with the farnesoid X receptor (FXR) and vitamin D receptor (VDR) may be involved in the regulation of bile acids. However, not all of these receptors are involved in CYP induction. A detailed discussion regarding the involvement of nuclear receptors in bile acid metabolism will follow in subsequent sections.

1.2 Bile acids

Bile acids are catabolic byproducts of cholesterol metabolism. Bile acids consist of a 5β C_{24} steroidal backbone. The major bile acids are cholic acid (CA), lithocholic acid (LCA), deoxycholic acid (DCA), ursodeoxycholic acid (UDCA) and chenodeoxycholic acid (CDCA). The structures of some major bile acids and their metabolites are shown in Fig.1.4. Hofmann and his colleagues published a recommended nomenclature for bile acids (Hofmann et al., 1992). The bile acid structure consists of a 19 carbon saturated sterol nucleus, an α-oriented hydroxyl group at C_3 and a branched five carbon saturated side chain terminating in a carboxylic acid. Bile salts also have a β-oriented hydrogen at C_5 resulting in a bend in the steroid nucleus (Vlahcevic et al., 1996; Hofmann, 1999b).
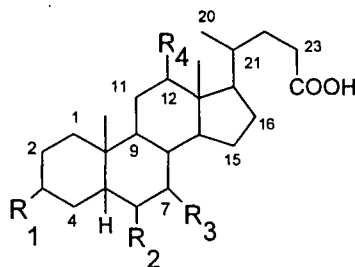
	R_1	R_2	R_3	R_4	Bile acid/metabolite (Abbreviations*)
1.	α-OH	H	α-OH	α-OH	cholic acid (CA)
2.	α-OH	H	α-OH	H	chenodeoxycholic acid (CDCA)
3.	α-OH	H	H	α-OH	deoxycholic acid (DCA)
4.	α-OH	H	β-OH	H	ursodeoxycholic acid (UDCA)
5.	α-OH	H	H	H	lithocholic acid (LCA)
6.	α-OH	β-OH	β-OH	H	β-muricholic acid (β-MCA)
7.	α-OH	β-OH	α-OH	H	α-muricholic acid (α-MCA)
8.	O	H	H	H	3-ketocholanic acid (3KCA)
9.	α-OH	O	H	H	6-ketolithocholic acid (6KLCA)
10.	α-OH	α-OH	H	H	hyodeoxycholic acid (HDCA)
11.	β-OH	H	H	H	isolithocholic acid (ILCA)
12.	α-OH	β-OH	H	H	murideoxycholic acid (MDCA)

Fig.1.4 Basic structures of bile acids
* Abbreviations for the various bile acids used are according to Hofmann et al. (1992). The abbreviations for 3KCA, ILCA and 6KLCA are new, but follow a similar pattern as used in Hofmann et al. (1992) and are used throughout this thesis.

Unconjugated bile acids have a pKa of 5-6. The pKa of the bile acid is reduced upon conjugation with glycine and taurine. Glycine conjugates have a pKa of 3.9 while taurine conjugates have a pKa value < 1. Bile acid conjugation through Phase II biotransformation reactions results in complete ionization of the bile salts, increased solubility but decreased diffusion across plasma membranes (Carey, 1984; Fini and Roda, 1987). *In vivo,* conjugated bile acids exist in ionized form and hence are called bile salts.

1.2.1 Biosynthesis and circulation of bile acids

Bile acid synthesis takes place in the liver. Cholesterol is metabolized to 7α-hydroxycholesterol by cholesterol 7α-hydroxylase which is encoded by the CYP7A gene. A second pathway involves the conversion of cholesterol to oxysterol, which is then acted upon by oxysterol 7α-hydroxylase regulated by the CYP7B gene (Fig.1.5). The 7α-hydroxylated sterols are precursors in the formation of CA and CDCA, respectively (Russell, 1999). Bile acids are conjugated with the amino acids glycine and taurine in the liver before being secreted into bile and stored in the gall bladder. The uptake of bile acids in hepatocytes is a highly efficient process.
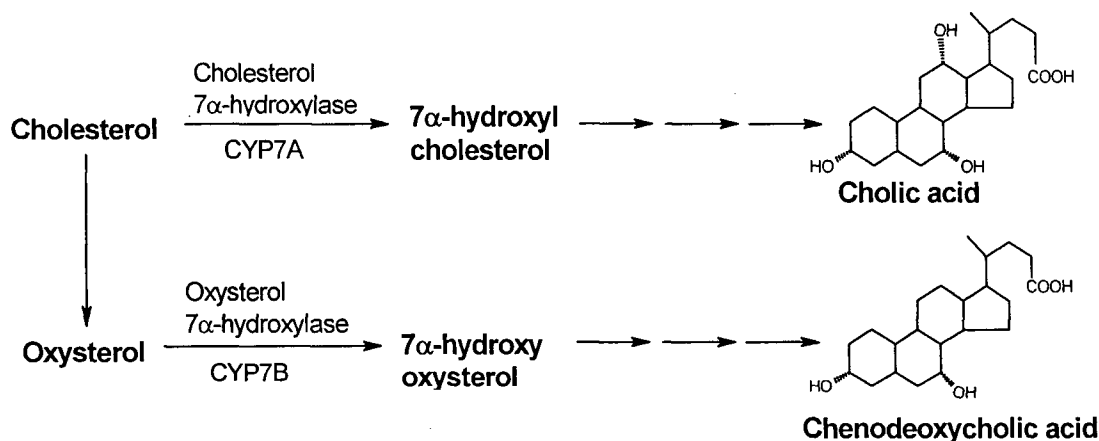
Fig.1.5 Biosynthesis of bile acids.

Cholesterol 7α-hydroxylase pathway regulated by the CYP7B gene mediates the formation of cholic acid from cholesterol. Oxysterol 7α-hydroxylase pathway regulated by the CYP7B gene mediates the formation of chenodeoxycholic acid from oxysterol (Russell, 1999).

CDCA and CA are formed directly in the hepatocyte from cholesterol and are called primary bile acids. Bacterial biotransformation of bile acids occurs on the side chain during enterohepatic cycling of bile acids, and their structure is altered. Deconjugation occurs on the side chain to form unconjugated bile acid and glycine or taurine. Some of the conjugated bile acids are absorbed, returned to the liver, or reconjugated. The C-7 hydroxy group is attacked by anaerobic bacteria in the colon. Bacterial dehydratases act to remove the hydroxy group to form 7-deoxy bile acids. Dehydroxylation of CA leads to the formation of DCA. Similarly, the 7-dehydroxylation of CDCA leads to the formation of LCA. LCA and DCA are known as secondary bile acids.

Approximately 95% of bile acids return to the liver via the portal circulation and 5% of the bile acid pool escapes uptake and is excreted. The diminished level of bile acids is replenished by new synthesis from cholesterol in the liver (See Fig.1.6) (Russell, 1999).
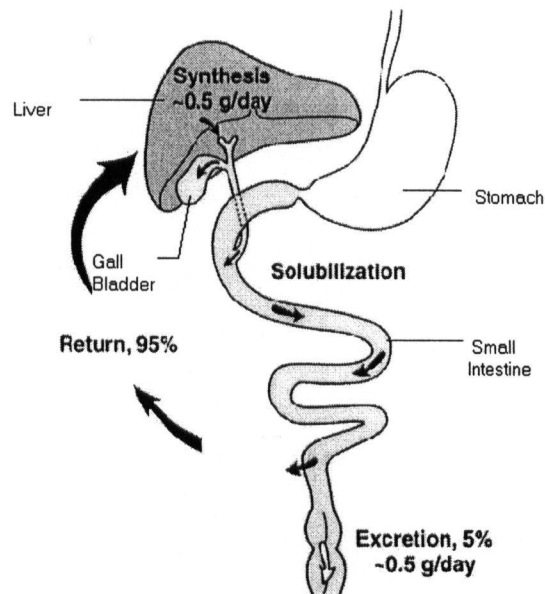
Fig.1.6 Circulation of bile acids in humans

Bile acids are released into the small intestine through a common bile duct. A major portion of the bile acids return to the liver by portal circulation and a small percent is excreted (Russell, 1999).

1.2.2   Bile salt transporters

Unconjugated bile acids are weak acids that are uncharged at the physiological pH and thus can traverse cell membranes by passive diffusion. Conjugated bile salts such as taurocholate and glycocholate are present predominantly in anionic form, have lower pKa values and require active transport mechanisms for cellular uptake. Bile salt transport occurs against a chemical and electric gradient and is a carrier-mediated, sodium-dependent, energy requiring system. The enterohepatic circulation of bile salts is assisted by numerous hepatobiliary membrane transporter systems in hepatic and extrahepatic tissues. Various membrane transport systems involved in bile acid circulation are summarized in Table 1.4. A discussion of the various transporters and their role in bile acid transport follows.

Table 1.4
Bile salt transporters

Location	Transporter, Abbreviation (Gene Nomenclature)	Function
Basolateral membrane of hepatocyte	sodium taurocholate cotransporting polypeptide, NTCP (SLC10A1)	Na^+-dependent bile salt uptake
	organic anion transport proteins, OATPs, (SLC21A)	Na^+-independent bile salt uptake, multispecific
	multidrug resistance associated proteins, MRP3, (ABCC3)	bile salt efflux, multispecific
Canalicular membrane of hepatocyte	multidrug resistance-1 P-glycoprotein, MDR1, (ABCB1)	ATP-dependent, excretion of xenobiotics into bile
	canalicular bile salt export pump, SPGP, (ABCB11)	ATP-dependent transport of monovalent bile salts into bile
	familial intrahepatic cholestasis-1, FIC1, (ATP8B1)	potential aminophospholipid translocating ATPase
Cholangiocytes	ileal sodium-dependent bile salt transporter, ABST, (SLC10A2)	bile salt efflux during cholestasis
	multidrug resistance associated proteins, MRP3, (ABCC3)	transports returning bile salts to portal circulation during obstructive cholestasis
Intestine	organic anion transporting polypeptides, OATP3, (SLC21A7)	Na^+-dependent bile salt uptake from intestinal lumen
	ileal sodium-dependent bile salt transporter, ABST, (SLC10A2)	primary carrier for sodium-dependent bile salt uptake from intestine by ileum
	multidrug resistance associated proteins, MRP3, (ABCC3)	transports returning bile salts to portal circulation
Kidney	ileal sodium-dependent bile salt transporter, ABST, (SLC10A2)	bile salt uptake from glomerular filtrate
	multidrug resistance associated proteins, MRP2 (ABCC2)	postulated to facilitate renal excretion of bile salt conjugates in cholestasis

a) Sodium taurocholate co-transporting polypeptide (NTCP)

The sodium taurocholate co-transporting polypeptide (NTCP) is located and expressed in the basolateral membrane of hepatocytes. It is responsible for the uptake of sodium-dependent conjugated bile salts from the portal blood (See Fig.1.7.) (Meier and Stieger, 2002). NTCP is involved mainly in the sodium-dependent uptake of taurine and glycine conjugated bile salts. This Na^+-dependent pathway accounts for > 80% of conjugated taurocholate uptake but < 50% of unconjugated cholate uptake (Kullak-Ublick et al., 2000). NTCP (gene symbol SLC10A1) has been isolated from rat, mouse, rabbit and human liver (Hagenbuch et al., 1991; Hagenbuch and Meier, 1994; Cattori et al., 1999; Kramer et al., 1999). It consists of seven or nine transmembrane spanning domains with an exoplasmic N terminus and cytoplasmic C terminus (Hagenbuch et al., 1991; Hagenbuch and Meier, 1994; Kullak-Ublick et al., 2000). Bile salt uptake via NTCP is unidirectional with a co-transport of two Na^+ for one taurocholate molecule, and is driven by both the transmembrane Na^+ gradient, which in turn is maintained by Na^+-K^+-ATPase, and the intracellular electrical potential derived from the outward diffusion of K^+ (Kullak-Ublick et al., 2000; Meier and Stieger, 2002).

b) Organic anion transport proteins (OATPs)

Sodium-independent hepatocellular uptake of bile salts is mediated by several members of organic anion transport proteins (OATPs). OATPs are multispecific transporter systems with a wide substrate preference for mostly amphiphathic organic compounds, including conjugated and unconjugated bromosulphothalein, bilirubin, cardiac glycosides and other neutral steroids, linear and cyclic peptides, mycotoxins, selected organic cations and numerous drugs (Trauner and Boyer, 2003). Na^+-independent bile salt uptake is mediated largely by facilitated exchange with intracellular anions such as glutathione (Kullak-Ublick et al., 2000). Three different classes of OATP (gene symbol SLC21A3), namely OATP1, OATP2 and OATP4, have been identified.

OATP1 (SLC21A1) is localized to the basolateral membrane of hepatocytes, the apical membrane of kidney proximal tubular cells, and choroid plexus epithelial cells (Bergwerk et al., 1996; Angeletti et al., 1997) (See Fig. 1.7). Developmentally, OATP1 expression precedes expression of NTCP, and its mRNA can be detected at day 16 of gestation in developing rat liver (Dubuisson et al., 1996). OATP1 is a highly versatile, multispecific transport system that transports a wide variety of amphiphathic substrates with differing affinities. Specific substrates for OATP1 include bile salts, thyroid hormones including triiodothyronine (T_3) and thyroxine (T_4), steroid hormones and steroid conjugates, leukotriene C_4 and other glutathione conjugates, neutral steroids such as ouabain, the angiotensin-converting enzyme inhibitors enalapril and temocaprilat, opiod receptor antagonists enkephalin and deltorphin II and organic cations such as N-propylajmalinium (Trauner and Boyer, 2003).

Based on the homology with OATP1, a second OATP2 (SLC21A5) was cloned originally from a rat brain cDNA library. OATP2 is also highly expressed in liver and kidney. OATP2 is localized to the basolateral membrane of hepatocytes, retina, endothelial cells of blood-brain barrier, and basolateral membrane of choroid plexus epithelial cells. The substrate specificity of OATP2 is similar, but not identical, to that of OATP1 with similar affinities for taurocholate and cholate. Moreover, OATP2 transports ouabain with higher affinity and is unique in mediating high affinity transport of the cardiac glycoside, digoxin. Similar to OATP1, the driving force for OATP2-mediated uptake appears to be exchange with glutathione and glutathione conjugates (Noe et al., 1997).

The third OATP family member involved in hepatic bile salt uptake in rat liver is OATP4 (SLC21A10). OATP4 is the full-length isoform of rat liver-specific transporter 1 (rLST-1). It is located in the basolateral membrane of hepatocytes and shares 43-44% amino acid identity with OATP1 and OATP2 (Cattori et al., 2000). OATP4 transports estrone-3-

sulfate, estradiol 17β-glucuronide, prostaglandin E_2, the thyroid hormones T_3 and T_4 and gadoxetate (Cattori et al., 2000). OATP4 appears to be primarily involved in the hepatic clearance of anionic peptides including microcystin and cholecystokinin. OATP4 works in concert with OATP1 and OATP2 in the basolateral membrane of rat hepatocytes. (Kullak-Ublick et al., 2000; Meier and Stieger, 2002).

OATP3 is a multispecific transport system in the small intestine (Cattori et al., 2000). OATP3 is not expressed in liver, in contrast to initial reports and may be important for intestinal bile salt uptake. OATP3 has similar broad susbtrate specificity but much lower affinities than OATP4.

Human liver expresses four OATPs (OATP-A, OATP-B, OATP-C and OATP8) (Trauner and Boyer, 2003). The most important sodium-independent bile transporter of human liver is OATP-C (SLC21A6), which is also called LST-1, OATP2, or OATP6 (Kullak-Ublick et al., 2001). It is located in the basolateral membrane of human hepatocytes and transports taurocholate with lower affinity than NTCP (Kullak-Ublick et al., 2000). OATP-C exhibits large overlapping substrate specificity with other OATPs of human liver, but a unique property of OATP-C is transport of unconjugated bilirubin (Cui et al., 2001). Although OATP-C shares many substrates with rat OATP4, it remains uncertain whether the two proteins represent truly orthologous gene products. OATP8 is 80% identical with OATP-C and shares the same selective basolateral expression in human hepatocytes (Konig et al., 2000). OATP-A was cloned from human liver, its hepatic expression level is low and its overall contribution to hepatic bile salt uptake is minor. Its predominant expression is in brain, where it is involved in the transport of various drugs and opioid peptides across the blood brain barrier (Abe et al., 1999; Gao et al., 2000). Finally, OATP-B (SLC21A9) is expressed at the basolateral membrane

of human hepatocytes, but its spectrum of substrates does not include bile salts (Kullak-Ublick et al., 2001).

c)   **Multidrug resistance associated proteins (MRP)**

ATP-dependent transport systems in liver are members of the ATP-binding cassette (ABC) superfamily. They transport biliary constituents across the canalicular membrane against steep concentration gradients. ABC proteins belong to the multidrug resistance P-glycoprotein (MDR) family also known as ABC-B family or the multidrug-resistance protein (MRP) family. A typical ABC transporter consists of 12 or more membrane spanning domains that determine the substrate specificity and two intracellular nucleotide-binding loops that are highly conserved and contain Walker A and B motifs for binding and hydrolysis of ATP (Hooiveld et al., 2001).

Basolateral efflux of bile salts is dependent on the MRP subfamily. MRP proteins are normally expressed at low levels but may be induced during cholestatic conditions. In humans, this family consists of six members (MRP1-6) (Borst et al., 1999; Keppler and Konig, 2000). The hepatic expression of the MRP4 and MRP5 proteins is low, and their physiological function and subcellular localization are not known (Hooiveld et al., 2001). Three members of the family have been identified in rat (MRP2,-3,-6), five in mouse (MRP1,-2,-4,-5,-6) and one in rabbit (MRP2) (Cole et al., 1992; Mayer et al., 1995). The first member of the MRP family, MRP1, was cloned from a multidrug resistant small lung cancer cell line and is minimally expressed in normal liver where it has been reported to be localized in the basolateral membrane of hepatocytes (Cole et al., 1992; Mayer et al., 1995). Substrates for the MRP family include glucuronides and glutathione conjugates of endogenous and exogenous compounds (Konig et al., 1999; Keppler and Konig, 2000). MRP1 and MRP3 are able to transport the divalent anionic bile salts such as sulfated taurocholate, taurolithocholate and glucuronidated bile salts with high affinity. In addition, MRP3 can also transport monovalent bile salts such as tauro- and

30

glycocholate, while human MRP3 transports only glycocholate to a significant degree (Hirohashi et al., 1999; Hirohashi et al., 2000). Because MRP1 and MRP3 are able to transport divalent anionic bile salts that are eliminated in urine, the induction of MRP1 and MRP3 during cholestasis may increase the renal excretion of bile salts as a major mechanism for bile salt elimination in patients with chronic, long-standing cholestasis (Trauner and Boyer, 2003).

d)   Bile salt export pump (BSEP)

The canalicular membrane contains a bile salt export pump (BSEP) for monovalent bile salts. The canalicular BSEP was originally known as sister of P-glycoprotein (SPGP) (Trauner and Boyer, 2003). Functional expression of the rat SPGP gene demonstrated that SPGP functions as an ATP-dependent bile salt transporter with transport characteristics comparable with canalicular rat liver plasma membrane vesicles (Gerloff et al., 1998). Rat BSEP is a 1,321-amino acid protein with 12 membrane spanning domains, four potential N-linked glycosylation sites and a molecular mass of 160 kDa. Comparison of ontogenic expression of the BSEP gene with that of MRP2 demonstrated that BSEP is undetectable before birth, whereas MRP2 was observed in liver of 16-day-old fetuses, indicating that biliary excretion of monovalent bile salts by BSEP does not take place until birth (Zinchuk et al., 2002). BSEP transports various bile salts at similar rates as ATP-dependent transport in canalicular rat liver plasma membrane vesicles. In addition to taurocholate, BSEP also mediates ATP-dependent transport of glycocholate, taurodeoxycholate and tauroursodeoxycholate (Kullak-Ublick et al., 2000; Meier and Stieger, 2002). The mouse BSEP gene was localized to a region in mouse chromosome 2, which has been linked to genetic gallstone susceptibility (Lammert et al., 2001). Targeted inactivation of this gene, as observed in SPGP knockout mice, results in nonprogressive but persistent intrahepatic cholestasis, due to the *de novo* formation and biliary excretion of muricholic acid (Wang et al., 2003). SPGP knockout mice fed a CA-enriched diet show severe

31

cholestatic symptoms such as jaundice, weight loss, elevated plasma bile acid, elevated transaminase, cholangiopathy, liver necrosis, high mortality, and changes in mRNA levels of major liver genes (Wang et al., 2001a). This suggests that BSEP is a major canalicular bile salt transport system.

e)   Familial intrahepatic cholestasis-1 (FIC1)

FIC1 (ATP8B1), a P-type ATPase mutated in "familial intrahepatic cholestasis", belongs to a family of putative aminophospholipid transporters. FIC1 has been localized to the canalicular membrane and to bile duct epithelium (See Fig. 1.7) (Ujhazy et al., 2001) but is also highly expressed in extrahepatic tissues including the intestine and pancreas (Bull et al., 1998; Eppens et al., 2001). The detailed function of FIC1 is unclear, but mutations of this transporter result in variants of familial intrahepatic cholestasis, suggesting that it must play a direct or indirect role in canalicular bile salt excretion (Bull et al., 1998; Eppens et al., 2001). Of note, these patients have a prominent reduction in the biliary excretion of hydrophobic bile salts such as lithocholate and chenodeoxycholate relative to cholate conjugates, indicating that FIC1 could directly excrete highly hydrophobic bile salts (Stieger, 2001). Apart from this, FIC1 could also play an indirect role in bile secretion by maintaining the canalicular membrane asymmetry between the inner and the outer layer and maintaining phosphatidylethanolamine and serine within the inner bilayer of the plasma membrane, or regulating the docking of vesicles fusing with the canalicular membrane (Oude Elferink and van Berge Henegouwen, 1998). High levels of expression of FIC1 in extrahepatic tissues such as pancreas, small intestine, and kidney suggests a more general role in the regulation of secretory processes (Bull et al., 1998) and may explain some of the extrahepatic features associated with these syndromes such as pancreatitis, diarrhea, and nephrolithiasis. The biochemical function of FIC1 in bile acid transport has so far

not been identified clearly. Generation of FIC1 knockout mice should shed light on the physiological function of FIC1 (Stieger, 2001).

f)   Ileal sodium-dependent bile salt transporter (ISBT)

Na^+-dependent bile salt uptake occurs via the ileal bile salt transporter (ISBT or IBAT) also known as the apical sodium-dependent bile salt transporter (ASBT). This transport system has been identified in the apical membrane of cholangiocytes and proximal renal tubular cells (See Fig. 1.7). ISBT was originally cloned from hamster intestine (Wong et al., 1995), followed by human (Wong et al., 1994), rat (Shneider et al., 1995), rabbit (Kramer et al., 1999), and mouse (Saeki et al., 1999) ileum. Both primary and secondary conjugated and unconjugated bile salts are substrates for ISBT, the highest affinity being reported for conjugated dihydroxy bile salts (Oelkers et al., 1997). In contrast to NTCP, which transports some non-bile salt substrate in addition to bile salts, the substrate specificity of ISBT appears to be strictly limited to bile salts. ISBT is the major intestinal bile salt uptake system in humans as emphasized by ISBT gene mutations that result in bile salt malabsorption (Wong et al., 1995; Oelkers et al., 1997).
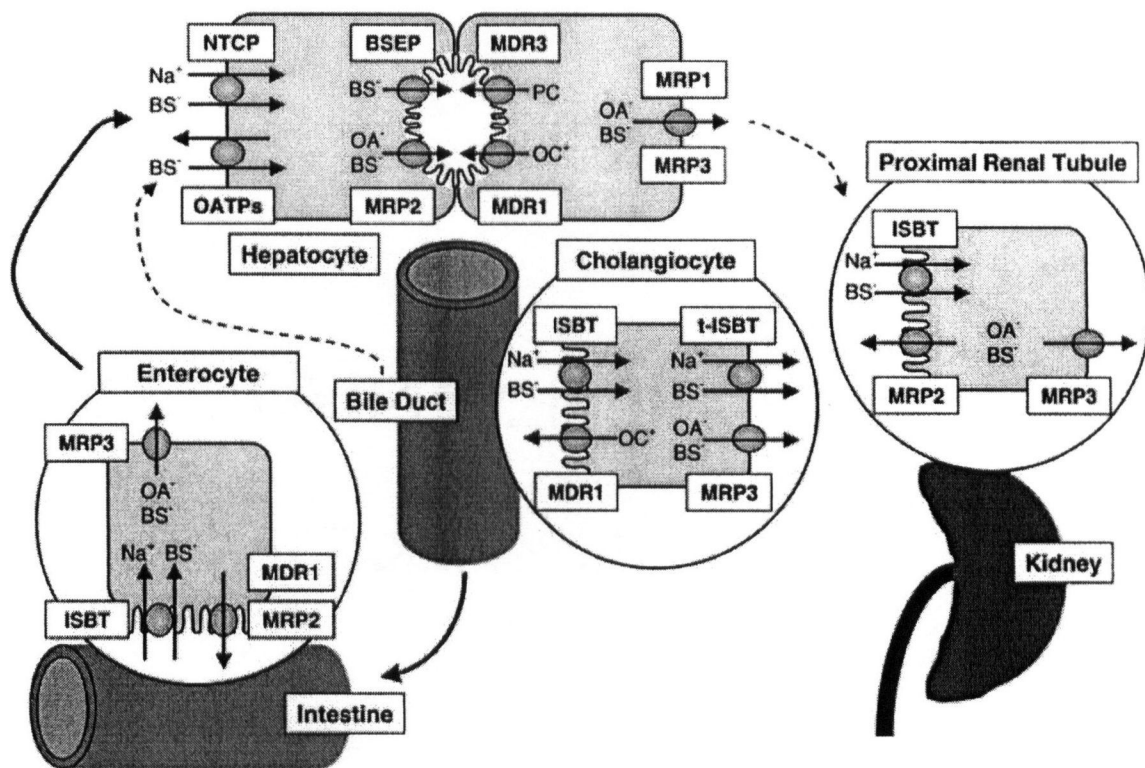
Fig. 1.7 Bile salt transporters

Hepatobiliary transport systems in liver and extrahepatic tissues in humans. Bile salts (BS⁻) are taken up by hepatocytes via the basolateral Na⁺/taurocholate cotransporter (NTCP) and organic anion transporting proteins (OATPs). Monovalent BS⁻ are excreted via the canalicular bile salt export pump (BSEP) while divalent BS⁻ together with anionic conjugates (OA⁻) are excreted via the canalicular conjugate export pump (MRP2). The phospholipid export pump (MDR3) facilitates excretion of phosphatidylcholine (PC), which forms mixed micelles in bile together with BS⁻ and cholesterol. Cationic drugs are excreted by the multidrug export pump (MDR1). Other basolateral isoforms of the multidrug resistance-associated protein (MRP1 and MRP3) provide an alternative route for the elimination of BS⁻ and nonbile salt anionic conjugates from hepatocytes into the systemic circulation. BS⁻ are reabsorbed in the terminal ileum via ileal Na⁺-dependent bile salt transporter (ISBT) and effluxed by MRP3. Similar mechanisms exist in proximal renal tubules and cholangiocytes where an additional, truncated isoform (t-ISBT) may be involved in BS⁻ efflux from cholangiocytes. MRP2 is also present in the apical membrane of enterocytes and proximal renal tubules, while MDR1 is also found in intestine and bile ducts (Taken from Trauner M and Boyer J, 2003).

1.2.3 Cytotoxicity of bile acids

Bile acids play an important role in the absorption of fats and fat-soluble vitamins and in the maintenance of cholesterol homeostasis. However, bile acids are known to be cytotoxic byproducts of cholesterol metabolism. The cytotoxicity of bile acids is due to their structure. The bile acid molecule is relatively planar. It has a hydrophobic face that consists of non-hydroxy substituents and a hydrophilic face made up of hydrophilic substituents. Bile acids are surface active, naturally occuring amphipathic molecules (See Fig. 1.8). Thus, they have the ability to form micelles above a particular concentration (critical micellar concentration, CMC) and can act as solubilizers, surfactants or detergents. The inherent detergent properties of bile acids causes disruption of cell membranes and tissue degradation leading to toxicity (Vyvoda et al., 1977; Scholmerich et al., 1984). Above the CMC, conjugated bile acids form polymeric aggregates or micelles with lipids. The lipids that form micelles include phosphatidylcholine (PC), fatty acid anion mixtures, and monoglycerides.
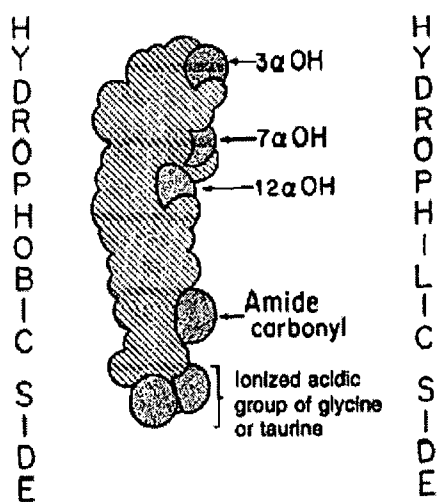
Fig. 1.8 The bile acid molecule

Bile acids are planar, surface active, amphiphatic molecules. It is due to this nature that they exhibit surfactant like action (Hofmann, 1999a).

The attributes that make bile acids powerful solubilizers of membrane lipids are also responsible for bile acid cytotoxicity at abnormally high concentrations (Roberts et al., 1997; Hofmann, 1999a). The efficient coupling of bile acids with binding proteins in cytosol keeps the concentration of bile acids within the hepatocyte extremely low (less than < 3 μM). In healthy individuals, intracellular bile acid uptake is followed by rapid elimination. A defect in canalicular transport or physical obstruction to bile flow causes bile to accumulate within the hepatocyte. With impaired elimination (e.g. in cholestasis), the bile acid-binding capacity of cytosolic proteins is exceeded. Bile acids enter other organelles, damaging cell membranes and impairing their functions. Bile acids induce apoptosis and necrosis by damaging the mitochondria (Roberts et al., 1997). The cytotoxicity of bile acids is also related to their structure. The number of hydroxy groups on the bile acid molecule is inversely related to toxicity so that the fewer the number of hydroxy groups, the higher the toxicity. Naturally occurring dihydroxylated CDCA and DCA bind tightly to tissue, have a longer retention time, are hydrophobic and hence, highly cytotoxic. LCA is the most hydrophobic cytotoxic bile acid. CA has intermediate hydrophobicity and is non-cytotoxic at low concentrations, but cytotoxic at very high concentrations. UDCA, although a dihydroxylated bile acid, does not bind to tissue, is more hydrophilic and is devoid of cytotoxic properties (Scholmerich et al., 1984; Quist et al., 1991).

1.2.4 Bile acids in cancer

Evidence implicating the involvement of bile acids in the development of colon carcinoma has been put forth recently (Berta et al., 2003; De Gottardi et al., 2004; Pai et al., 2004; van Faassen et al., 2004). Colon cancer incidence is positively related to dietary fat intake and negatively related to the amount of fiber consumed (Cummings et al., 1992). A high fat intake elevates the amount of sterols in the colon by stimulating hepatic synthesis of cholesterol

and bile acids (Narisawa et al., 1978). Clinical case-control studies show that patients with tumors had significantly more DCA and LCA in their feces than control patients without tumors (Imray et al., 1992). It was shown that adenoma patients have a higher serum DCA concentration than healthy controls (Bayerdorffer et al., 1995). Animal experiments show that bile acids act as tumor promoters in rodents. Feeding rodents high fat diets resulted in higher tumor yield and an increased fecal bile acid concentration (Nagengast et al., 1995). In one study, a DCA-enriched diet led to damage of the colonic mucosa thereby provoking increased cell renewal. This was accompanied by increased cell proliferation, which might be the mechanism leading to colonic carcinogenesis (Hori et al., 1998). Impaired elimination of bile acids in the small intestine is sometimes associated with tumors. Studies show that ileum resection in rats fed a DCA-enriched diet resulted in colon tumors (Kanamoto et al., 1999). Another study in humans found a strong association between genetic polymorphism of the gene for the bile acid transporter, ISBT, and the risk of colorectal adenoma (Wang et al., 2001b). A small prospective study suggested that a high ratio of DCA to CA in serum is associated with an increased incidence of colorectal cancer. A high level of unconjugated DCA in serum is regarded as being a biomarker for habitual colonic exposure to the cancer-promoting DCA (Bayerdorffer et al., 1993). A role for bile acids in the development of breast cancer in women has been proposed (Costarelli and Sanders, 2002).

Toxic bile acids impair mitochondrial function, leading to an inhibition of oxidative phosphorylation and enhanced formation of toxic oxygen species by the mitochondrial respiratory chain. This results in oxidative stress, ATP depletion, and an increase in intracellular Ca^{2+} concentration with stimulation of hydrolases. This could lead to hydrolysis of lipid membranes and structural proteins causing cell death by necrosis.

1.2.5   Bile acids in cholestasis

Cholestasis (Greek: *chole*, bile and *stasis*, standing still), defined as cessation or obstruction to bile flow, can cause nutritional imbalances related to malabsorption of lipids and fat-soluble vitamins. The obstruction causes bile salts or acids, the bile pigment bilirubin, and fats (lipids) to accumulate in liver instead of being eliminated (Hofmann, 2002). Cholesterol accumulation, fat malabsorption, elevated bile acid and alkaline phosphatase blood levels are the usual indications observed in cholestasis. The primary symptoms of cholestasis include itching, jaundiced skin or eyes, nausea, vomiting and white stools. Puritis, a metabolic bone disease, and fatigue are other manifestations of this disorder that contribute to a poor quality of life for patients (Glasova and Beuers, 2002). Anabolic steroids, non steroidal anti-inflamatory drugs (NSAIDS) such as nimesulide, antibiotics such as erythromycin, barbiturates, benzodiazepines, neuroleptics such as phenothiazines, angiotensin converting enzyme inhibitors such as fosinopril, antihyperglycemics such as troglitazone, and certain antifungals have been reported to cause or induce cholestasis (Jezequel et al., 1994). Drug-induced cholestasis may lead to abdominal pain and dark urine (Erlinger, 1997). Cholestasis during pregnancy is due to the increased sensitivity of bile ducts to estrogen. It develops during the second and third trimesters of pregnancy and disappears within two to four weeks after the infant's birth but may reappear again during subsequent pregnancies. Pregnancy-induced cholestasis tends to run in families (Hofmann, 1999b; Hofmann, 2002).

In chronic cholestatic liver disease in humans, levels of hydrophobic bile acids, CA, LCA and CDCA, are increased in liver. These hydrophobic bile acids have been shown to be highly detrimental. Hepatic levels of bile acids in endstage cholestasis are illustrated in Fig. 1.9 (Fischer et al., 1996). However, the level of DCA is decreased significantly ($P < 0.01$) as shown in Fig.1.9.
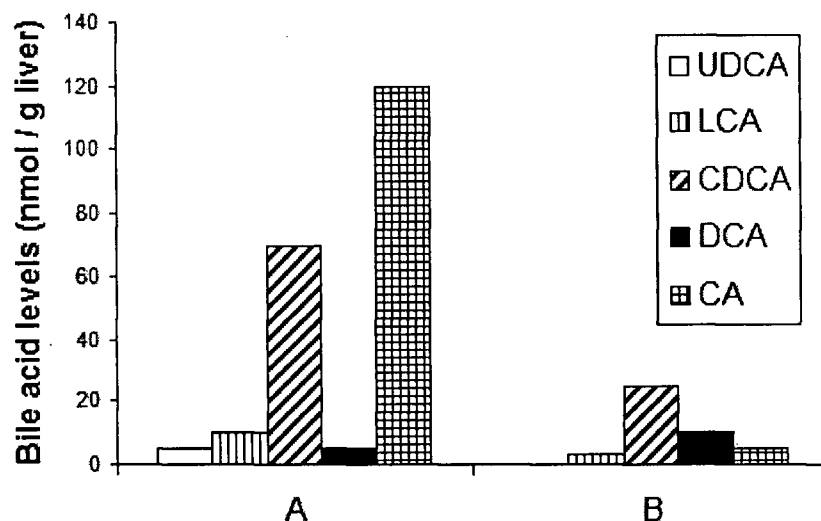
Fig.1.9 Comparison of hepatic levels of bile acids in end-stage cholestasis and normal liver

Hepatic levels of bile acids (nmol/g liver, wet tissue) in end–stage chronic cholestasis (A), and in normal liver tissue (B). LCA, lithocholic acid; DCA deoxycholic acid; CA, cholic acid; CDCA, chenodeoxycholic acid; UDCA, ursodeoxycholic acid (Adapted from Fischer et al., 1996).

1.2.6 Biotransformation of bile acids

Bile acid toxicity is attenuated by hydroxylation at several positions on the steroidal backbone. Hydroxylation (Phase-I metabolism) converts bile acids to hydrophilic products and thus facilitates clearance. All possible hydroxylation positions for bile acids are shown in Fig. 1.10. The major Phase I metabolites of these bile acids are listed in Table 1.5.

Bile acid → CYP, NADPH, O_2 → **Possible bile acid hydroxylation sites**
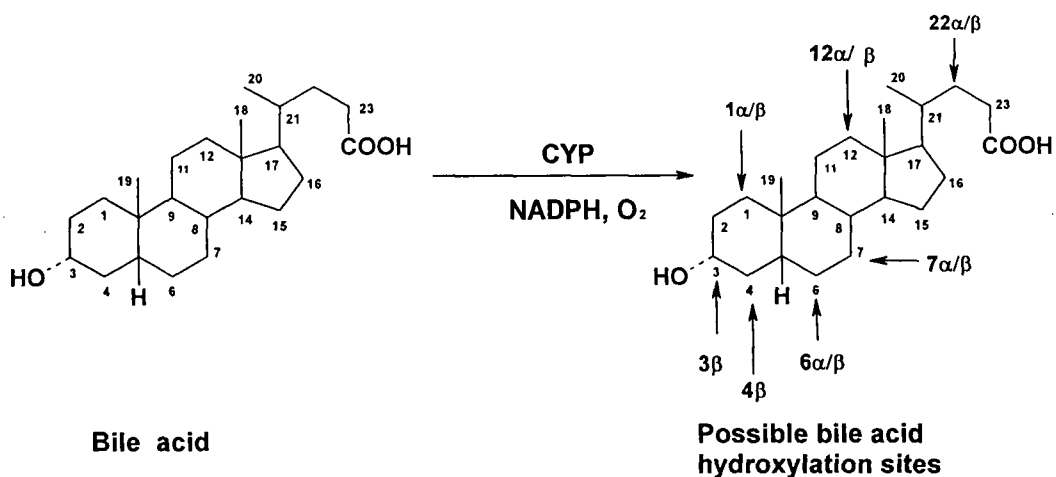
Fig. 1.10 Regio-and stereospecific hydroxylation sites of bile acids.

The various hydroxylation positions for bile acids are C_1, C_3, C_4, C_6, C_7, C_{12} and C_{22} on the steroidal ring system. Arrows indicate possible or observed bile acid hydroxylation positions.

a)   Biotransformation of LCA

Biotransformation of LCA has been examined in different species using various analytical techniques. *In vitro* hepatic microsomal metabolism of LCA in male Sprague-Dawley rats showed MDCA as the major metabolite followed by 6KLCA, CDCA, α-MCA and β-MCA, respectively. These metabolites were identified using TLC techniques (Zimniak et al., 1989). Metabolism of LCA in male Sprague-Dawley rats also supports the formation of MDCA as the major metabolite along with β-MCA (Dionne et al., 1994).

The 6β-hydroxylation of LCA, to form MDCA, was studied using cDNA-expressed hamster CYP3A10 and hamster liver microsomes by Chang et al. (1993). LCA metabolites were identified using TLC techniques. Results from this study showed that hamster CYP3A10 played an important role in the hydroxylation of LCA. The Vmax and Km values for 6β-hydroxylation were 164 pmol/min/mg protein and 25 μM respectively (Chang et al., 1993).

In an attempt to identify human liver enzymes catalyzing the hydroxylation of bile acids, recombinant expressed human CYP enzymes and human liver microsomes were incubated with taurochenodeoxycholic acid (TCDA) and LCA, and metabolites were analyzed using GC/MS. Recombinant expressed CYP3A4 was the only enzyme found to be active in bile acid biotransformation (Araya and Wikvall, 1999). A strong correlation was found between 6α-hydroxylation of TCDCA, a Phase II metabolite, CYP3A4 levels and testosterone 6β-hydroxylation. A strong correlation was also obtained between 6α-hydroxylation of LCA, CYP3A4 levels and testosterone 6β-hydroxylation. TAO, an effective inhibitor of CYP3A and testosterone 6β-hydroxylation, was shown to inhibit 6α-hydroxylation of TCDCA almost completely at a concentration of 10 μM. The apparent Km for 6α-hydroxylation of TCDA by human liver microsomes was 716 μM. The study concluded that CYP3A4 is active in hydroxylation of taurochenodeoxycholate and lithocholate in human liver (Araya and Wikvall, 1999).

In vitro studies using human liver microsomes carried out by Xie et al., 2001, pointed to HDCA, followed by MDCA and CDCA, as major metabolites of LCA. The metabolite detection in this study was carried out using TLC. Anti-CYP3A antibody totally inhibited LCA 6α-hydroxylation by human liver microsomes. Recombinant CYP3A4 efficiently hydroxylated LCA while CYP3A5 was observed to be less active. This study concluded that LCA hydroxylation by human liver microsomes is mediated primarily by CYP3A enzymes (Xie et al., 2001).

Metabolism of LCA by recombinant CYP3A4 using GC/MS identified 3KCA as a major metabolite followed by HDCA and two new minor metabolites, namely, 6α-hydroxy-3-oxo-5β-cholanic acid (m/z 461) and 1β-hydroxy LCA (m/z 391) (Bodin et al., 2005). However, CDCA and MDCA were not identified as CYP3A4-catalyzed metabolites.

In vivo Phase I LCA metabolites, such as 3-ketocholanic acid (3KCA) and isolithocholic acid (ILCA) have been found in human bile (Norman, 1964; Norman and Palmer, 1964; Whitney et al., 1983). The LCA metabolites identified in different studies and from various species are shown in Table 1.5.

b)   Biotransformation of other unconjugated bile acids

The biotransformation of ^{14}C-labeled CDCA was studied in patients with intrahepatic cholestasis, by Bremmelgaard and Sjovall. The ^{14}C-labeled metabolites were isolated from urine and were identified after subsequent derivatization using gas-liquid chromatography-mass spectrometry (GLC/MS). CDCA was metabolized to hyocholic acid (HCA), α-muricholic acid (α-MCA), taurolithocholate (TLCA), and taurohyodeoxycholate (THDCA) as major metabolites (Bremmelgaard and Sjovall, 1980). Recently, *in vitro* studies performed by Bodin et al. (2005), identified metabolites of CDCA namely, 3α,6α,7α-trihydroxy-5β-cholanic acid (major), following incubation with recombinant CYP3A4 (Bodin et al., 2005). The various Phase–I metabolites of CDCA obtained from the literature are compiled in Table 1.5.

Biotransformation of CA was also observed in patients with intrahepatic cholestasis using radiolabeled CA. The radioactive labeled and derivatized metabolites detected by GLC/MS from the urine of patients include 1β,2β,6α-hydroxy cholanoic acid; 3α,6α,7α,12α-tetrahydroxy-5β-cholanoic acid; 1ξ,3α,7α,12α-tetrahydroxy-cholanoic acid; 3α,6α-dihydroxy-12α-acetoxy-7-oxo-5β-cholanoic acid; 3-hydroxy,12-keto-cholanoic acid and DCA (See Table 1.5) (Bremmelgaard and Sjovall, 1980). Recombinant CYP3A4 metabolizes CA to 3-dehydro-CA as its major product (Bodin et al., 2005). Recently, a new metabolite, 3α,6α,7β,12α-tetrahydroxy-5β-cholanoic acid has been identified in the SPGP gene knockout mouse cholestatic model. Tetrahydroxylated bile acids have been observed to be increased in these

SPGP gene knockout mice (Perwaiz et al., 2003). Characterization of the involvement of CYP enzymes in these CA biotransformations remains to be investigated.

The major metabolites of DCA obtained from patients with intrahepatic cholestasis using GLC/MS are 1β,3α,12α-trihydroxy-5β-cholanoic acid; 6α-hydroxy DCA; 3α,6α,12α-trihydroxy-5β-CA and 1β-hydroxy-DCA (Bremmelgaard and Sjovall, 1980). Recently, 3-dehydro-DCA and 1β-hydroxy-DCA have been identified as major recombinant CYP3A4-catalyzed metabolites of DCA (Bodin et al., 2005).

A number of UDCA metabolites have been identified from serum and urine of pregnant women with intrahepatic cholestasis. The metabolites were identified using GC/MS and are shown in Table 1.5 (Meng et al., 1997). *In vitro* studies using recombinant CYP3A4 showed 3-oxo-UDCA as a major metabolite of UDCA (Bodin et al., 2005).

It should be noted that most of the metabolites of these unconjugated bile acids are formed either by oxidation or hydroxylation. Hydroxylation and oxidation of substrates is a characteristic of hepatic CYP enzymes. The CYP enzymes involved in biotransformation of these bile acids have not been identified.

Table 1.5
Phase I metabolites of bile acids

Bile acid	Metabolite	Trivial name	Species/Enzyme	Research group
Lithocholic acid	5β-cholanic acid-3β-ol	isolithocholic acid	human	Norman and Palmer, 1964
(5β-cholanic acid-3α-ol)	5β-cholanic acid-3α, 6β, 7β-triol	β-muricholic acid	rat, mice	Dionne et al., 1994, Stedman et al., 2004
	5β-cholanic acid-3α, 6α-diol	hyodeoxycholic acid	human, rCYP3A4	Araya and Wikvall, 1999, Xie et al., 2001 Bodin et al., 2005
	5β-cholanic acid-3α, 6β-diol	murideoxycholic acid or	rat	Dionne et al., 1994; Zimniak et al., 1989
		murocholic acid	hamster	Staudinger et al., 1989, Chang et al., 1993 Stedman et al., 2004
	3oxo 5β-cholanic acid	3-ketocholanic acid	rat, rCYP3A4 human	Xie et al., 2001, Bodin et al, 2005 Sakai et al., 1980
	5β-cholanic acid-3α, 7α-diol	chenodeoxycholic acid	rat	Zimniak et al., 1989, Stedman et al., 2004
	3α, 6oxo 5β-cholanic acid	6-ketolithocholic acid	rat	Zimniak et al., 1989,
	5β-cholanic acid-3oxo-6α-diol		rCYP3A4	Bodin et al, 2005
	5β-cholanic acid-1β, 3α-diol	1β-hydroxy-LCA	rCYP3A4	Bodin et al, 2005
	5β-cholanic acid-3α, 6β, 7α-triol	α-muricholic acid	mice	Stedman et al., 2004
	5β-cholanic acid-3α, 7α- 12α-triol	cholic acid	mice	Stedman et al., 2004
	5β-cholanic acid-3α, 7β- diol	ursodeoxycholic acid	mice	Stedman et al., 2004
	5β-cholanic acid-3α, 12α- diol	deoxycholic acid	mice	Stedman et al., 2004
Chenodeoxycholic acid	5β-cholanic acid-3α, 6α, 7α-triol	hyocholic acid	human, pig	Bremmelgaard and Sjovall, 1980
(5β-cholanic acid-3α, 7α-diol)	5β-cholanic acid-3α, 6β, 7α-triol	α-muricholic acid	rat	Bremmelgaard and Sjovall, 1980
	3oxo 5β-cholanic acid	3 ketocholanic acid	rCYP3A4	Bodin et al, 2005
Cholic acid	5β-cholanic acid-3α, 12α-diol	deoxycholic acid	human	Norman and Palmer, 1964
(5β-cholanic acid-3α, 7α-12α-triol)	5β-cholanic acid-3α, 6α, 7β, 12α- tetraol		mice	Perwaiz et al., 2003
	5β-cholanic acid-3α, 6α, 7α, 12α- tetraol		human	Bremmelgaard and Sjovall, 1980
	5β-cholanic acid-1ξ, 3α, 7α, 12α- tetraol		human	Bremmelgaard and Sjovall, 1980

Table 5 continued-

Deoxycholic acid (5β-cholanic acid-3α, 12α-diol)	5β-cholanic acid-1β, 3α, 12α-triol	1β-hydroxy-DCA	human, rCYP3A4	Bremmelgaard and Sjovall, 1980, Bodin et al, 2005
	5β-cholanic acid-3α, 6α, 12α-triol		human	Bremmelgaard and Sjovall, 1980
	5β-cholanic acid-3α, 6α, 7α, 12α- tetraol		human	Bremmelgaard and Sjovall, 1980
	5β-cholanic acid-3oxo, 12α-ol	3-dehydro-DCA	rCYP3A4	Bodin et al, 2005
Ursodeoxycholic acid (5β-cholanic acid-3α,7β-diol)	5β-cholanic acid-3α, 12α-diol	deoxycholic acid	human	Meng et al, 1997
	5β-cholanic acid-3α, 7α-diol	chenodeoxycholic acid	human	Meng et al, 1997
	5β-cholanic acid-3α, 7α, 12α-triol	cholic acid	human	Meng et al, 1997
	5β-cholanic acid-3β, 7β-diol	isoursodeoxycholic acid	human	Meng et al, 1997
	5β-cholanic acid-3α, 6β, 7β-triol		human	Meng et al, 1997
	5β-cholanic acid-3α, 4β-diol		human	Meng et al, 1997
	5β-cholenoic acid-3-oxo-3α,12α-diol		human	Meng et al, 1997
	5β-cholanic acid-3α, 7β, 22-triol		human	Meng et al, 1997
	5β-cholanic acid-3α, 5β, 7β-triol		human	Meng et al, 1997
	5β-cholanic acid-3α, 4β, 7α-triol		human	Meng et al, 1997
	5β-cholanic acid-3α, 4β, 12α-triol		human	Meng et al, 1997
	5β-cholanic acid-1β, 3α, 7β-triol		human	Meng et al, 1997
	5β-cholanic acid-3α, 6α, 7β-triol		human	Meng et al, 1997
	5β-cholanic acid-3α, 4β, 7α, 12α-tetraol		human	Meng et al, 1997
	5ξ-cholanic acid-3α, 4ξ, 7β-triol		human	Meng et al, 1997
	5β-cholanic acid-3oxo-7β-ol		rCYP3A4	Bodin et al, 2005

The table shows various Phase-I metabolites of unconjugated bile acids as compiled from different sources of literature. The involvement of specific CYP enzymes in the metabolism of most of these bile acids is not yet identified. r-recombinant.

1.3 Nuclear receptors in bile acid metabolism

NORs are involved in regulating primary bile acid synthesis, transport, and enterohepatic bile acid re-circulation in the liver and within the intestine. Nuclear receptors appear to play a role in cholesterol and bile acid regulation as sensors to maintain normal homeostasis. FXR, PXR, VDR, and CAR are identified as 'bile acid' receptors that regulate bile acid metabolism. The specific and overlapping functions of these nuclear receptors increase the complexity of liver metabolism and suggest the existence of functionally redundant defenses against bile acid toxicity as shown in Fig. 1.11 (Zhang et al., 2004).

Bile acids

Phase I
CYPs

Phase II
UGT, SULT, GST

Transporters
MRP2, MDR1, OATP2

Bile acid metabolism
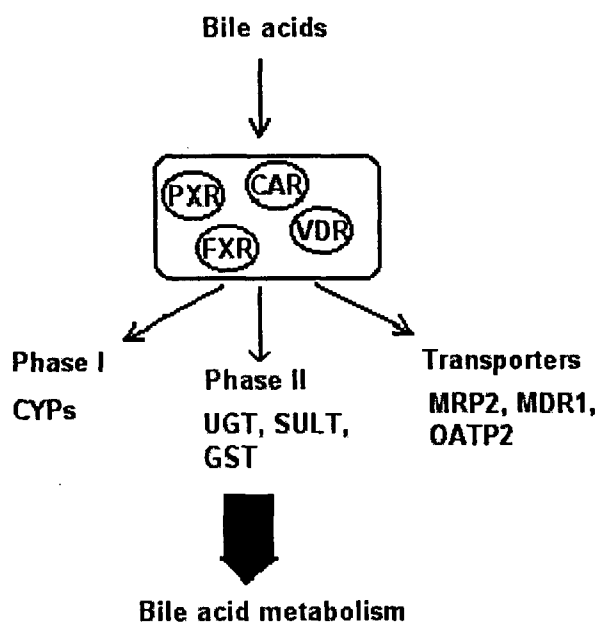
Fig.1.11 Redundancy of receptors in bile acid homeostasis

Activation of nuclear receptors by bile acids and regulation of Phase I and Phase II enzymes and drug transporters eventually helps in homeostasis of bile acids.

Bile acids appear to be natural ligands for FXR. FXR was originally identified as a receptor activated by farnesol, an intermediate in cholesterol synthesis. A major role of FXR as a bile acid receptor has been put forth (Makishima et al., 1999). FXR is active as a heterodimer

46

with RXR and is expressed in liver, intestine, and kidney. CDCA is the most potent FXR agonist. FXR regulates expression of several genes including cholesterol 7α-hydroxylase and the apical sodium-dependent bile acid transporter (Grober et al., 1999). Bile acid activated FXR represses the expression of CYP7A1 and CYP8B enzymes involved in hepatic bile acid synthesis, through an indirect pathway. Bile salts regulate gene expression through the liver X receptor (LXR-α) together with PXR and FXR receptors (Xie et al., 2001; Ekins et al., 2002) (See Fig. 1.12). At high concentrations, bile salts bind to FXR, leading to up-regulation of proteins involved in bile salt trafficking and down-regulation of enzymes involved in bile salt biosynthesis. FXR gene knockout mice have impaired resistance to bile acid-induced hepatotoxicity (Sinal et al., 2000). A synthetic FXR agonist, GW4064, has proven to be hepatoprotective in rat models of intra- and extrahepatic cholestasis (Liu et al., 2003). All these studies show an indispensable role for the nuclear receptor, FXR, in mediating protection against bile acid toxicity.

The human orphan receptor, steroid X receptor (SXR), and its rodent ortholog, PXR, regulate CYP3A expression in liver and intestine. Both PXR and SXR bind to inverted (IR-6) and direct response elements (DRE-4) localized in the promoter regions of human or rodent CYP3A genes (Kliewer et al., 1998; Palut et al., 2002). PXR represses the CYP7A1 gene involved in the synthesis of bile acids from cholesterol. It induces OATP2 gene expression that is involved in the enterohepatic circulation of bile acids and it also regulates the expression of CYP3A genes in metabolism of secondary bile acids (especially LCA) (Staudinger et al., 2001). LCA and its 3-keto metabolite bind to PXR, which confers resistance to LCA toxicity. PXR protects against liver damage induced by LCA and thus serves as a physiological sensor of LCA (See Fig. 1.13) (Staudinger et al., 2001; Xie et al., 2001). As shown in Fig. 1.9, the concentration of LCA in livers of cholestatic patients is approximately 6 μM. LCA

concentrations of 5-10 µM were reported in livers of cholestatic patients and in rat models of biliary cholestasis (Setchell et al., 1997). LCA activates PXR at these concentrations (Staudinger et al., 2001). The PXR knockout mouse model exhibits heightened levels of LCA toxicity compared with wild-type animals. Also, induction of CYP3A11 and OATP2 gene expression is observed in wild-type mice as compared to PXR knockout mice upon LCA treatment, indicating that PXR functions as a receptor for LCA and regulates LCA metabolism *in vivo* (Staudinger et al., 2001).

PXR functions as a heterodimer with the RXR (See Fig. 1.13). Ligands such as LCA bind to PXR and induce the expression of CYP3A, which catalyzes the metabolism of xenobiotic and endogenous substrates including LCA (Mangelsdorf and Evans, 1995; Ekins et al., 2002). PXR and VDR, after heterodimerization with RXR, are capable of sensing the concentration of secondary bile acids, including LCA, and inducing their metabolism in the liver and intestine (Staudinger et al., 2001; Xie et al., 2001; Makishima et al., 2002). A key PXR and VDR target is the CYP3A gene which converts LCA to the non-toxic HDCA (Makishima, 2005).

The above discussed mechanisms of the involvement of nuclear receptors in regulation of bile acid metabolism have been described suitably in Fig. 1.12 (Makishima, 2005).
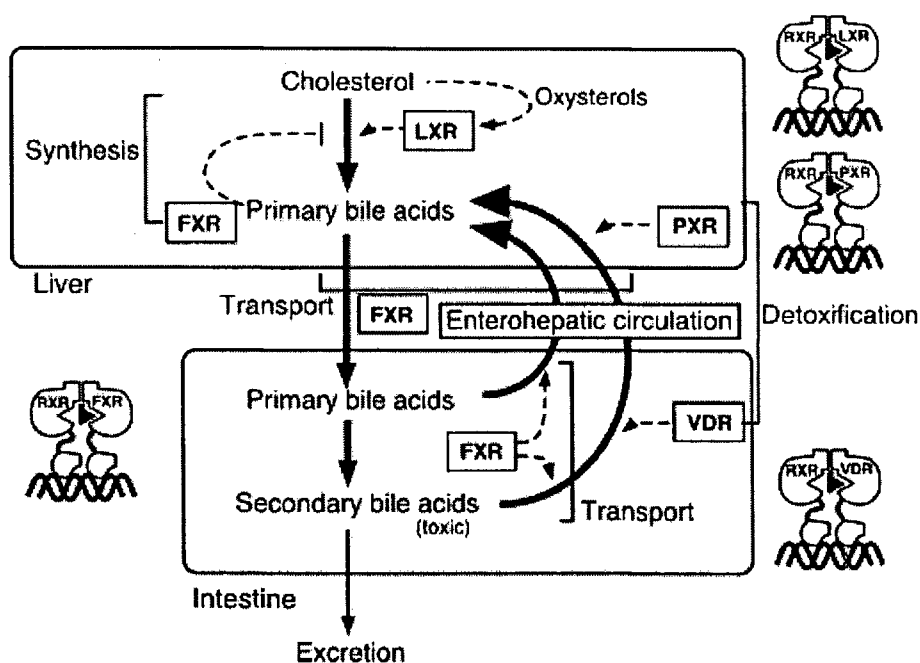
Fig. 1.12 Regulation of bile acid biotransformation by nuclear receptors

Bile acid synthesis is stimulated by LXR in rodents. Negative feedback regulation of bile acid synthesis is mediated by FXR. FXR represses bile acid import in hepatocytes and stimulates their biliary excretion. FXR induces the expression of intestinal bile acid-binding protein. PXR and VDR are involved in detoxification of secondary bile acids (Taken from Makishima, 2005).

CAR normally resides in the cytoplasm of untreated mouse liver and hepatocytes, but undergoes a cytosolic-nuclear translocation upon PB stimulation, at least in mouse liver and primary rat hepatocytes (Handschin and Meyer, 2003; Maglich et al., 2003). The identity of CAR as a xenobiotic receptor was first revealed when selective androstane metabolites inhibited its constitutive ability. CAR was shown to activate the phenobarbital response element (PBRE) found in promoters of PB-inducible CYP2B genes. The activation of CAR has been shown to reduce hepatotoxicity of LCA by induction of cytosolic sulfotranferase (SULT) and increased LCA sulfation. It regulates SULT expression by binding to the CAR response elements found within the SULT gene promoters (Saini et al., 2004). This function of CAR was also observed to be independent of CYP3A (Saini et al., 2004). CAR heterodimerizes with RXR and activates the

49

expression of xenobiotic metabolizing enzymes (Willson and Kliewer, 2002). A comparison of responses of PXR and CAR to LCA treatment demonstrates that CAR predominantly mediates induction of CYP3A11 and the MRP3 transporter. CAR is also a major regulator of the OATP2 gene involved in bile acid transport.

Several groups have recently demonstrated the existence of cross-talk between CAR, PXR and their target CYP genes. Such reciprocal regulation is accomplished via recognition of each other's DNA response elements as shown in Fig. 1.13. The PBRE of CYP2B contains two imperfect DR-4 type nuclear receptor binding sites that show affinity for SXR. SXR was also found to regulate CYP2B in cultured cells and in transgenic mice (Xie et al., 2000b). In the same manner, CAR can activate CYP3A through SXR/PXR response elements (Moore et al., 2000; Xie et al., 2000b; Xie and Evans, 2001). The cross-regulation of CYP gene classes provides an explanation for the dual activation property of certain compounds including bile acids. This reciprocal regulation of CYP genes by multiple receptors reveals the existence of a metabolic safety network to protect against the toxic effect of xenobiotics and endobiotics.
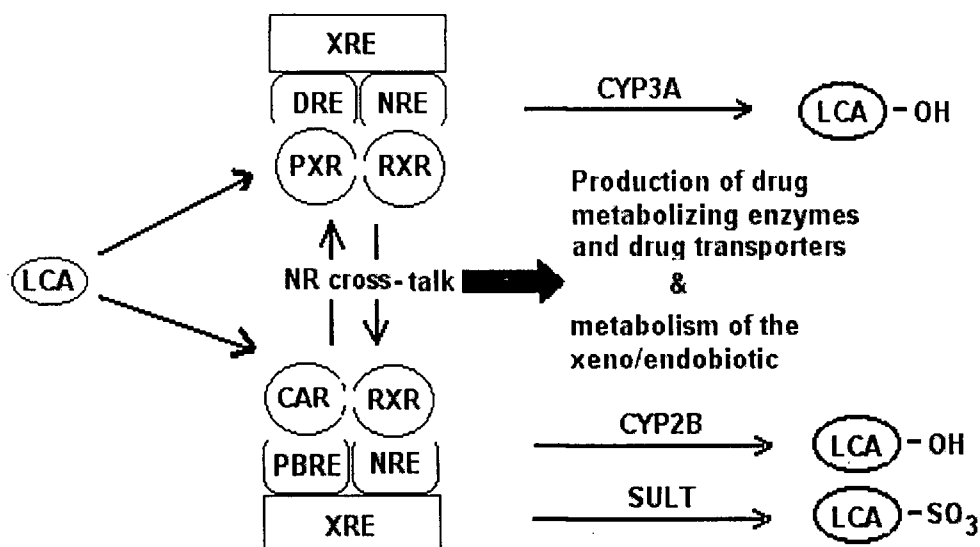
Fig.1.13 PXR and CAR cross-talk mediated metabolism of lithocholic acid

Bile acids such as LCA act as endobiotic activators to activate PXR and CAR which heterodimerize with RXR and bind to respective response elements and increase transcription of target genes. Response elements that are activated by both PXR and CAR allow direct cross-talk and reciprocal regulation of CYP genes generating a metabolic safety network to protect against toxicity. Activation of these receptors induces Phase I (e.g. CYP3A, and CYP2B) and Phase II (e.g. sulfotransferase, SULT) enzymes and drug transporters. The PXR receptor along with its xenobiotic response elements (XRE) induces CYP3A. Similarly, CAR along with its XRE induces CYP2B. XRE-xenobiotic response element; DRE-DNA response element, NRE-nuclear response element; NR-nuclear receptor, PBRE-phenobarbital response element.

1.4   Scope of this study

The purpose of this study was to generate an understanding of various hepatic elimination pathways of the most toxic bile acid, LCA. A comprehensive study to identify all the LCA metabolites, the CYP enzymes and kinetic parameters involved in formation of these metabolites has not been reported previously. Earlier analytical methods developed to characterize Phase I metabolism of LCA utilized TLC or GC/MS (Zimniak et al., 1989; Dionne et al., 1994). A more simple and sensitive method to elucidate pathways and kinetic parameters for the oxidative metabolism of LCA using an analytical tool such as LC/MS was required. Most bile acids and their metabolites have a similar C_{24} 5β-cholestane steroidal backbone with the same molecular mass but variation in the position of hydroxyl groups (Fig. 1.4). LC/MS facilitated separation and detection of bile acid metabolites based on molecular mass as well as the composition of mobile phase was achievable. Thus, an assay using LC/MS was developed to analyze the various LCA metabolites.

Biotransformation of LCA in inducer treated hepatic microsomes was analyzed. This data, along with anti-CYP antibody inhibition experiments was used to identify specific CYP enzymes in LCA biotransformation. The identification of specific CYP enzymes involved in detoxification of bile acids will eventually help to reduce the risk of bile acid mediated disorders.

The catalytic activity of CYP enzymes in chronic cholestasis was reported to be altered (Chen and Farrell, 1996). A preliminary study to measure changes in the activity of individual CYP enzymes in an induced cholestatic rat model were carried out. Rat hepatic microsomes were prepared, and CYP enzyme levels and protein content were measured and compared to control rats. Catalytic activities of CYP enzymes were measured using specific marker rat CYP

enzymatic activities. This work is presented as a pilot study as an addendum to the LCA biotransformation study in the **APPENDIX**.

1.5   Rationale

Biotransformation of steroids, such as testosterone and cortisol, to their respective 6α/β-hydroxylated metabolites has been observed to be catalyzed by CYP3A in rats and humans (Sonderfan et al., 1987; Waxman and Chang, 1998; Furuta et al., 2003). Bile acids are also steroidal structures with a 5β-cholestane steroidal ring system (See Fig. 1.4). Hamster liver microsomal CYP3A10 was observed to be the major enzyme involved in biotransformation of LCA to its 6β-hydroxylated metabolite, MDCA. Xie et al. (2001) showed that recombinant CYP3A4 and human liver microsomes catalyze 6α-hydroxylation of LCA to HDCA as the major metabolite. Zimniak et al. (1989) identified many LCA metabolites using Sprague-Dawley rat liver microsomes (See Table 1.5) by TLC techniques but the CYP enzymes involved in this biotransformation were not identified. On the basis of these studies, the probable metabolites of LCA in rat liver are MDCA, CDCA, HDCA, 6KLCA and β-MCA and it is highly likely that rat CYP3A is involved in the biotransformation of LCA to some, but not all, of these metabolites. Because rat CYP2C enzymes are known to play a major role in steroid metabolism, it is likely that CYP2C enzymes will also catalyze biotransformation of bile acids. The purpose of this study was to develop a LC/MS based method to quantify formation of LCA metabolites by rat hepatic microsomes and to identify the CYP enzymes involved in LCA biotransformation.

1.6   Hypothesis

1. Rat CYP3A is involved in the hepatic biotransformation of LCA to CDCA.

1.7   Specific research objectives

- To develop an *in vitro* assay to analyze the hepatic biotransformation of LCA.

- To determine enzyme kinetic parameters involved in hepatic LCA biotransformation.

- To identify the CYP enzymes involved in hepatic biotransformation of LCA using CYP inducers and anti-CYP antibodies.

2. MATERIALS AND METHODS

2.1 Materials

2.1.1 Chemicals

Chemicals and reagents used in this study were obtained from the following sources:

Steraloids, Inc. (Newport, RI, U.S.A.):

α-Muricholic acid, β-muricholic acid, γ-muricholic acid, murideoxycholic acid, ursodeoxycholic acid, hyodeoxycholic acid, chenodeoxycholic acid, 6-ketolithocholic acid, isolithocholic acid and 3-ketocholanic acid.

Fisher Scientific (Ottawa, Ontario):

Methanol, isopropanol, dichloromethane

BDH chemicals (Toronto, Ontario, Canada):

Sodium hydroxide, sucrose, phenobarbitone disodium salt,

Boehringer Mannheim Canada Ltd. (Laval, Quebec, Canada):

Nicotinamide adenine dinucleotide phosphate tetra-sodium salt (NADPH, reduced form)

Eastman Kodak Company (Rochester, New York, U.S.A.):

3-Methylcholanthrene

J.T. Baker Chemical Co. (Phillipsburg, New Jersy, U.S.A):

Sodium dithionite

Praxair Canada Inc. (Mississauga, Ontario, Canada):

Carbon monoxide (CO) and nitrogen (N_2)

Sigma Chemical Co. (St Louis, MO, USA)

Dexamethasone

Dr. Jan Palaty, Children's & Women's Health Center (Vancouver, B.C., Canada).

Cholic-2,2,4,4-d_4 acid as an internal standard

Dr. Victor Ling (BC Cancer Agency, Vancouver, Canada)

5053 Pico Lab® Rodent Diet 20 as normal diet *(Richmond, IN, USA).*

2.1.2   Antibodies

Monospecific rabbit anti-rat CYP2C11 IgG, polyspecific rabbit anti-rat CYP2C and polyspecific rabbit anti-rat CYP3A IgG were prepared by the laboratory of Dr. Bandiera, Faculty of Pharmaceutical Sciences, UBC, as reported previously (Bandiera and Dworschak, 1992; Panesar et al., 1996; Wong and Bandiera, 1996).

2.1.3   Inducer treated hepatic microsomes

Pooled hepatic microsomes from male Long Evans rats (7 weeks of age) treated with MC (25 mg/kg/day for 4 days), male Long Evans rats (7 weeks of age) treated with PB (75 mg/kg bw/day for 4 days), female Long Evans rats treated with DEX (100 mg/kg bw/day for 4 days), male Long Evans rats (7 weeks of age treated with peanut oil, 0.8 ml/kg per day × 2 day) and female Long Evans rats (7 weeks of age, untreated) were obtained from the laboratory of

Dr. Bandiera, Faculty of Pharmaceutical Science, UBC. Pooled microsomes were prepared as described previously (Hrycay and Bandiera, 2003).

2.1.4 Animals

Adult male Wistar rats, male and female Long-Evans rats, and male Sprague-Dawley rats (200-225 g) were purchased from Charles River Canada Inc. (Saint-Constant, Quebec). After arrival, rats were allowed to recover for 3 to 5 days before treatment was initiated. Water was supplied *ad libitum* and the animals were housed in clear, polycarbonate cages containing corncob bedding (Anderson's Maumee, OH) in a room with controlled light (14 h) and dark (10 h) cycles and a constant room temperature (23^0C). Male Wistar rats were fed Pico Lab$^®$ Rodent Diet 5053 (control diet, Richmond, IN, USA) for 20 days. Long-Evans and Sprague-Dawley rats were fed Laboratory Rodent Diet 5001 (PMI Feeds Inc., Richmond, IN, USA). Liver microsomes prepared from male Wistar rats were used to develop and optimize the *in vitro* LCA biotransformation assay. Liver microsomes prepared from Long-Evans rats were used to study the effect of inducers on LCA biotransformation and antibody inhibition studies. Liver microsomes prepared from untreated male Sprague-Dawley rats were used to compare LCA biotransformation with microsomes prepared from untreated male Long-Evans and Wistar rats.

2.2 Methods

2.2.1 Animal treatments

To study the effect of treatment with CYP inducers on LCA metabolism, hepatic microsomes were prepared from Long-Evans rats treated with DEX and PB. Male Long-Evans rats (7 weeks of age) were injected *s.c.* with DEX (suspended in corn oil, 100 mg/kg bw/day for

4 days). Female Long-Evans rats (7 weeks of age) were injected *s.c.* with PB (dissolved in water, 75 mg/kg bw/day for 4 days).

2.2.2 Preparation of hepatic microsomes

Hepatic microsomes were prepared from individual male Wistar rats. Livers were removed immediately after decapitation, weighed, minced and placed into homogenizer tubes containing ice-cold 0.05 M Tris HCl, 1.15% KCl buffer. Livers were homogenized using a Potter-Elvehjem glass motar and motar driven pestle (Talboys Engineering Corp., Emerson, NJ, USA). The homogenate was centrifuged at 9,000 × g for 20 min at 5^0C using a Beckman J2-21 centrifuge (Beckman Instruments, Palo Alto, CA, USA). The supernatant was filtered through cheesecloth and centrifuged at 105,000 × g for 60 min at 5^0C using a Beckman LE-80 ultracentrifuge. The microsomal pellet was separated from glycogen and resuspended in ice-cold 10 mM EDTA containing 1.15% KCl using a homogenizer. The suspension was centrifuged at 105,000 × g for 60 min at 5^0C using a Beckman LE-80 ultracentrifuge. The resulting pellet was resuspended in 0.25 M sucrose. Aliquots were stored at -80^0C in cryovials (Ingram & Bell, Richmond, BC, Canada). In the case of DEX and PB-treated female Long-Evans and untreated male Sprague-Dawley rats, livers from each treatment group were pooled after initial homogenization. Microsomes were prepared as described above.

2.2.2 Determination of protein concentration

Protein concentrations of hepatic microsomes were measured using the Lowry protein assay (Lowry *et al.* 1951). Bovine serum albumin (BSA) was used as the standard. All samples were analyzed in duplicate at an absorbance of 650 nm using a Shimadzu UV-160 UV-visible recording spectrophotometer (Shimadzu Corporation, Kyoto, Japan).

2.2.4 Instrumentation

Chromatographic separation, detection and quantitation of LCA and its metabolites were carried out using a Fisons VG Quattro mass spectrometer (Micromass, Montreal, Canada) interfaced with a Hewlett-Packard (Avondale, PA, USA) 1090 II liquid chromatograph. MASSLYNX® (v3.1, Micromass) software was used for analysis and data acquisition.

2.2.5 Stock standard solutions

Stock solutions of LCA and its known metabolites (structures shown in Fig. 1.4) were prepared from authentic standards. Stock solutions (1 mg/ml) of LCA (5β-cholanic acid-3α-ol, m.wt.-376.57), α-muricholic acid (α-MCA, m.wt.- 408.57), β-muricholic acid (β-MCA, 5β-cholanic acid-3α, 6β, 7β-triol, m.wt.- 408.57), γ-muricholic acid (γ-MCA, 5β-cholanic acid-3α, 6α, 7α-triol, m.wt.- 408.57), murideoxycholic acid or murocholic acid (MDCA, 5β-cholanic acid-3α, 6β-diol, m.wt.- 392.57), ursodeoxycholic acid (UDCA, 5β-cholanic acid-3α, 7β-diol, m.wt.- 392.57), hyodeoxycholic acid (HDCA, 5β-cholanic acid-3α, 6α-diol, m.wt.- 392.57), chenodeoxycholic acid (CDCA, 5β-cholanic acid-3α, 7α-diol, m.wt.- 392.57), 6-ketolithocholic acid (6KLCA, 5β-cholanic acid-3α-ol-6-one, m.wt.- 390.56), isolithocholic acid (ILCA, 5β-cholanic acid-3β-ol, m.wt.- 376.57), and 3-ketocholanic acid (3KCA, 5β-cholanic acid-3-one, m.wt.- 374.56) were prepared in methanol. A working solution of the internal standard, cholic-2,2,4,4-d_4 acid (40 µg/ml, m.wt.- 412.57), was also prepared in methanol. All the stock solutions were stored at –20 ^{0}C. Aliquots of working solutions were used for each assay.

2.2.6 High-performance liquid chromatography

Samples (10 µl per injection) were separated on a Hewlett-Packard model 1090 II LC instrument using a XTerra™ MS C_{18} (2.1 mm x 150 mm, 3.5 µ) column and delivered at 0.15 ml/min at 40 ^{0}C. The mobile phase consisted of solvent A (50% methanol : 10% 10 mM ammonium acetate pH 4.6 : 40% water) and solvent B (85% methanol : 10% 10 mM ammonium acetate pH 4.6 : 5% water) delivered as a gradient as follows : 0-20 min solvent A 100%; 20-25 min solvent B 100%; 25-35 min solvent A 100%. The total run time was 35 min.

2.2.7 Electrospray mass spectrometry

The HPLC eluent was introduced into a stainless steel capillary probe held at 3 kV in a Fison VG Quattro mass detector via an electrospray ionization interface operating in negative ion mode. Quantitative determination of bile acids was performed by time-scheduled single ion recordings (SIR) using [M-H]⁻ ions. The following parameters were found to be optimal for bile acid detection: cone voltage 40 V, RF lens 3, 5 and 6 operated at 93, 196 and -3 V respectively with a source temperature was 160 ^{0}C. Bath gas flow and nebuliser gas flow were set at 250 L/hr and 20 L/hr, respectively. The low-mass and high-mass resolutions were set at 5.0/5.0 for MS1. SIR with respect to 6 channels at m/z of 411, 407, 391, 389, 375, 373 were monitored with a dwell time of 0.25 s/channel and an interchannel delay of 0.03 s.

2.2.8 Hepatic microsomal LCA biotransformation assay

Hepatic microsomal incubations were performed in clean, methanol-rinsed, borosilicate glass tubes with PTFE-lined caps. LCA (0.5–300 µM) was incubated with 0.5 mg/ml of hepatic microsomal protein (untreated male Wistar rats) for 30 min in a reaction mixture consisting of 1

mM NADPH and 46.5 mM potassium phosphate buffer at pH 7.4. All reactions were initiated using 10 µl of 10 mM NADPH in a final reaction volume of 1 ml. The reaction was terminated using 4 ml of 80:20 dichloromethane and isopropanol. A 10 µl aliquot of the internal standard, cholic-2,2,4,4-d_4 acid (40 µg/ml in methanol, 0.4 µg /ml of reaction mixture) was added to each sample and tubes were capped. Control samples in which the substrate, NADPH or microsomes were omitted were processed in a similar manner as test samples. A metabolite standard mixture (0.5 µM-100 µM for minor metabolites and 0.1 mM- 4 mM for major metabolites) was used routinely to assess the amount of metabolite formed in the assay. All test samples, standards and controls were subsequently processed by a double step, liquid-liquid extraction procedure. The samples were manually vortex-mixed for 1 min and then manually shaken upside down for 1 min. The separation of the aqueous and the organic phase was carried out by centrifugation at 2000 × g for 5 min at room temperature. The aqueous layer was transferred using individual Pasteur pipettes into a clean set of tubes and 4 ml of dichloromethane: isopropanol (80:20) was again added to the aqueous layer for a second extraction. The sample tubes were re-mixed, re-shaken and centrifuged for a second time as described above. The aqueous layer from each sample was removed by aspiration and the organic layers were pooled and evaporated to dryness under a gentle stream of nitrogen. Samples were reconstituted using 0.2 ml of mobile phase (67% methanol, 23% water and 10% 10 mM ammonium acetate, pH 4.6) with vigorous mixing for 30 sec and then filtered through a 3 mm, 0.45 µm syringe filter. A 10 µl aliquot was analyzed using conditions described in the **High-performance liquid chromatography and Electrospray mass spectrometry** sections of this thesis. The metabolites were identified using authentic standards. A summary of this methodology is shown in Fig. 2.1.

LCA (0.5-300 µM) was incubated with 0.5 mg/ml of microsomal protein for 30 min in a reaction mixture consisting of 1 mM NADPH and 46.5 mM potassium phosphate buffer at pH 7.4 $\longrightarrow$ Internal standard (cholic –2,2,4,4- d_4 acid) was added $\longrightarrow$ Extracted twice using 80:20 dichloromethane : isopropanol

Dried under a stream of N_2 and reconstituted in mobile phase $\longrightarrow$ Analyzed using LC/MS and Xterra™ MS C_{18} (2.1 mm x 150 mm, 3.5 µm column) $\longrightarrow$ Identification of metabolites using authentic standards

Fig. 2.1 Methodology used for lithocholic acid biotransformation assay

To determine if LCA metabolite formation was a CYP mediated process, the assay was performed in the absence of NADPH, with boiled microsomes, or following carbon monoxide treatment. Reactions were performed as described above. Microsomes were boiled for 5 min in the presence of phosphate buffer in borosilicate glass tubes on a hot water bath. In the case of carbon monoxide treatment, the gas was bubbled for 2 min into an incubation mixture containing buffer and hepatic microsomes.

LCA, at two different saturating substrate concentrations (100 µM for MDCA and ILCA; 250 µM for 3KCA), was incubated with pooled hepatic microsomes prepared from rats treated with CYP inducers including MC, PB and DEX to assess the contributions of CYP1A/1B, CYP2B and CYP3A. The experiments were carried out in duplicate using procedures described previously.

To identify the individual CYP enzymes involved in the biotransformation of LCA (100 µM for MDCA and ILCA; 250 µM for 3KCA), a panel of antibodies prepared against individual CYP enzymes was used. Rabbit monospecific anti-CYP2C11 IgG, rabbit polyspecific anti-CYP2C IgG and rabbit polyspecific anti-CYP3A IgG was incubated at 1, 2.5 and 5.0 mg

IgG/mg of microsomal protein. Antibody and hepatic microsomes were allowed to preincubate for 30 min at room temperature and subsequently replenished with the usual buffer system. LCA (100 μM for MDCA and ILCA; 250 μM for 3KCA) hydroxylation was initiated at 37^0C with the addition of NADPH and the subsequent procedures were carried out as described above.

2.2.9 LCA assay validation

To validate the assay for LCA hydroxylation, metabolite stability, limit of detection (LOD), inter- and intra-assay variability, and extraction efficiency were determined. Hepatic microsomal samples prepared from untreated male Wistar rats were used for assay validation. Assay validation was primarily restricted to MDCA, ILCA and 3KCA, unless otherwise stated.

a)   Standard (calibration) curves

Various concentrations of calibration standards were included in each experiment in duplicate and treated in the same manner as test samples. Calibration standard mixtures were prepared at concentrations of 0.5, 2.5, 5, 25, 50 and 100 μM for all metabolites *i.e.* α-MCA, β-MCA, γ-MCA, MDCA, HDCA, UDCA, CDCA, 6KLCA, ILCA, and 3KCA were prepared. During initial experiments, it was observed that formation of MDCA, ILCA and 3KCA in hepatic microsomal incubations exceeded the range 0.5-100 μM (5-1,000 pmol/ml of reaction mixture) of the standard curve. Hence, stock calibration standards at concentrations of 0.1-3 mM (1,000-30,000 pmol/ml of reaction mixture) were prepared for MDCA, ILCA and 3KCA. The calibration curves were determined by plotting peak area ratios (PARs; AUC of metabolite /AUC of I.S.) obtained using LC/MS *versus* concentrations of individual analytes.

b)   Stability of analytes

Bench-top stability of metabolite standards was assessed with hepatic microsomes prepared from untreated male Wistar rats spiked with metabolite standards (MDCA, ILCA, 3KCA) at concentrations of 0.1, 1 and 4 mM (1000, 10,000 and 40,000 pmol/ml of reaction mixture, respectively) in the absence of NADPH. These spiked microsomal samples were left on the bench-top overnight (24 h at room temperature at approximately 20^0C) and analyzed the next day. The relative stability of each analyte was determined by comparing the PARs of

64

MDCA, ILCA and 3KCA with the PARs of freshly prepared reference standards of the same concentrations, in the absence of hepatic microsomes. The freshly prepared reference standards were considered to be 100% stable. The stability was measured as follows:

$$\text{Stability of Sample} = (\text{PAR sample}/\text{PAR reference standard}) \times 100$$

The analytes were considered 'stable' if the measured PARs were within ± 10% of the reference PARs.

c) Limit of detection (LOD)

To determine the limit of detection, standard mixtures (MDCA, ILCA and 3KCA; n = 5) at concentrations of 25, 5, 2.5 and 0.5 pmol/ml of reaction mixture were prepared. The PARs of the metabolite standards were calculated. To determine the inherent noise in the assay, peaks occurring with the same retention times as authentic standards were quantified. LOD (defined as the smallest amount of analyte that can be detected with a corresponding peak area three times greater than that of the noise peak areas) was identified from the calculated results.

d) Variability of the assay

The reproducibility of the assay was determined by evaluating inter- and intra-assay variability (coefficient of variation, C.V.) for the following metabolites, MDCA, ILCA and 3KCA. Six sets of calibration curves were analyzed on 6 separate days (inter-assay) and on the same day (intra-assay). The reproducibility of the assay (C.V.) was determined from the variance observed for the mean of the replicates and a variability of < 20% for inter-assay and < 10% for intra-assay, was considered to be acceptable.

e)   Extraction recovery

The percent recovery of metabolite standards from the hepatic microsomal reaction mixture was determined. Metabolite concentrations of 0.5 to 100 µM for minor metabolites (β-MCA, γ-MCA, UDCA and 6KLCA) and 0.5 mM to 4 mM for major metabolites (MDCA, ILCA and 3KCA) were used. Two sets of samples, the non-extracted samples and the extracted samples, were prepared in duplicate. In the extracted samples, analytes were extracted twice by a liquid-liquid double-extraction procedure using dichloromethane: isopropanol (80:20), as outlined in Fig. 2.1. The choice of the extraction solvent mixture was taken from Stedman et al., (2004). The non-extracted samples containing the internal standard were prepared in mobile phase and injected directly onto the LC. The extraction recovery was determined as follows-

% Extraction recovery = (PARs of extracted samples from hepatic microsomal mixture / PARs of non-extracted samples) × 100

2.2.10 LCA microsomal assay optimization

Hepatic microsomal LCA biotransformation was analyzed as a function of incubation time, protein concentration and substrate concentration. Hepatic microsomal samples prepared from untreated male Wistar rats were used for optimization of the assay. Assay optimization was primarily restricted to MDCA, ILCA and 3KCA, unless otherwise stated.

a)   Time of incubation

LCA was incubated with a reaction mixture containing 1 mg/ml microsomal protein for different periods of time (1, 5, 10, 15, 20, 30, 45 and 60 min) and metabolites were extracted and analyzed as described in the **LCA microsomal assay** section. PARs of metabolite

formation were plotted for the metabolites MDCA, ILCA and 3KCA as a function of time. An optimal time for metabolite formation was selected from the linear portion of the plotted curves.

b)   Protein concentration

LCA was incubated for 30 min. in a reaction mixture containing different final microsomal protein concentrations of 1.867 mg/ml, 1 mg/ml, 0.75 mg/ml, 0.5 mg/ml and 0.25 mg/ml. Metabolites were extracted and analyzed as described in **LCA microsomal assay** section. PARs of the metabolite were plotted for MDCA, ILCA and 3KCA as a function of protein concentration. An optimal microsomal protein concentration was selected from the linear portion of the plotted curves.

c)   Saturating substrate concentration

LCA was incubated with a reaction mixture containing 0.5 mg/ml of microsomal protein, at various final concentrations of 0.5-300 µM for 30 min. Reactions were initiated using NADPH. Metabolites were extracted and analyzed as described in **LCA microsomal assay** section. PARs of metabolites MDCA, ILCA and 3KCA along with 6KLCA, UDCA, β-MCA were plotted as a function of substrate concentration. Metabolite formation was analyzed and the saturating concentration of LCA for each of the identified metabolites was determined.

3. RESULTS

3.1 LC/MS methodology and LCA microsomal assay

3.1.1 LC/MS identification and separation of bile acid standards

All bile acid standards under consideration gave negative ion mass spectra, confirming that the ions are mainly produced by deprotonation, *i.e* by formation of $[M-H]^-$ ions. Collision induced dissociation of these unconjugated bile acids was not possible and hence structure elucidation by analysis of fragmentation patterns using LC/MS/MS could not be carried out. Following the analytical work described by Stedman et al. (2004) and building on initial experimentation, an LC/MS assay system was developed as described in the **MATERIALS AND METHODS** section. Fig. 2.2 shows the separation of a diluted mixture of bile acid standards (each consisting of 20 μM) prepared from a stock solution of 1 mg/ml. The bile acids were eluted according to their polarity and appeared in different ion channels according to their m/z of 411, 407, 391, 389, 375, and 373 respectively. The retention time of α-MCA was the lowest, suggesting that it was the most polar bile acid. LCA was eluted with the highest retention time, and was the most non-polar bile acid with a single hydroxy group. The retention times for γ-MCA, UDCA and 6KLCA were approximately the same. Effective separation of four bile acids with the same m/z of 391 was seen, with MDCA eluting first, followed by UDCA, HDCA and CDCA, respectively. Similar retention times were also observed for CDCA and ILCA. Baseline separation of the isomers, α-MCA and β-MCA, was not obtained but they could be easily distinguished by spiking. In contrast, baseline separation of the isomers ILCA and LCA was very distinct. The internal standard, cholic-2,2,4,4-d₄ acid had a distinct m/z of 411 and did not interfere with any of the other bile acids (See Fig 2.2).

Separation of a standard mixture of all known LCA metabolites
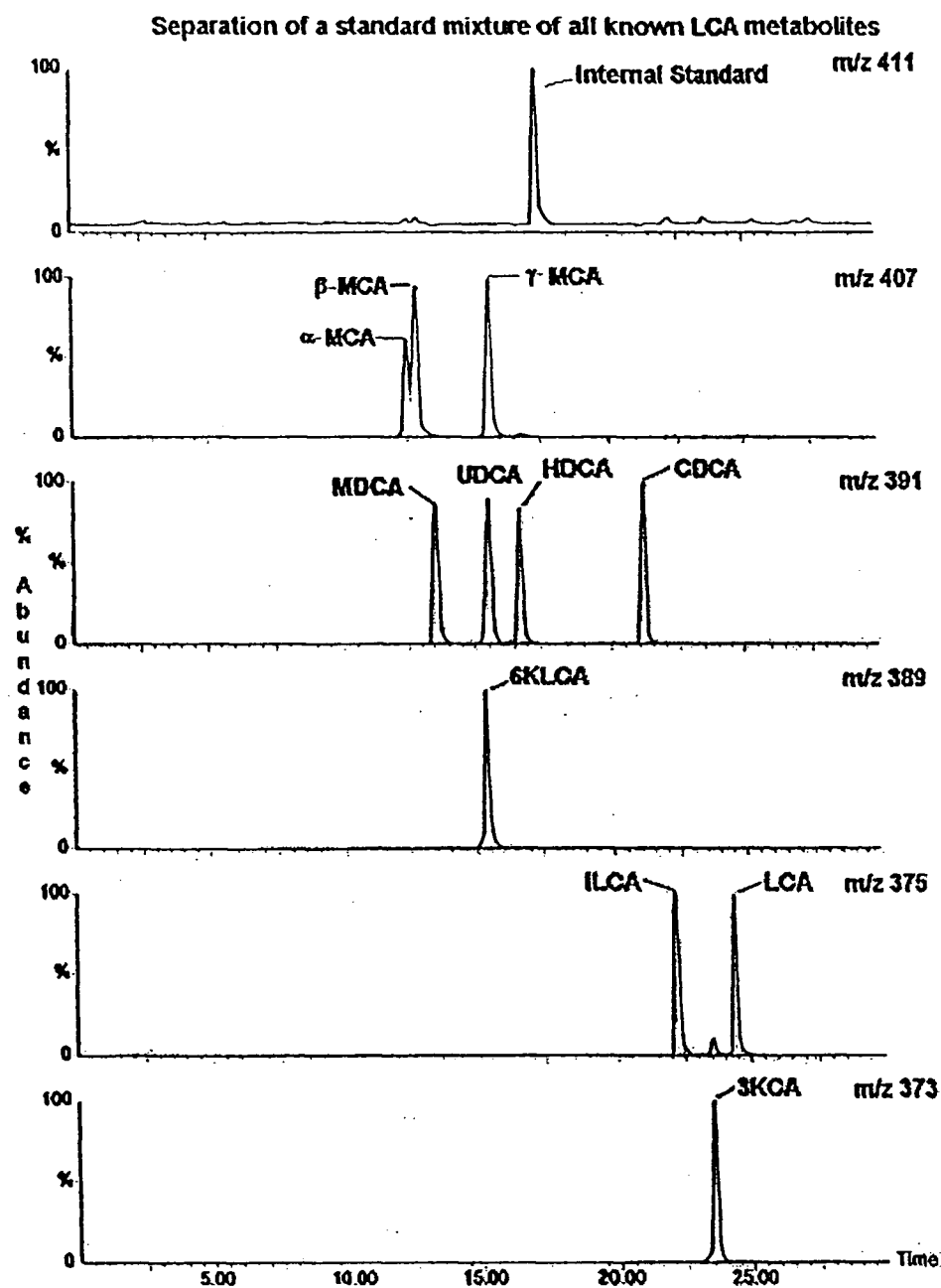
Fig. 2.2. Identification and separation of bile acid standards.

Representative chromatogram showing resolution of a mixture of authentic metabolite standards (20 µM each). Metabolite separation was carried out using LC/MS parameters as described in the **MATERIALS AND METHODS** section. Metabolite identification was performed by co-chromatography and spiking with authentic standards.

69

2.2.2 LCA assay validation

a) Standard (calibration) curves

The calibration curves of authentic metabolite standards are shown in Fig. 2.3a and 2.3b. The response obtained by LC/MS detection for the minor (β-MCA, UDCA, 6KLCA) and major metabolites (MDCA, ILCA, 3KCA) was linear with respect to the concentration ranges chosen for the minor (0.5 –100 µM or 5-1000 pmol/ml of reaction mixture) and major (0.1 mM-3 mM or 1,000-30,000 pmol/ml of reaction mixture) metabolite standards, respectively. The mean slope values for the metabolite standards are summarized in Table 2.1.
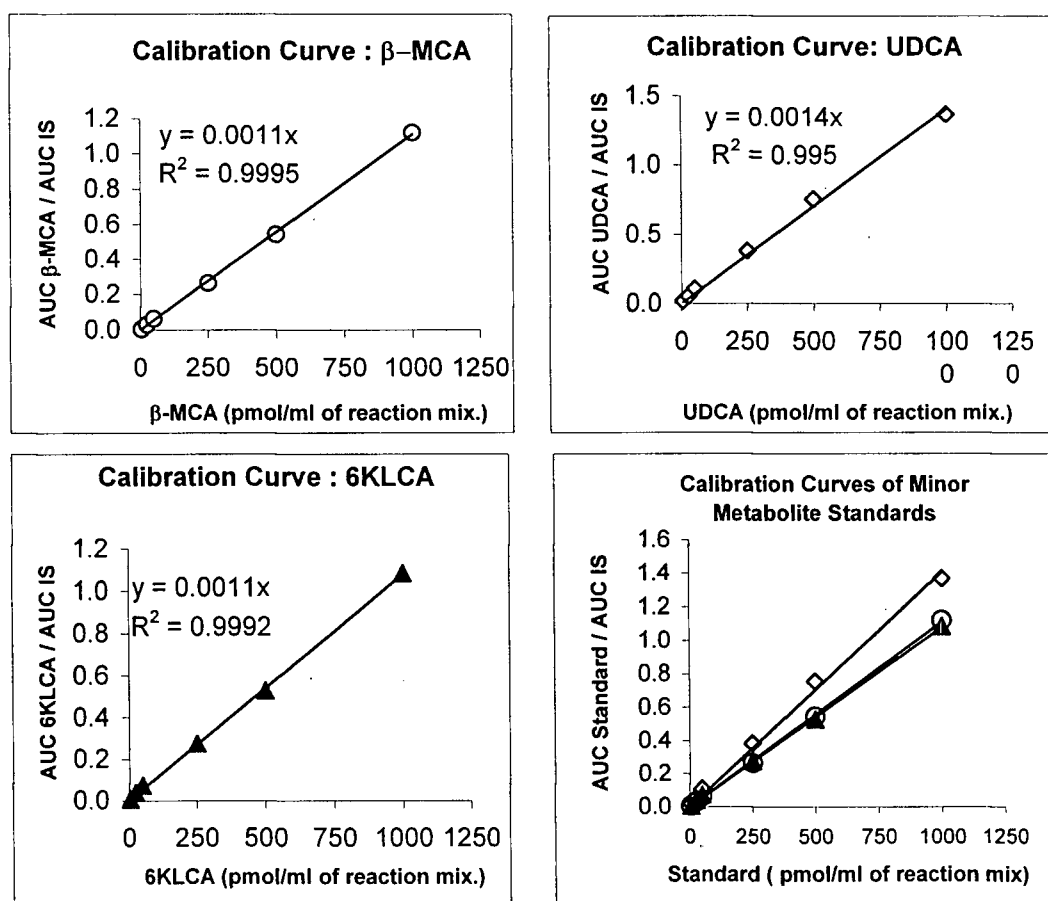
Fig. 2.3a Representative calibration curves for minor metabolites

The figure shows the calibration curves for the minor metabolites β-MCA(-o-), UDCA(-◊-) and 6KLCA(-▲-). The response obtained by LC/MS detection was linear over the range of concentration of 0.5 –100 µM (5-1000 pmol/ml of reaction mixture) chosen for the minor metabolites. The y intercept for all the standard curves passed through the origin.
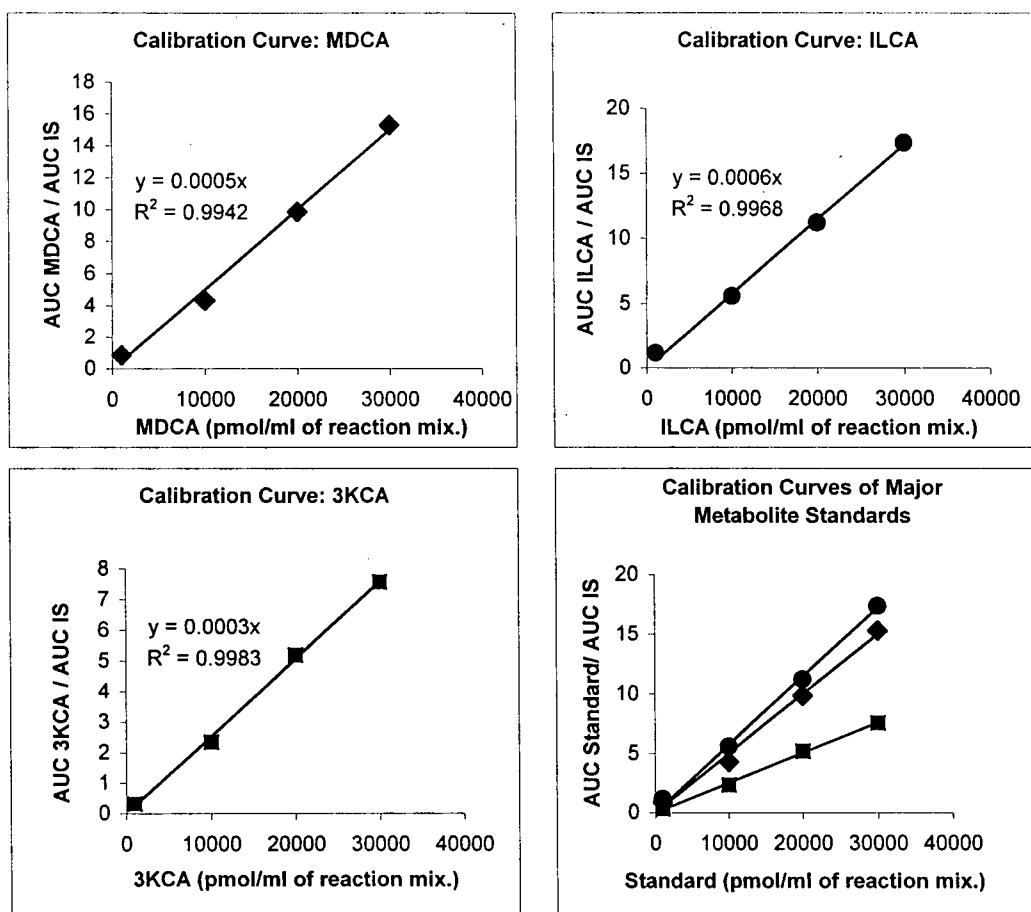
Fig.2.3b Representative calibration curves for MDCA, ILCA and 3KCA.

The figure shows the calibration curves for the minor metabolites MDCA (-♦-), ILCA(-●-), and 3KCA(-■-). The response by LC/MS detection was linear over the range of concentration of 0.1 mM-3 mM (1,000-30,000 pmol/ml of reaction mixture) chosen for the metabolites. The y intercept for all the standard curves passed through the origin.

Table 2.1
Mean slopes of minor and major LCA metabolite standards

Metabolite Standard	β-MCA	UDCA	6KLCA	MDCA	ILCA	3KCA
n=6 Mean Slope ± S.E.M	0.0017 ± 0.00003	0.0014 ± 0.00012	0.0011 ± 0.00001	0.00048 ± 0.00002	0.00055 ± 0.00004	0.00028 ± 0.00001
Conc. Range in stock soln.	0.5 μM- 100 μM	0.5 μM- 100 μM	0.5 μM- 100 μM	0.1 mM- 3 mM	0.1 mM- 3 mM	0.1 mM- 3 mM

71

b)   Stability of analytes

Bench-top stability of metabolite standards (MDCA, ILCA and 3KCA) was assessed in the concentration range of 0.1- 4 mM as described previously. The stability values calculated are shown in Table 2.2 below. Setting the stability of the reference standards at 100%, it can be seen that the analytes were stable in the presence of rat liver microsomes after 24 h at room temperature (approximately 20^0C) and were within ± 10% of the PARs of the reference samples.

Table 2.2
Stability of MDCA, ILCA and 3KCA in presence of rat liver microsomes

Concentration in mM	Stability of sample expressed as (PAR Sample / PAR Reference standard) x 100		
	MDCA	ILCA	3KCA
0.1	103	95.9	92.2
1	101	94.1	91.7
4	97.9	92.4	96.1

c)   Limit of detection (LOD)

The LOD was described as mentioned in the **MATERIALS AND METHODS** section. The LOD for MDCA and ILCA was 2.5 pmol/ml of reaction mixture. The LOD for 3KCA was 5 pmol/ml.

d)   Variability of the assay

The reproducibility of the assay was determined by evaluating inter- and intra-assay variability. The reproducibility (in terms of coefficient of variation, C.V.) of the assay for MDCA, ILCA and 3KCA was calculated as described previously. The intra-assay and inter-assay variability values for the major metabolites are listed in Tables 2.3 and 2.4, respectively. The inter-assay variability for the metabolites in the concentration range of the standard curve was less than 20% (Table 2.3). Similarly, the intra-assay variability for the metabolites in the concentration range of the standard curve was less than 10% (See Table 2.4). Limit of

72

quantitation (LOQ) is the smallest peak area of the analyte that could be measured with a C.V. of less than 15%. Based on the values shown in Table 2.4, it could be suggested that the LOQ values for MDCA, ILCA and 3KCA will be between the LOD values mentioned above and 1,000 pmol/ml of reaction mixture.

Table 2.3
Inter-assay variability (n = 6)

Analyte	Concentration of the analyte			
mM (stock solution)	0.5	1	2	3
pmol/ml (reaction mixture)	5,000	10,000	20,000	30,000
C.V.%				
MDCA	11.6	9.5	11.5	14.6
ILCA	4.2	12.8	11.8	14.2
3KCA	16.1	12.0	11.0	10.2

The inter-assay variability of MDCA, ILCA and 3KCA was assessed at the concentrations mentioned above. The C.V. (%) was observed to be less than 20%.

Table 2.4
Intra-assay variability (n = 6)

Analyte	Concentration of analyte			
mM (stock solution)	0.1	1	2	3
pmol/ml (reaction mixture)	1,000	10,000	20,000	30,000
C.V. %				
MDCA	2.4	5.6	6.1	3.8
ILCA	4.2	5.4	5.4	3.3
3KCA	4.7	5.2	6.0	4.6

The intra-assay variability of MDCA, ILCA and 3KCA was assessed at the concentrations mentioned above. The C.V. (%) was observed to be less than 10%.

d) Extraction recovery

Extraction recovery was determined as mentioned in the **MATERIALS AND METHODS** section. The extraction efficiency of all metabolites, except 3KCA, was between 90-100%. The percent recovery of 3KCA was found to be approximately 60%. The reason for

the lower extraction recovery of 3KCA is not known. Other extraction procedures to enhance the recovery of 3KCA were not attempted. The extraction efficiency of the internal standard was calculated independently and was found to be 100%.

3.1.3 LCA assay and identification of metabolites

LCA incubation procedures were carried out and metabolites were analyzed as described in the **MATERIALS AND METHODS** section. A representative chromatogram of LCA and its metabolites is illustrated in Fig. 2.4. The figure shows the separation of LCA metabolites from an extracted reaction mixture (final LCA concentration of 50 μM, incubation time of 30 min, protein concentration of 0.5 mg/ml). Effective separation of all LCA metabolites was achieved. Metabolite identification was carried out by spiking with authentic standards and co-chromatographic comparison. Of the authentic standards under consideration, β-MCA, MDCA, ILCA, UDCA, 6KLCA, and 3KCA were identified to be LCA metabolites produced by liver microsomes from male Wistar rats (See Fig. 2.4). On the other hand, no peaks were found corresponding to the retention times for α-MCA, γ-MCA. Thus, it is unlikely that α-MCA, γ-MCA are LCA metabolites. PARs of each metabolite were calculated. MDCA, ILCA and 3KCA were observed to be major metabolites. β-MCA, UDCA and 6KLCA were identified as minor metabolites. In addition, five other peaks (M-1, m/z 407; M-2, m/z 407; M-3, m/z 391; M-4, m/z 391 and M-5, m/z 389) were also characterized as minor metabolites but remained unidentified. With respect to the retention times observed, it is possible that M-4 could be HDCA.

Separation and identification of LCA metabolites from an incubated sample
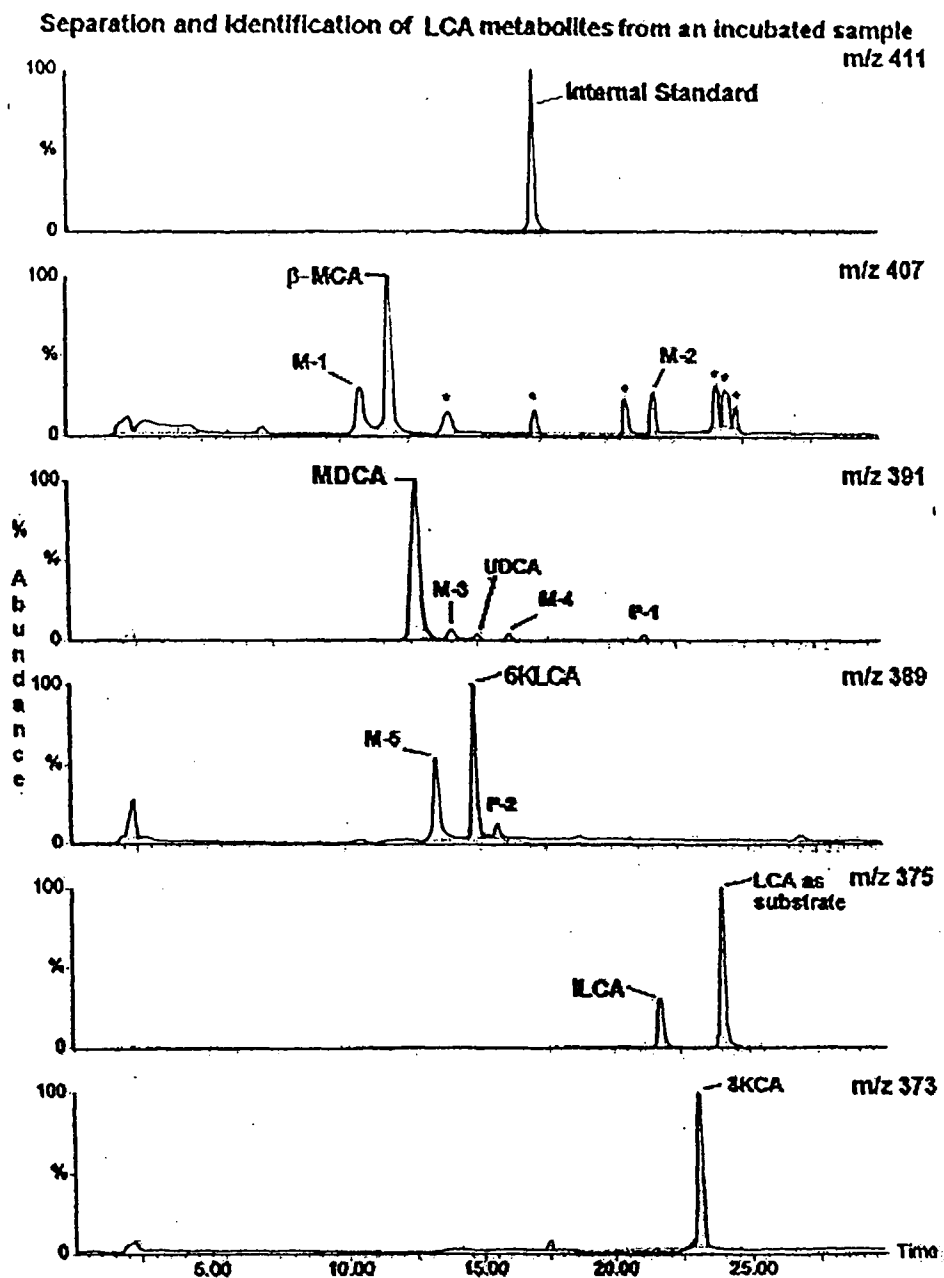
Fig. 2.4 Identification and separation of LCA metabolites from an incubated sample.

Representative chromatogram showing separation of LCA metabolites from an extracted reaction mixture (final LCA concentration 50 µM, incubation time 30 min, protein concentration 0.5 mg/ml). Metabolite separation was carried out using LC/MS as described in the **MATERIALS AND METHODS** section. Metabolite identification was performed by co-chromatography and spiking with authentic standards. M-1 to M-5 indicate peaks of unidentified metabolites.

• indicates peaks also obtained in the blank and the controls. It is possible that M-4 could be hyodeoxycholic acid (HDCA).

Two additional small peaks, named P-1 (m/z 391) and P-2 (m/z 389), were observed to increase as the substrate concentration increased suggesting that they could be metabolites of LCA. Of these, P-1 was observed to have the same retention time as CDCA (m/z 391, See Fig. 2.2 and 2.4). Because CDCA was previously reported to be a metabolite of LCA in rat, it was important to establish the identity of P-1 (Zimniak et al., 1989). To resolve this issue, control samples were prepared with increasing substrate concentration in the absence of microsomes. The PARs of P-1 and P-2 were plotted *versus* increasing LCA concentration (10 μM–50 μM final concentration). It was observed that as the concentration of LCA increased, the PARs of P-1 and P-2 increased in a linear manner (See Fig. 2.5). This was an indication that P-1 and P-2 were not metabolite peaks but were probably LCA contaminants. Thus, it is unlikely that CDCA was a LCA metabolite in this assay.

Remaining peaks (represented by '*') did not interfere with LCA, its metabolites or the internal standard but also appreared in the blank and the control samples not containing either NADPH, microsomes or the substrate. Thus, these were not considered to be LCA metabolites.
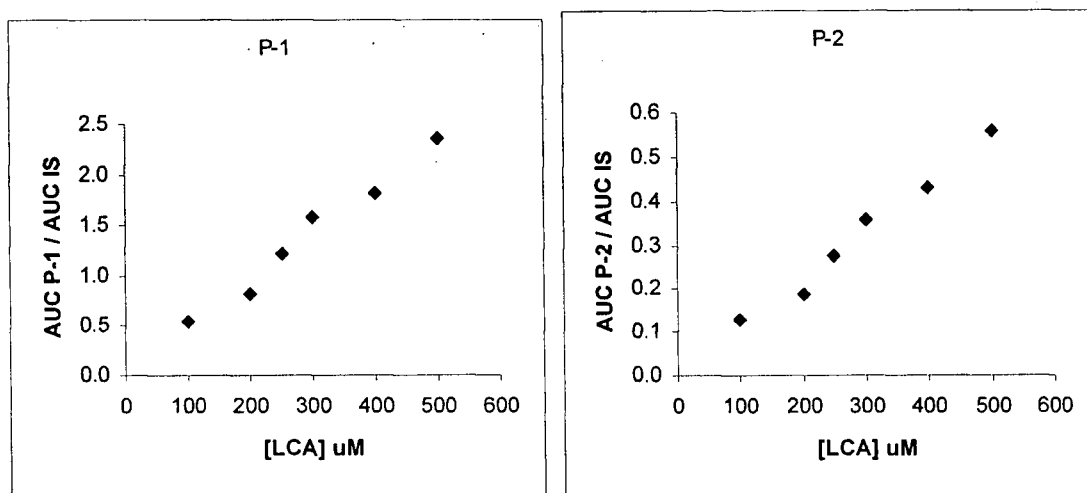
Fig. 2.5 Characterization of P-1 and P-2

3.1.4 LCA assay optimization

a) Time of incubation

LCA (100 μM) was incubated in the reaction mixture (as described in **MATERIALS AND METHODS**) containing 1 mg/ml microsomal protein at timed intervals of 1, 5, 10, 15, 20, 30, 45 and 60 min, respectively. Individual metabolite formation curves were plotted as PARs of metabolite formed *versus* time in min. Metabolite formation curves for MDCA, ILCA and 3KCA (shown in Fig. 2.6) and other metabolites were linear with respect to time in the range of 0 to 30 min. Hence, a 30 min incubation time was considered optimal for further experiments.
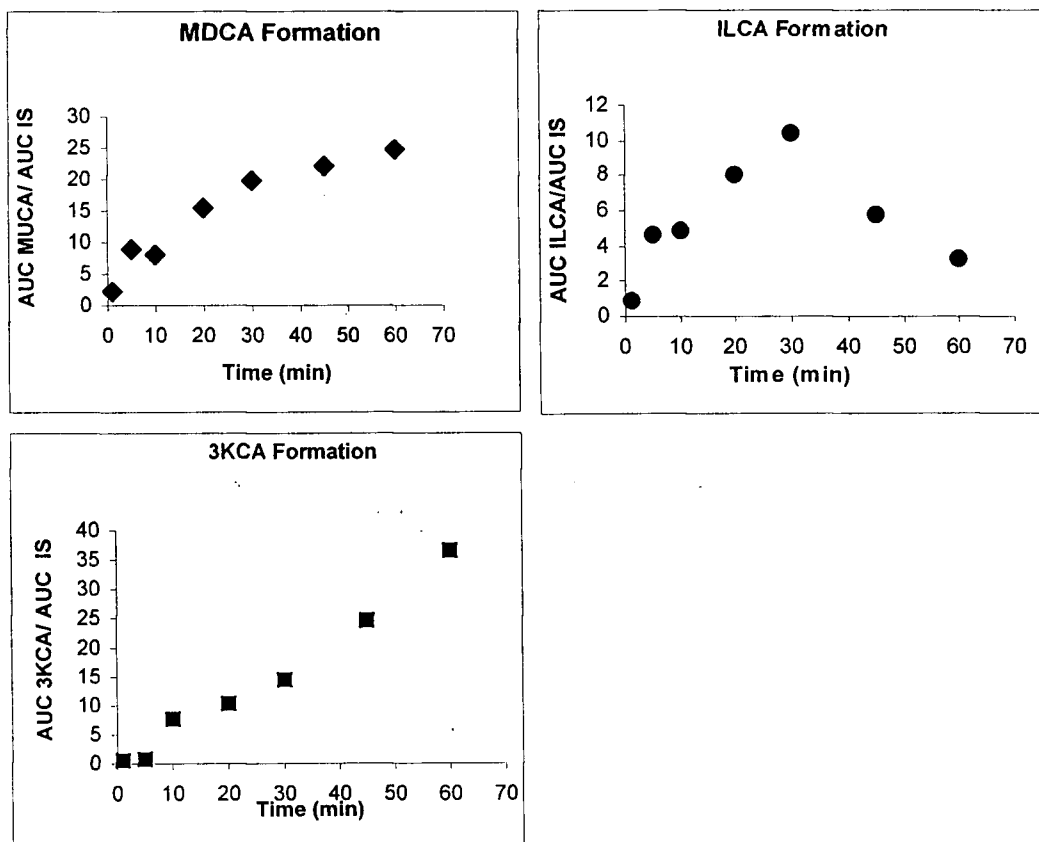
Fig. 2.6 Time dependent formation of major LCA metabolites.

LCA (100 μM) was incubated with a reaction mixture containing 1mg/ml of microsomal protein, for 1, 5, 10, 15, 20, 30, 45 and 60 min, respectively. Reactions were initiated with 1mM NADPH. Metabolite formation curves were plotted as shown above. Metabolite formation curves were linear at 30 min for MDCA, ILCA and 3KCA formation and was considered to be optimal and used for further experiments.

b) Protein concentration

LCA was incubated in the reaction mixture as described in *Materials and Methods* at different final protein concentrations of 1.867 mg/ml, 1 mg/ml, 0.75 mg/ml, 0.5 mg/ml and 0.25 mg/ml for 30 min. Metabolite formation curves were plotted with PARs of metabolite formed versus protein concentration. Metabolite formation was linear in the range of 0.25-0.75 mg/ml for MDCA, ILCA and 3KCA (Fig. 2.7). A final protein concentration of 0.5 mg/ml in the reaction mixture was used in further experiments.
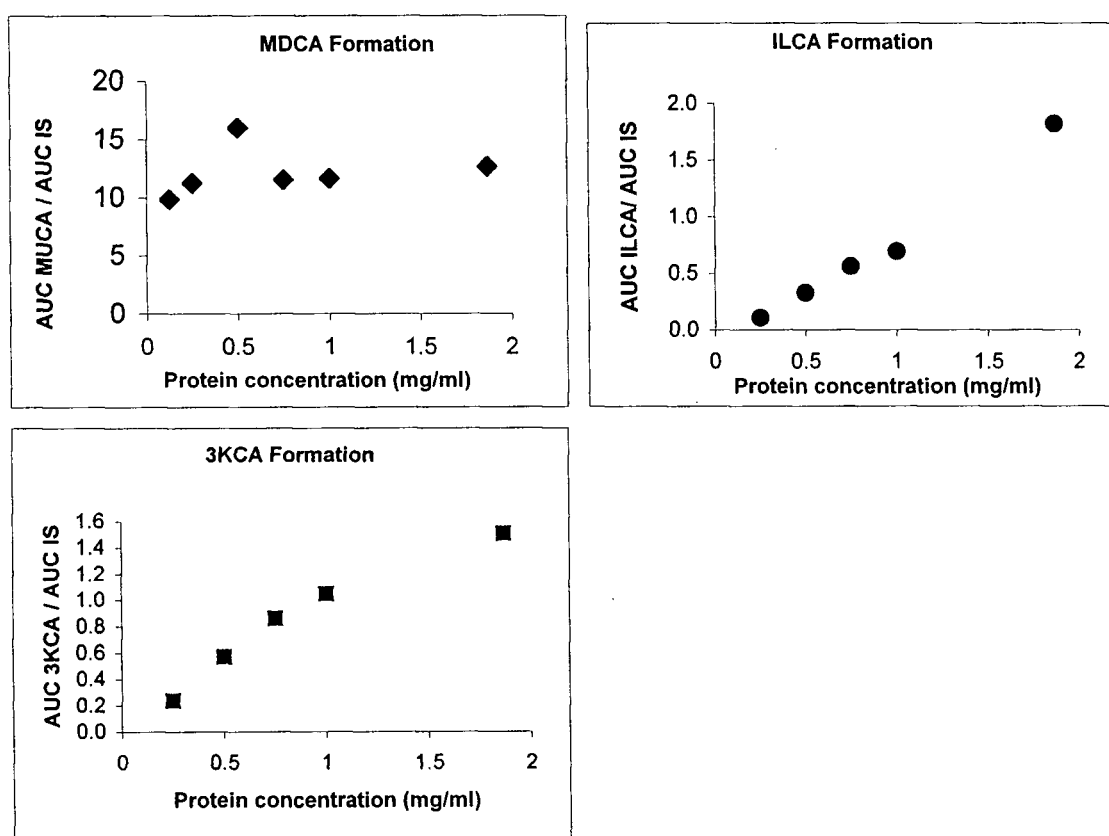
Fig. 2.7 Protein dependent formation of major LCA metabolites.

LCA (100 μM) was incubated with a reaction mixture containing 1.867 mg/ml, 1 mg/ml, 0.75 mg/ml, 0.5 mg/ml and 0.25 mg/ml of microsomal protein, respectively at incubation time of 30 min. Reactions were initiated with 1mM NADPH. Metabolite formation curves were plotted as shown above. Metabolite formation curves for MDCA, ILCA and 3KCA were linear at 0.5 mg/ml of protein, which was considered optimal and used in further experiments.

c) Saturating substrate concentration

Various LCA concentrations in the range of 0.5 to 300 μM (see Fig. 2.8) were used in the reaction mixture and analysis of metabolite formation was carried out as described earlier. Rate of formation of MDCA, UDCA, 6KLCA, ILCA and 3KCA was monitored. At all substrate concentrations tested, MDCA, 3KCA and ILCA were observed to be the major metabolites, and 6KLCA and UDCA were identified as minor metabolites. Metabolite formation increased linearly with increasing LCA concentration initially and then remained constant. A saturating substrate concentration of 100 μM was observed for MDCA, ILCA, and the minor metabolite UDCA. The saturating substrate concentrations for 6KLCA and 3KCA were observed to be 50 μM and 250 μM, respectively. Interestingly, the formation of β-MCA was linear to 10 μM but decreased rapidly thereafter, suggesting possible product inhibition or formation of secondary metabolites. Metabolite formation curves for the metabolites, β-MCA, MDCA, UDCA, 6KLCA, ILCA and 3KCA, are shown in Fig. 2.8.

In summary, LCA (50 μM for 6KLCA; 100 μM for MDCA and ILCA; and 250 μM for 3KCA) was incubated with 0.5 mg/ml of protein for 30 min. The assay was carried out in a reaction mixture consisting of 1 mM NADPH and 46.5 mM potassium phosphate buffer at pH 7.4.
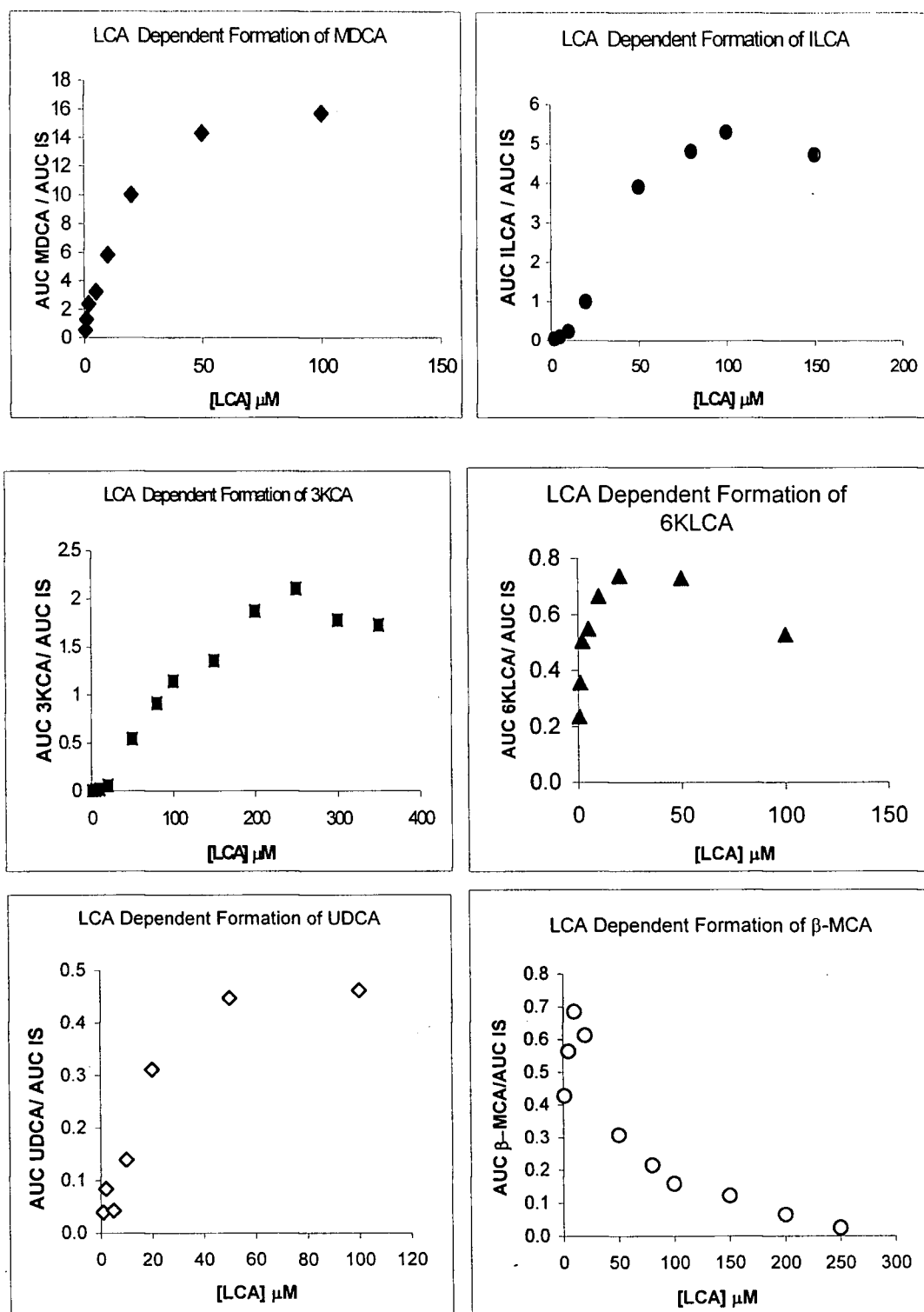
Fig. 2.8 LCA dependent formation of MDCA, ILCA, 3KCA UDCA, 6KLCA and β-MCA.

LCA (at saturating concentration of 50 μM for 6KLCA; 100 μM for MDCA and ILCA; and 250 μM for 3KCA) incubated with 0.5 mg/ml of protein for 30 min in a reaction mixture consisting of 1 mM NADPH and 46.5 mM potassium phosphate buffer at pH 7.4 were identified as optimal conditions to study LCA biotransformation.

3.2 Reaction kinetics

Metabolite formation for MDCA, 6KLCA, UDCA, 3KCA and ILCA followed typical Michelis-Menten (M-M) kinetics (Fig. 2.9). Kinetic constants (Km and Vmax) were calculated for the metabolites from triplicate determinations and are summarized in Table 2.5.
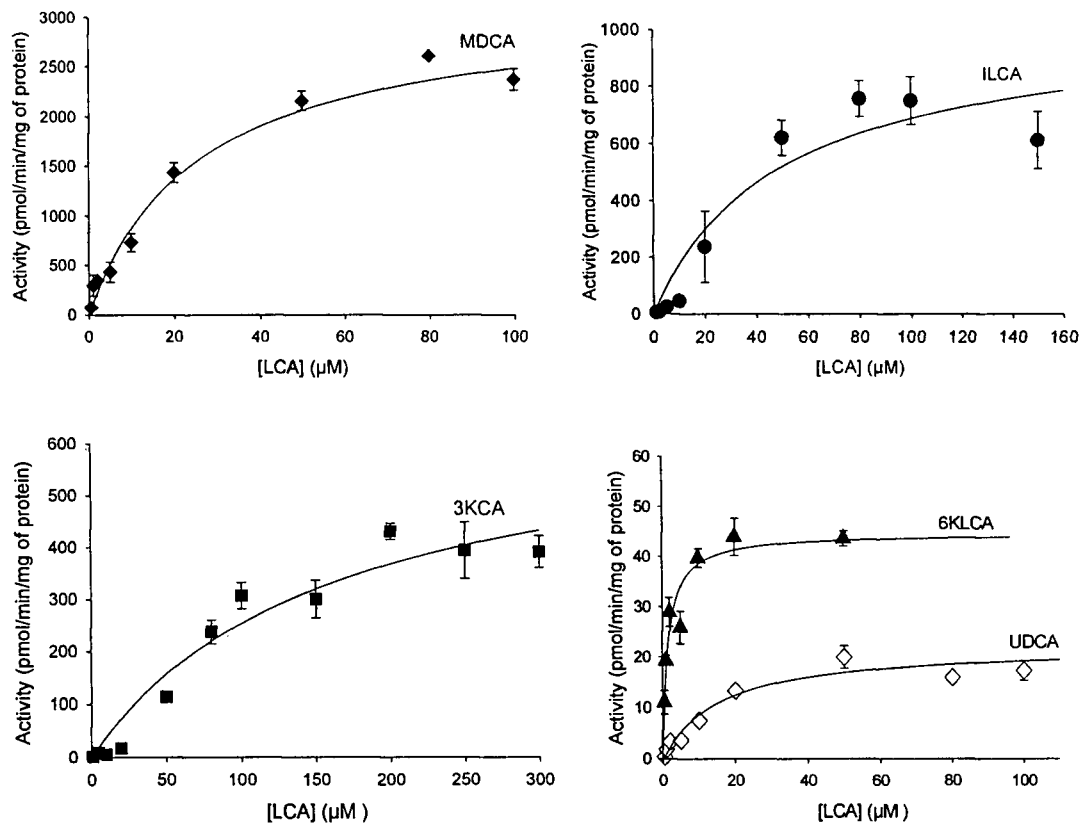
Fig. 2.9 Michaelis-Menten kinetics of MDCA, ILCA, 3KCA, 6KLCA and UDCA

Activity is plotted as a function of substrate concentration for MDCA, ILCA, 3KCA, 6KLCA and UDCA. The graphs were plotted from triplicate determinations.

Table 2.5
Kinetic constants for LCA metabolites.

Metabolite	Vmax* (pmol/min/mg of protein)	Km* (μM)
MDCA	2790 ± 114	19.9 ± 2.80
ILCA	1020 ± 175	48.9 ± 21.3
3KCA	668 ± 98.1	163 ± 49.6
UDCA	22.4 ± 1.70	15.3 ± 3.70
6KLCA	44.5 ± 2.10	1.60 ± 0.300

*Vmax and Km values calculated from triplicate determinations.

The reaction velocity observed for MDCA (2793.1 pmol/min/mg of protein) was the highest among the metabolites, followed by ILCA, 3KCA, 6KLCA and UDCA. The Km value for 6KLCA (1.6 μM) was the lowest among the metabolites. The highest Km value (162.6 μM) was observed for 3KCA.

3.3 Biotransformation of LCA in different strains of rats

The method developed was used to compare the metabolism of LCA in male Long-Evans, Wistar and Sprague-Dawley rats. The amount of metabolite formed in each case is summarized in Table 2.6.

Table 2.6
LCA metabolism in different strains of rat

	Activity in pmol/min/mg of protein in reaction mixture		
Untreated Strain	**MDCA**	**ILCA**	**3KCA**
Male Long-Evans	2900	803	512
Male Wistar	2590	444	270
Male Sprague-Dawley	2170	621	240

Average values obtained from two sets of experiments are listed in Table 2.6.

It can be seen from the above table that metabolite formation in male Long-Evans rats was higher (1.2-2 fold) than in male Wistar and Sprague-Dawley rats for MDCA, ILCA and 3KCA, respectively.

3.4   Identification of CYP enzymes in LCA biotransformation

To assess the involvement of CYP in LCA metabolite formation, the assay was performed in the absence of NADPH, with boiled microsomes, or following carbon monoxide treatment. Metabolite formation was not observed in any of these cases.

3.4.1   Effect of CYP inducers on LCA biotransformation

Metabolism of LCA was studied using hepatic microsomes prepared from Long-Evans rats treated with CYP inducers in order to identify the CYP enzymes involved. LCA at two different saturating substrate concentrations (100 μM for MDCA and ILCA; 250 μM for 3KCA) was incubated with pooled hepatic microsomes prepared from rats treated with MC, PB and DEX representing the involvement of CYP1A/1B, CYP2B and CYP3A, respectively. The experiments were carried out using optimal assay conditions described in the **RESULTS**. The results are summarized in Table 2.7.

The formation of MDCA, (a 6β-hydroxylated metabolite), and ILCA (a 3β-isomer of LCA) in hepatic microsomes from MC-treated male rats was decreased by 60% and 50%, respectively, compared to peanut oil treated male rat liver microsomes used as control.

The formation of MDCA and ILCA in hepatic microsomes from PB-treated male rats was suppressed 80% and 70%, respectively, compared to control rats. However, 3KCA formation was not altered as much. In PB-treated female rats, the metabolism of MDCA, ILCA and 3KCA was not altered compared to untreated female rat liver microsomes used as control.

In DEX-treated male and female rats, the formation of MDCA was suppressed 35% whereas the formation of 3KCA was increased 2.7-and 2.2-fold, respectively. ILCA formation was not altered by DEX treatment.

A comparison of data obtained with hepatic microsomes from male and female control rats indicated increased formation of the three major metabolites (MDCA, 2.5-fold; ILCA, 39-fold; and 3KCA, 1.2-fold) in male compared to female rats. This data has been summarized in Table 2.7.

<div align="center">

Table 2.7
Effect of inducers on formation of major metabolites in LCA biotransformation

</div>

<div align="center">

Activity in pmol/min/mg of protein in reaction mixture

</div>

	MDCA	ILCA	3KCA
MC male	1010 ± 171	403 ± 70.0	486 ± 117
PB male	633 ± 150	231 ± 55.0	394 ± 106
DEX male†	1810	765	1380
Control male	2900 ± 302	803 ± 83.0	512 ± 49.7
PB female†	1250	23.2	585
DEX female	781 ± 122	33.2 ± 10.0	1050 ± 169
Control female	1220 ± 182	25.3 ± 1.40	461 ± 19.0

Incubations were carried out at two saturating substrate concentrations, 100 μM LCA (for MDCA and ILCA) and 250 μM (for 3KCA), respectively, with optimal assay conditions as discussed in the **RESULTS**. Metabolite formation using inducer treated male and female Long-Evans rat liver microsomes was compared with peanut oil treated male and untreated female rat liver microsomes used as controls. † Values based on only 2 sets of experiments.

3.4.2 CYP inhibition studies

To identify the individual CYP enzymes involved in biotransformation of LCA, a panel of antibodies prepared against individual CYP enzymes was used. Rabbit monospecific anti-CYP2C11 IgG, rabbit polyspecific anti-CYP2C IgGs and rabbit polyspecific anti-CYP3A IgG were incubated at 1, 2.5 and 5.0 mg IgG/mg of microsomal protein, allowed to preincubate for 30 min at room temperature and subsequently replenished with the usual buffer system. LCA hydroxylation was initiated at 37^0C with NADPH and the procedures were carried out as described in the **MATERIALS AND METHODS** section.

MDCA and 3KCA formation (panels a and b; Fig. 2.10) was inhibited 50% by polyspecific anti-CYP2C IgG and 40% by polyspecific anti-CYP3A IgG at 5 mg IgG/mg protein as compared to the control IgG. ILCA and the minor unidentified metabolite M-2 formation (panels c and d, respectively) were inhibited 30% by polyspecific anti-CYP3A IgG at 5 mg IgG/mg protein but were uninhibited by polyspecific anti-CYP2C IgG. Polyspecific anti-CYP3A antibody inhibited M-4 and M-5 formation (panels e and f) by more than 50% at all IgG concentrations (5, 2.5 and 1 mg IgG/mg of protein) used in the assay. CYP2C11 was expected to be involved in metabolite formation based on the inducer treated studies, but monospecific anti-CYP2C11 IgG was not effective in inhibiting formation of any of the metabolites. UDCA formation (panel g) was inhibited 20% by polyspecific anti-CYP3A IgG. However, increased formation of UDCA and M-4 (approximately 50 to 100% increase) by preincubation with anti-CYP2C and anti-CYP2C11 IgG was observed. All these results are shown in Fig. 2.10.

a-CYP dependent MDCA formation

b-CYP dependent 3KCA formation

c-CYP dependent ILCA formation

d-CYP dependent M-2 formation

e-CYP dependent HDCA/ M-4 formation

f-CYP dependent M-5 formation

g-CYP dependent UDCA formation
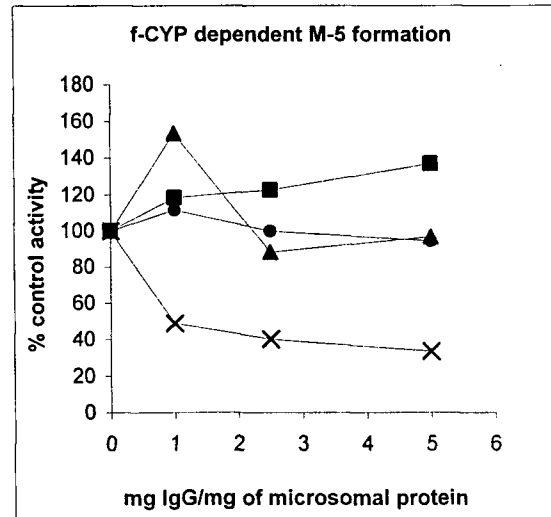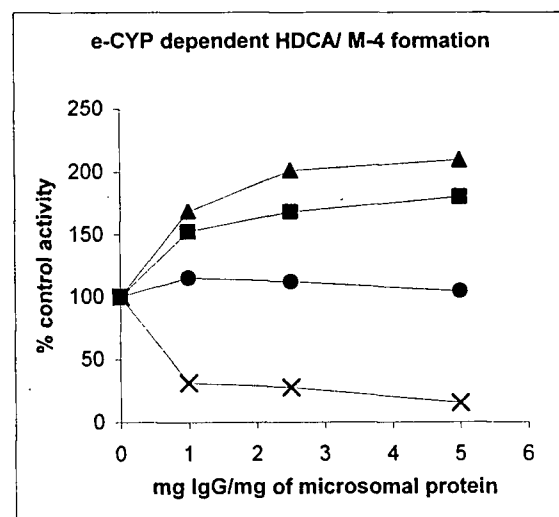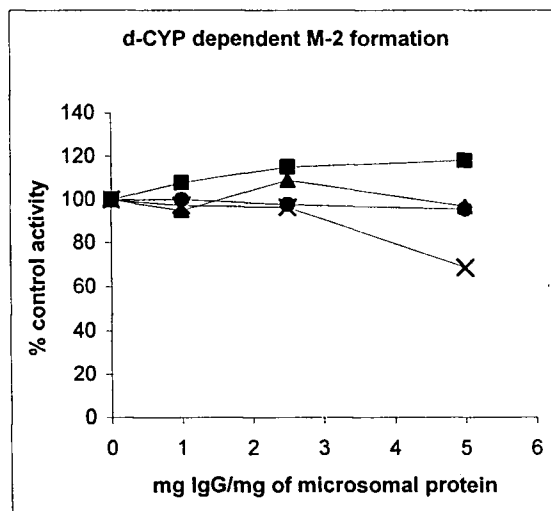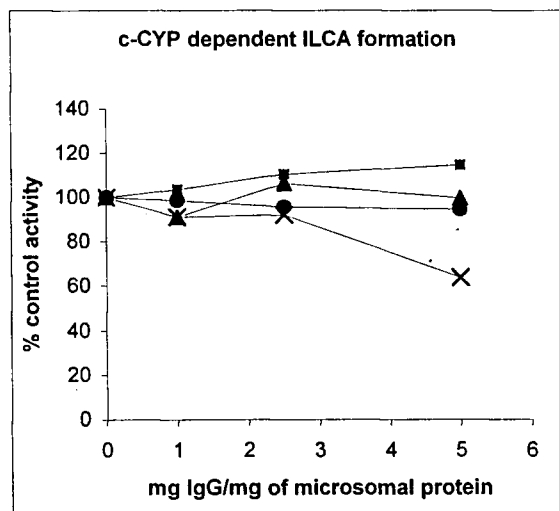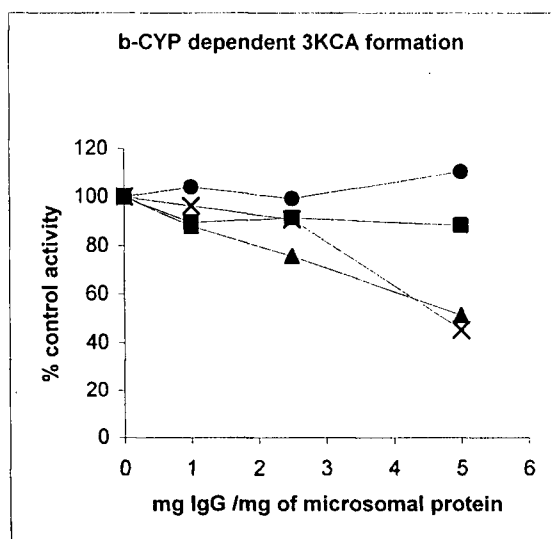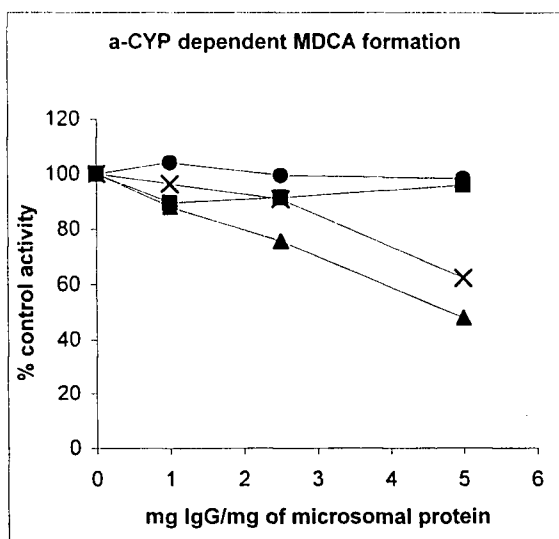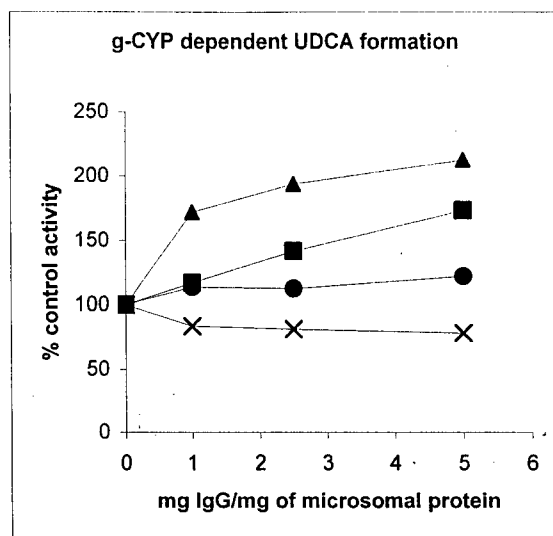
Fig. 2.10 CYP dependent antibody inhibition

Antibody inhibition experiments were carried out using liver microsomes from untreated male Long-Evans rats. LCA was incubated (as described in the **MATERIALS AND METHODS** section) in presence of rabbit control IgG (–•–), monospecific anti-rat CYP2C11 IgG (–■–), polyspecific anti-rat CYP3A IgG (–×–) and polyspecific anti-rat CYP2C IgG (–▲–). Anti-rat CYP2C IgG inhibited MDCA formation (panel a) and anti-rat CYP3A IgG inhibited 3KCA (panel b) formation by 50%, respectively, at 5 mg IgG/mg of protein. Anti-rat CYP3A IgG inhibited MDCA, ILCA (panel c) and M-2 (panel d) formation at 5 mg IgG/mg protein, whereas complete inhibition of metabolites, M-1 and M-3 (not shown), was observed. Anti-rat CYP3A IgG also inhibited M-4 (panel e) and M-5 (panel f) formation by more than 50%. UDCA formation (panel g) was inhibited partially by anti-CYP3A IgG. Monospecific anti-rat CYP2C11 IgG was not effective in inhibiting the formation of any metabolites.

4. DISCUSSION

LCA is the only endogenous mono-hydroxy bile acid. The high lipophilicity of LCA, combined with its ability to form micelles, enables it to penetrate almost all cell membranes and renders it the most toxic bile acid (Hofmann, 1999a). LCA accumulation in the body leads to cholestasis, hepatic disorders and even colorectal cancer (Narisawa et al., 1974; Hofmann, 1999a). LCA can also act as a ligand for nuclear receptors such as PXR that regulate CYP enzymes (Staudinger et al., 2001). Conjugation of LCA with amino acids or with glucuronyl or sulfate moieties fails to eliminate the cholestatic potential of LCA, because the 3-O-glucuronide of LCA is a more potent cholestatic agent than the parent compound (Oelberg et al., 1984). On the other hand, hydroxylation converts LCA into more hydrophilic bile acids which are eliminated more easily, and this process thereby acts as a detoxification mechanism (Radominska-Pyrek et al., 1987). In the rat, hydroxylation constitutes a major pathway of LCA detoxification. The present study investigated the *in vitro* biotransformation of LCA in rat hepatic microsomes.

4.1 LC/MS methodology and LCA biotransformation assay

4.1.1 LC/MS identification and separation of bile acid standards

LC/MS is an effective method to obtain good sensitivity, selectivity, detection and separation of unconjugated bile acids. The mobile phase consisting of two solvents, A (methanol : 10 mM ammonium acetate pH 4.6 : water (50:10:40)) and B (methanol : 10 mM ammonium acetate pH 4.6 : water (85:10:5)), delivered as a gradient, was modified from the method of Stedman et al. (2004). This method was able to resolve a mixture of unconjugated bile acid standards (α-MCA, β-MCA, γ-MCA, MDCA, UDCA, HDCA, CDCA, 6KLCA, ILCA, LCA, 3KCA and cholic-2,2,4,4-d_4 acid) (Fig. 2.2) but did not resolve two trihydroxylated isomers of

muricholic acid, α-MCA and β-MCA (Fig. 2.2). It should be possible to resolve α-MCA and β-MCA using a chiral column. Another trihydroxylated isomer of muricholic acid, γ-MCA (m/z 407) was well resolved from α-MCA and β-MCA (Fig. 2.2). Baseline separation of LCA, and its β-isomer, ILCA, was possible in our LC/MS system (Fig. 2.2). The LC/MS system offers several advantages over other analytical methods. The resolution and detection of these bile acid standards using a HPLC system with UV detection would have been more difficult because bile acids do not have a conjugated diene system that can assist UV detection. The identification of bile acids using LC/MS is less tedious than GC/MS because there is no need for derivatization (acetylation or methylation), which is required for identification using GC/MS. Identification of metabolites by TLC often lacks good resolving power and is tedious. One major disadvantage of analyzing bile acids using LC/MS is that unconjugated bile acids cannot be fragmented easily and hence structure elucidation using LC/MS/MS is ruled out.

The hepatic *in vitro* metabolism of LCA was studied previously. Zimniak et al. (1989) used TLC for the identification of unconjugated bile acids. The mobile phase (isooctane-ethyl acetate-acetic acid, 10:10:2) used in their study was able to resolve β-MCA, HDCA, MDCA, CDCA, 6KLCA. The bile acids were identified using Krowiki's reagent. Zimniak et al. (1989) also used radiolabelled LCA and carried out acetylation/methylation of LCA metabolites for identification using GC/MS. Using TLC and GC/MS, Dionne et al. (1994), identified the formation of MDCA and β-MCA as metabolites of LCA. Recently, Bodin et al. (2005) identified 3KCA, HDCA, 6α-hydroxy-3-oxo-5β-cholanic acid (m/z 461) and 1β-hydroxy LCA (m/z 391) using GC/MS as metabolites of LCA.

Unconjugated bile acids such as α-MCA, β-MCA, CA, CDCA, UDCA, MDCA and DCA were identified by Stedman et al. (2004) in liver homogenates of bile duct ligated and sham operated mice injected with LCA. Validation and assay optimization of the LC/MS

89

method used in this study has not been reported. The identification of individual hepatic CYP enzymes involved in the formation of various LCA metabolites was also not carried out by Stedman et al. (2004).

4.1.2 Extraction recovery

A liquid-liquid extraction procedure was used in the present study. The choice of extraction solvent (dichloromethane:isopropanol, 80:20) was taken from Stedman et al. (2004). The recovery of bile acid standards was in the range of 90-100% except for 3KCA (60% recovery) as mentioned in the RESULTS section. A recovery of 50% or greater is considered to be adequate by some researchers (Karnes et al., 1991) but we would prefer the recovery of 3KCA to be closer to that of the other metabolites. A better extraction system is needed to increase the recovery of 3KCA. 3KCA has similar lipophilicity as LCA. Thus, increasing the concentration of dichloromethane in the dichloromethane:isopropanol extraction solvent to 90:10 may increase the recovery of 3KCA and also eliminate the need for a double step extraction. Solid phase extraction procedures using a Bond Elute C_{18} cartridge may also be used.

4.1.3 Identification of LCA metabolites

The incubation of LCA with rat liver microsomes and NADPH led to the formation of MDCA, ILCA and 3KCA as major metabolites followed by UDCA, 6KLCA, and β-MCA as minor metabolites, along with five minor unidentified metabolites M-1 to M-5 (See Fig 2.4). No metabolite peaks corresponding to α-MCA and γ-MCA were obtained. CDCA was reported previously to be a minor metabolite (4.9% of total metabolites formed) of LCA in a Sprague-Dawley rat microsomal system (Zimniak et al., 1989). *In vitro* studies using human liver microsomes carried out by Xie et al. (2001) pointed to HDCA, followed by MDCA and CDCA,

as major metabolites of LCA. Both studies used TLC techniques for metabolite identification. CDCA was not observed as a metabolite, but was identified as a contaminant of LCA in our study. During initial experiments, we surmised that the peak corresponding to CDCA (P-2) represented a metabolite. However, later experiments (See Fig. 2.5) confirmed that CDCA was present as a contaminant in the substrate solution. It is possible that CDCA was a contaminant in the studies performed by Zimniak et al. (1989) and Xie et al. (2001).

Structural identification of the unknown metabolites, M-1 to M-5, was not possible. NMR and other techniques are needed in order to identify these metabolites. It is possible that M-4 is hyodeoxycholic acid (HDCA, m/z 391), based on the retention time using HDCA as an authentic standard. The exact identity of this metabolite peak could not be established even after spiking the incubated sample with standard HDCA due to the close proximity of the M-4 peak with other metabolite peaks (See in Fig. 2.4.) HDCA was identified as a major metabolite in human microsomes (Xie et al., 2001). HDCA was also observed to be a LCA metabolite using hepatic microsomes from male Sprague-Dawley rats (Zimniak et al., 1989).

4.1.4. LCA biotransformation assay

Optimal assay conditions for analyzing LCA biotransformation consisted of substrate concentrations of 50 μM (LCA) for 6KLCA formation, 100 μM (LCA) for MDCA and ILCA formation, and 250 μM (LCA) for 3KCA formation. Substrate was incubated with hepatic microsomes at 0.5 mg/ml of protein for 30 min in a reaction mixture consisting of 1 mM NADPH and 46.5 mM potassium phosphate buffer at pH 7.4.

In patients suffering from end-stage cholestasis, the hepatic level of LCA was calculated to be approximately 6 μM (Fischer et al., 1996). In a second study, concentrations of 5 to 10 μM were reported in livers of cholestatic patients and in rat models of biliary cholestasis (Setchell et

al., 1997). This concentration of LCA is within the range of LCA (0.5 – 300 μM) used in our assay system.

Examination of the reaction products of LCA biotransformation indicated that hydroxylation occured primarily at the 6β-position of LCA, and led to formation of MDCA, which accounted for more than 60% of total metabolites formed. MDCA formation followed typical Michaelis-Menten kinetics. The rate of formation (Vmax = 2793.1 pmol/min/mg of protein) of MDCA was 2.5- and 4-fold greater than that of ILCA and 3KCA, respectively. MDCA was identified as a major 6β-hydroxylated LCA metabolite in previous studies. Using hepatic microsomes from male Sprague-Dawley rats, MDCA was the major metabolite followed by 6KLCA, CDCA, α-MCA and β-MCA in that order (Zimniak et al., 1989). Dionne et al. (1994) also reported that metabolism of LCA in male Sprague-Dawley rats led to formation of MDCA as the major metabolite along with β-MCA.

ILCA was the second most abundant metabolite of LCA in our assay system. It is interesting that ILCA (β-isomer of LCA) was identified as a metabolite in this study because ILCA was not reported as a metabolite in previous *in vitro* LCA biotransformation studies, but was reported as a major metabolite in human feces (Norman and Palmer, 1964). ILCA formation was not observed with boiled microsomes, in the absence of NADPH, or following carbon monoxide treatment, indicating that formation of ILCA is mediated by the CYP enzyme system. ILCA formation followed typical Michaelis-Menten kinetics.

The rate of 3KCA formation was the lowest (Vmax = 667.7 pmol/min/mg of protein) and the Km (162.6 μM) value was the highest of the three major metabolites. A high Km value for 3KCA suggests decreased formation of this 3-keto metabolite at low LCA concentrations (Table 2.5). The saturating concentration of LCA for 3KCA formation was 250 μM, which was the highest of all the metabolites studied. In *in vivo* studies performed by Sakai et al. (1980),

3KCA was the major metabolite in rats fed a LCA-enriched diet. In a recent *in vitro* study, 3KCA was identified as the major metabolite (74%) of LCA formed by recombinant CYP3A4 (Bodin et al., 2005).

A minor keto-metabolite formed as a result of CYP-mediated oxidation was 6KLCA. 6KLCA had a low Km value (1.6 μM, Table 2.5) indicating higher binding affinity than any other metabolite. The low Km value suggests that formation of 6KLCA occurs even at low substrate concentrations.

UDCA was obtained as a minor metabolite in our *in vitro* assay. The formation of UDCA is of interest because it is used as a therapeutic agent in the treatment of gallstones and cholestasis in humans (El-Rifai and Gottrand, 2004). UDCA is also recommended for the treatment of intra-hepatic cholestasis (Lengyel and Feher, 2004). UDCA formation followed typical Michaelis-Menten kinetics with a LCA saturating concentration of 100 μM. The role of UDCA as a possible intermediate in the formation of the trihydroxylated LCA metabolite, β-MCA, in rat hepatic microsomes was speculated by Zimniak et al. (1989). However, β-MCA formation decreased rapidly with increasing substrate concentrations (See Fig. 2.8). This observation suggests that β-MCA, and not UDCA, acts as an intermediate and undergoes further metabolism.

4.1.5 Biotransformation of LCA in different strains of rat

It should be noted that the hepatic microsomal metabolism assay for LCA was validated and optimized using male Wistar rats but the next set of experiments, which were designed to identify the CYP enzymes involved in LCA metabolism, were carried out using male Long-Evans rats. To determine if there was a strain difference in LCA metabolism, the rates of formation of the major metabolites (MDCA, ILCA and 3KCA only) were compared in male

Long-Evans, Wistar and Sprague-Dawley rats. Two substrate concentrations (100 μM for MDCA and ILCA and 250 μM for 3KCA) were used. Long-Evans rats were found to have greater activity towards LCA, as compared to the other two strains. Strain differences in xenobiotic metabolism have been observed previously. Significant strain differences in the metabolism of alprenolol using liver microsomes from male Wistar and Dark Agouti rats (Wistar > Dark Agouti), has been reported (Narimatsu et al., 1995). In another study, a marked strain difference in acetohexamide reductase activity was observed with liver microsomes from male Fischer 344, Sprague-Dawley and Wistar rat strains. Higher activity was reported for Fischer 344 rats (Imamura et al., 1995).

4.1.6 Identification of CYP enzymes involved in LCA biotransformation

Experiments to identify CYP enzymes involved in LCA biotranformation were carried out using microsomes from Long-Evans rats treated with inducers or antibodies as inhibiting agents.

a)   Identification of CYP enzymes in formation of MDCA

In the present study, MDCA formation was decreased in hepatic microsomes prepared from MC-, PB- and DEX-treated rats compared to control rats. Decreased MDCA formation in liver microsomes from MC- and PB-treated rats suggests that CYP1A and CYP2B do not contribute significantly to MDCA formation and that CYP enzymes normally present in untreated rats are involved. Also, formation of MDCA was observed to be greater in control male compared to control female rats (Table 2.7) suggesting the involvement of male predominant enzymes such as CYP2C11. In antibody inhibition studies, MDCA formation was inhibited primarily by polyspecific anti-CYP2C IgG (approximately 50% inhibition by anti-CYP2C IgG at 5 mg IgG/mg microsomal protein, Fig. 2.10). Polyspecific anti-CYP3A IgG also

inhibited MDCA formation by approximately 30% at 5 mg IgG/mg microsomal protein. Complete inhibition of MDCA formation by anti-CYP2C or anti-CYP3A IgG was not observed. Moreover, MDCA formation was not affected by monospecific anti-CYP2C11 IgG (Fig 2.10) suggesting that CYP2C (but not CYP2C11) and CYP3A enzymes are involved in MDCA formation. This result namely, the involvement of CYP2C in 6β-hydroxylation of LCA to form MDCA, has not been published previously.

The formation of 6β-hydroxylated steroidal metabolites is characteristic of CYP3A enzymes as observed in previous studies with testosterone and cortisol (Sonderfan et al., 1987; Waxman and Chang, 1998; Furuta et al., 2003). In the case of bile acids, formation of MDCA from LCA was observed to be CYP3A10-mediated in hamster liver (Chang et al., 1993). Xie et al. (2001) also showed that 6β-hydroxylation of LCA using recombinant CYP3A4 or human liver microsomes leads to the formation of MDCA. Surprisingly, this 6β-hydroxylated metabolite of LCA was not observed using recombinant CYP3A4 in studies carried out by Bodin et al. (2005).

b)   **Identification of CYP enzymes involved in 3KCA formation**

DEX treatment of male and female Long-Evans rats resulted in increased 3KCA formation (2.5-fold increase relative to control rats, Table 2.7) suggesting the involvement of CYP3A enzymes. Antibody inhibition experiments with polyspecific anti-CYP3A IgG and polyspecific anti-CYP2C IgG showed that CYP3A enzymes account for up to 50% of 3KCA formation, and that CYP2C enzymes, but not CYP2C11, also contribute to 3KCA formation. It should be noted that studies to identify the CYP enzymes involved in formation of 3KCA from LCA have not been reported previously.

c) Identification of CYP enzymes involved in ILCA formation

ILCA formation was higher by 40-fold in control male than female rats indicating a prominent role for male rat specific enzymes such as CYP2C11. However, neither monospecific anti-rat CYP2C11 IgG nor polyspecific anti-rat CYP2C IgG inhibited ILCA formation (panel c, Fig. 2.9). Partial inhibition (approximately 40% inhibition at 5 mg IgG/mg of protein) by polyspecific anti-rat CYP3A IgG suggests the involvement of CYP3A and other CYP enzymes in ILCA formation. The identity of the other CYP enzymes is unknown. Decreased ILCA formation was observed with MC- and PB-treated male rat liver microsomes, which suggests that CYP1A and CYP2B enzymes do not contribute significantly to ILCA formation. Studies identifying the CYP enzymes involved in ILCA formation have not been reported previously.

d) Identification of CYP enzymes involved in the formation of minor metabolites

The effect of CYP inducers on the formation of minor metabolites such as UDCA, 6KLCA and other unidentified metabolites was not investigated. However, experiments using anti-CYP antibodies could form a basis for identification of the individual CYP enzymes involved in the formation of these metabolites.

UDCA (5β-cholanic acid-3α, 7β- diol) is produced by 7β-hydroxylation of LCA. Polyspecific anti-CYP3A IgG inhibited UDCA formation by 20% at all concentrations suggesting a minor involvement of CYP3A.

The minor unidentified metabolite, M-4, could be HDCA as suggested previously. HDCA is a 6α-hydroxylated metabolite of LCA. Polyspecific anti-CYP3A IgG inhibited M-4 formation by up to 80% (at 5 mg IgG/mg of microsomal protein) indicating the involvement of CYP3A in the formation of M-4. Identification of CYP enzymes involved in HDCA formation

has been investigated previously. HDCA formation was inhibited by approximately 80% using polyspecific anti-CYP3A IgG at 1.25 mg IgG/mg human microsomal protein (Xie et al., 2001). Using a panel of human liver microsomes, Araya and Wikvall (1999), also suggested the involvement of CYP3A in 6α-hydroxylation of LCA. Biotransformation of LCA using recombinant CYP3A4 led to the formation of HDCA, which accounted for 12% of the total metabolites formed according to studies performed by Bodin et al. (2005). Collectively, these studies suggest that HDCA formation is mediated by CYP3A enzymes in humans and rats.

Interestingly, formation of metabolite peaks of UDCA and M-4 increased in the presence of polyspecific anti-rat CYP2C IgG (approximately a 50% increase) and monospecific anti-rat CYP2C11 IgG (approximately a 100% increase) at 5 mg IgG/mg of microsomal protein (Fig. 2.10, panel e and g). These results remain unexplained in this study. UDCA and M-4 are minor metabolites and hence repetition of the antibody inhibition experiments would be necessary to assess the reproducibility of these results.

The formation of the minor metabolite, M-2, was observed to be partially catalyzed by CYP3A (Fig. 2.10, panel d). Formation of another minor metabolite, M-5 was inhibited 70% (at 5 mg IgG/mg of microsomal protein) indicating CYP3A involvement. Metabolite peaks, M-1 and M-3, were not observed in the presence of anti-CYP3A IgG suggesting that their formation is predominantly catalyzed by CYP3A.

In summary, the data from the induction and antibody inhibition experiments suggests that CYP3A and CYP2C enzymes (but not CYP2C11) are involved in the biotransformation of LCA. Because formation of MDCA, ILCA and 3KCA was not inhibited by more than 60% in any of the antibody inhibition experiments, other CYP enzymes are likely to be involved. Recently, studies performed in mice provided evidence of a CYP3A independent CAR-mediated pathway in bile acid detoxification (Saini et al., 2004). This orphan nuclear receptor

was first shown to function as a xenobiotic receptor by activating CYP2B genes (Bertilsson et al., 1998; Blumberg et al., 1998; Honkakoski et al., 1998; Kliewer et al., 1998; Wei et al., 2000; Xie and Evans, 2001; Xie et al., 2001). Araya and Wikvall (1999) calculated a correlation coefficient of 0.47 between the rate of LCA hydroxylation and the S-mephenytoin *N*-demethylase (a CYP2B6 marker), using human microsomal samples. Although the inducer treatment and antibody inhibition experiments performed in the present study do not suggest that CYP2B is involved in LCA metabolism, it is possible that in other species such as in mice and humans, CYP2B enzymes could play some role in LCA hydroxylation. Thus, further experiments to explore the involvement of CYP2B (using mice and human microsomal samples) in LCA hydroxylation are required to investigate this possibility.

4.2   Possible mechanisms for CYP-mediated formation of ketone metabolites

Two ketone metabolites (3KCA and 6KLCA) were identified in this study. Oxidation reactions leading to a ketone product via a geminal diol intermediate can be catalyzed by CYP enzymes (See Fig. 2.11). β-Hydroxylation at an existing α-hydroxy position is required to form a geminal diol intermediate. Thus, for formation of 3KCA from LCA (a 3α-hydroxylated bile acid), the hydroxy group of the substrate has to be α-oriented. Formation of 3KCA will not be facilitated if a hydroxy group occupies the 3β-position. Incubation of epi-DCA (3β-hydroxy DCA) with recombinant CYP3A4 did not form the 3-oxo-metabolite (Bodin et al., 2005). Similarly, it could be speculated that formation of 3KCA from ILCA (3β-hydroxylated LCA) is not possible (See Fig. 2.11). Accordingly, it can be suggested that formation of 6-keto bile acids, such as 6KLCA, can occur by β-hydroxylation of an existing 6α-hydroxylated substrate, such as HDCA, via a geminal diol intermediate and not through MDCA (a 6β-hydroxy bile acid). In humans, similar CYP-mediated reactions catalyzed by CYP11B2, CYP19, CYP27 and

CYP51 are observed (Fischer et al., 1991; Holmberg-Betsholtz et al., 1993; Korzekwa et al., 1993; Bureik et al., 2002).

Alternative mechanisms involving direct dehydrogenation of a hydroxyl group to form 3KCA and 6KLCA by peroxycytochromes are possible. Oxidation could also be catalyzed via a dehydrogenase reaction, which utilizes $NADP^+$ from NADPH during CYP-mediated hydroxylation, or $NADP^+$ can be present as a contaminant in NADPH. However, microsomal incubation performed without NADPH, with CO treatment, or using boiled microsomes showed no metabolite formation. This result confirms that both oxidation products (3KCA and 6KLCA) were formed by CYP-catalyzed reactions. On the basis of antibody inhibition studies carried out in this study, it could be concluded that 3KCA formation is mediated primarily by CYP2C and CYP3A enzymes (Fig. 2.10). CYP2C-mediated bile acid oxidation leading to a ketone product is a new finding but CYP3A-mediated bile acid oxidation to a ketone has been described recently. A recent report by Bodin et al. (2005) demonstrated recombinant CYP3A4-mediated 3KCA formation, and indicated that LCA is not the only bile acid to undergo oxidation (Table 1.5). DCA, CDCA, LCA, UDCA and CA were metabolized to their respective 3-keto metabolites, with 100% conversion of CA to 3-oxo-cholic acid (Bodin et al., 2005). Experiments performed by Bodin et al. (2005) in the presence of a CYP3A4 inhibitor, TAO, and replacement of NADPH with $NADP^+$ did not result in formation of the keto-metabolites, thus strengthening the primary role of CYP3A enzymes in their formation. Keto products with oxidation at C_3, C_7 or C_{12} positions on the 5β-cholestane ring system have been found in human feces (Tandon et al., 1984). LCA oxidation at C_6 seems to occur in rat liver microsomal samples (male and female rats in all strains used in this work; Zimniak et al., 1989) but was not reported in the CYP3A4 recombinant system used by Bodin et al. (2005).

Oxidative biotransformation of bile acids such as LCA is of clinical importance as well, because it is known that keto metabolites lead to formation of reactive oxygen species (ROS) and formation of ROS is a major cause of liver toxicity (De Maria et al., 1996).
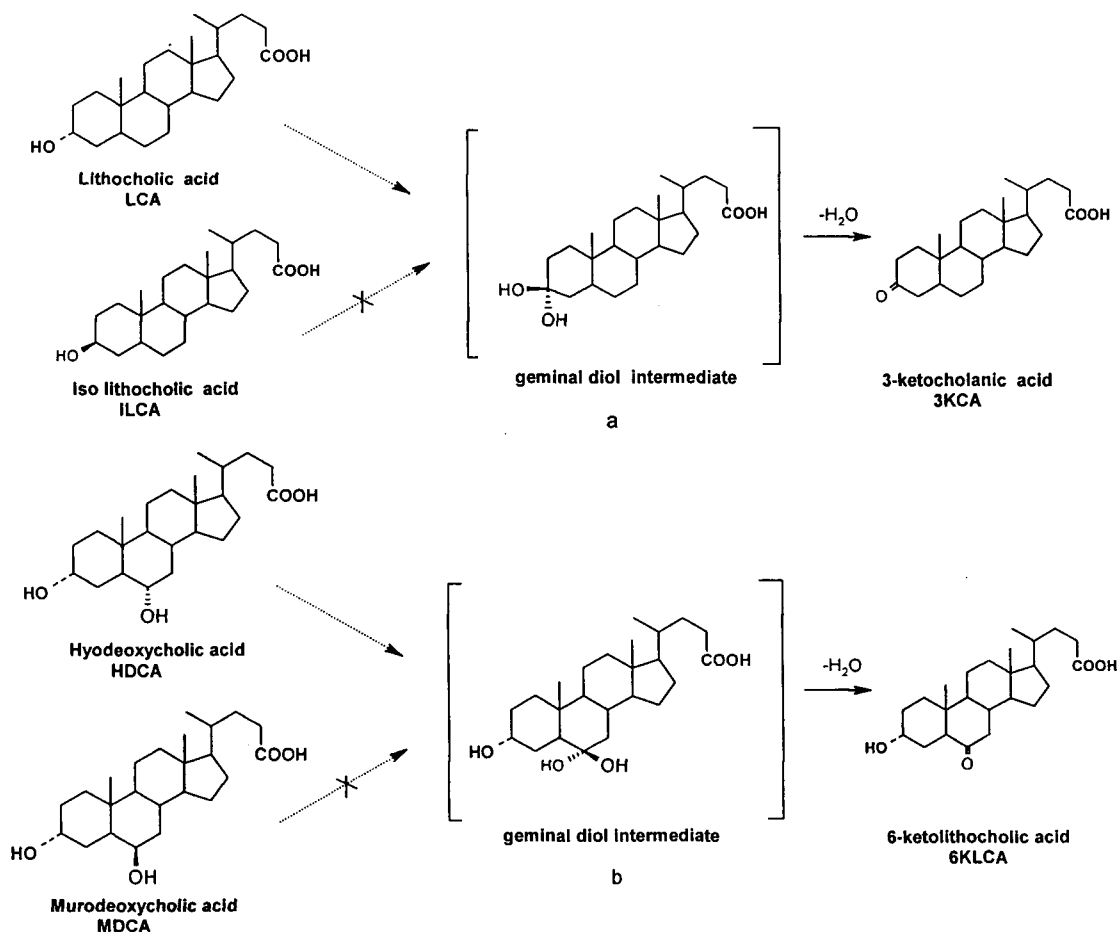
Fig. 2.11 Proposed mechanisms for CYP-mediated LCA oxidation.

Suggested mechanisms of oxidation to form oxo-lithocholic acid metabolites by CYP3A. β-hydroxylation occurs to form a geminal diol intermediate at an already existing α-hydroxyl position. Formation of 3KCA is facilitated due to the 3α-hydroxylated substrate, i.e. LCA, via β-hydroxylation to form a geminal diol intermediate and not through ILCA, the 3β-hydroxylated LCA (panel a). Formation of 6KLCA is facilitated due to the 6α-hydroxylated substrate, i.e. HDCA, via β-hydroxylation to form a geminal diol intermediate and not through MDCA, the 6β-hydroxylated bile acid (panel b).

4.3   Scheme for hepatic LCA biotransformation pathways

On the basis of the results of the present study, a scheme for CYP-mediated formation of

LCA metabolites is proposed as shown in Fig. 2.12.
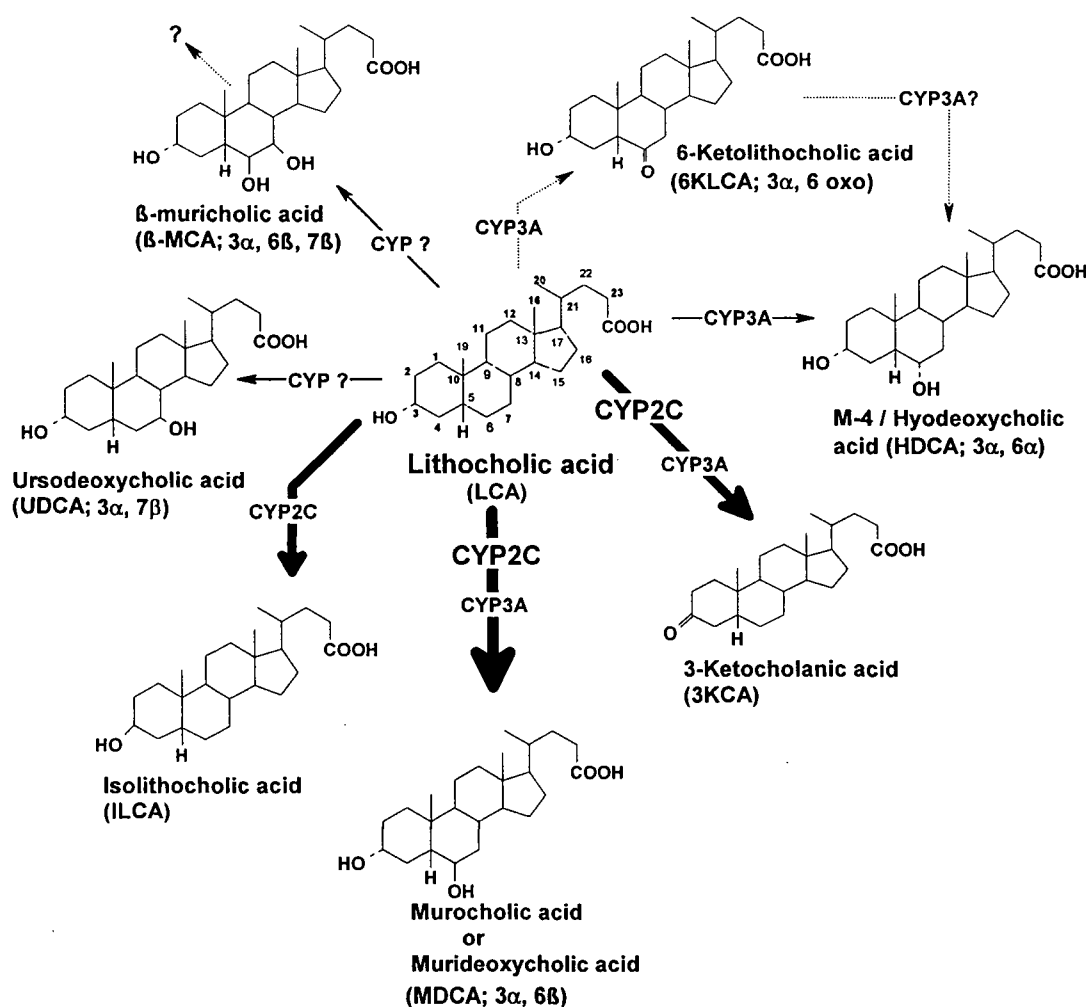
Fig. 2.12. Profile for CYP-mediated LCA biotransformation in rat hepatic microsomes

Results obtained indicate formation of MDCA, ILCA and 3KCA as major metabolites (shown by bold arrows) and UDCA, 6KLCA and β-MCA as minor metabolites. The scheme shows that formation of MDCA and 3KCA is mediated by CYP2C (other than CYP2C11) and CYP3A enzymes. The identity of the specific CYP2C enzymes involved in ILCA formation was not established. The CYP enzymes mediating formation of β-MCA and UDCA were not identified. It could be speculated from this data and the mechanism suggested in the **DISCUSSION** that CYP3A could be involved in 6KLCA formation but this needs to be verified (dotted arrows). The minor metabolites M-4 / HDCA, M-3 and M-5 are formed by CYP3A enzymes. Metabolism of β-MCA to other metabolites is possible (dotted arrows).

In summary, the biotransformation of LCA by rat hepatic microsomes was characterized and the reaction products were identified using LC/MS. The identity of metabolites, their rates of formation and their kinetic parameters provide a sound foundation for future studies of hepatic bile acid metabolism. Further experiments are required to verify the sequence of formation of the secondary metabolites. This work is the first of its kind to suggest a major role for CYP2C and CYP3A enzymes in LCA biotransformation. The identification of individual CYP2C, CYP3A, and other CYP enzymes involved in LCA biotransformation remains to be investigated.

4.4   Conclusions

1.   LC/MS can be used to study the biotransformation of LCA to its metabolites.

2.   MDCA, ILCA and 3KCA are the major metabolites and β-MCA, 6KLCA and UDCA are minor metabolites of LCA obtained using untreated male rat liver microsomal system.

3.   Further biotransformation of some LCA metabolites (e.g. β-MCA) is possible.

4.   Rat CYP2C (but not CYP2C11) and CYP3A are involved in the biotransformation of LCA.

4.5   Future experiments

1.   **LCA biotransformation in recombinant CYP enzymes and human liver microsomes.**

The method discussed in this thesis can be used effectively to study the biotransformation of LCA using recombinant CYP enzymes and human liver microsomes. The knowledge of the CYP enzymes involved in LCA biotransformation will eventually help to devise means that alleviate LCA-mediated disorders such as cholestasis.

2.   **Development of the LC/MS assay for detection and quantitation of CDCA metabolites.**

The method used in this assay can be applied to study the biotransformation of other bile acids such as CA, DCA, and CDCA. All these bile acids are involved in various disorders such as cholestasis, formation of gallstones, and colon cancer.

3.   **LC/MS analysis for tetrahydroxylated bile acids.**

Hepatic levels of tetrahydroxylated bile acids are increased in SPGP gene knockout cholestatic mice (Perwaiz et al. 2003). If authentic standards are available, a LC/MS method can be developed to analyze these bile acids and identify their role in bile acid mediated toxicity.

4.   **Development of an assay to analyze the metabolism of UDCA.**

UDCA is a hepatoprotective bile acid. It is metabolized to a number of metabolites as described previously (See Table 1.5). UDCA is also known to induce its hepatoprotective action through induction of CYP enzymes. Bile acids have been implicated in breast cancer, colorectal

cancer, liver damage and cholestasis. A rodent cholestatic and carcinogenic model will help to study the expression of CYP enzymes in these diseased conditions. The diseased condition combined with subsequent treatment of UDCA is expected to alleviate bile acid mediated toxicity. The mechanism by which UDCA shows its healing effects is still obscure and this knowledge combined with a metabolic UDCA profile can be useful in providing better treatment for cholestasis and cancer.

5.   Study of metabolism in intestinal microsomes.

Nuclear transporters and receptors are abundant in the intestine. Also, bile acids are known to cause colon cancer. The study of bile acid metabolism in intestinal microsomes in the control rodent and diseased rodent model could highlight the roles that nuclear receptors and transporters play in the intestine.

5. REFERENCES

Abe T, Kakyo M, Tokui T, Nakagomi R, Nishio T, Nakai D, Nomura H, Unno M, Suzuki M, Naitoh T, Matsuno S and Yawo H (1999) Identification of a novel gene family encoding human liver-specific organic anion transporter LST-1. *J Biol Chem* **274:**17159-17163.

Angeletti RH, Novikoff PM, Juvvadi SR, Fritschy JM, Meier PJ and Wolkoff AW (1997) The choroid plexus epithelium is the site of the organic anion transport protein in the brain. *Proc Natl Acad Sci U S A* **94:**283-286.

Araya Z and Wikvall K (1999) 6alpha-hydroxylation of taurochenodeoxycholic acid and lithocholic acid by CYP3A4 in human liver microsomes. *Biochim Biophys Acta* **1438:**47-54.

Bacher MA and Gibson GG (1988) Chlorophenoxyacid herbicides induce microsomal cytochrome P-450 IVA1 (P-452) in rat liver. *Chem Biol Interact* **65:**145-156.

Bandiera S and Dworschak C (1992) Effects of testosterone and estrogen on hepatic levels of cytochromes P450 2C7 and P450 2C11 in the rat. *Arch Biochem Biophys* **296:**286-295.

Bandiera S, Ryan DE, Levin W and Thomas PE (1986) Age- and sex-related expression of cytochromes p450f and P450g in rat liver. *Arch Biochem Biophys* **248:**658-676.

Bandiera SM (2001) *Cytochrome P450 Enzymes as Biomarkers of PCB Exposure and Modulators of Toxicity*. The University Press of Kentucky, Kentucky.

Barnett CR, Gibson GG, Wolf CR, Flatt PR and Ioannides C (1990) Induction of cytochrome P450III and P450IV family proteins in streptozotocin-induced diabetes. *Biochem J* **268:**765-769.

Bayerdorffer E, Mannes GA, Ochsenkuhn T, Dirschedl P, Wiebecke B and Paumgartner G (1995) Unconjugated secondary bile acids in the serum of patients with colorectal adenomas. *Gut* **36:**268-273.

Bayerdorffer E, Mannes GA, Richter WO, Ochsenkuhn T, Wiebecke B, Kopcke W and Paumgartner G (1993) Increased serum deoxycholic acid levels in men with colorectal adenomas. *Gastroenterology* **104**:145-151.

Bellward GD, Chang T, Rodrigues B, McNeill JH, Maines S, Ryan DE, Levin W and Thomas PE (1988) Hepatic cytochrome P-450j induction in the spontaneously diabetic BB rat. *Mol Pharmacol* **33**:140-143.

Bergwerk AJ, Shi X, Ford AC, Kanai N, Jacquemin E, Burk RD, Bai S, Novikoff PM, Stieger B, Meier PJ, Schuster VL and Wolkoff AW (1996) Immunologic distribution of an organic anion transport protein in rat liver and kidney. *Am J Physiol* **271**:G231-238.

Berta L, Fronticelli Baldelli C, Fazzari A, Radice E, Bargoni A, Frairia R and Gaetini A (2003) Sex steroid receptors, secondary bile acids and colorectal cancer. A possible mechanism of interaction. *Panminerva Med* **45**:261-266.

Bertilsson G, Heidrich J, Svensson K, Asman M, Jendeberg L, Sydow-Backman M, Ohlsson R, Postlind H, Blomquist P and Berkenstam A (1998) Identification of a human nuclear receptor defines a new signaling pathway for CYP3A induction. *Proc Natl Acad Sci U S A* **95**:12208-12213.

Blumberg B, Sabbagh W, Jr., Juguilon H, Bolado J, Jr., van Meter CM, Ong ES and Evans RM (1998) SXR, a novel steroid and xenobiotic-sensing nuclear receptor. *Genes Dev* **12**:3195-3205.

Bodin K, Lindbom U and Diczfalusy U (2005) Novel pathways of bile acid metabolism involving CYP3A4. *Biochim Biophys Acta* **1687**:84-93.

Borst P, Evers R, Kool M and Wijnholds J (1999) The multidrug resistance protein family. *Biochim Biophys Acta* **1461**:347-357.

Bremmelgaard A and Sjovall J (1980) Hydroxylation of cholic, chenodeoxycholic, and deoxycholic acids in patients with intrahepatic cholestasis. *J Lipid Res* **21**:1072-1081.

Bull LN, van Eijk MJ, Pawlikowska L, DeYoung JA, Juijn JA, Liao M, Klomp LW, Lomri N, Berger R, Scharschmidt BF, Knisely AS, Houwen RH and Freimer NB (1998) A gene encoding a P-type ATPase mutated in two forms of hereditary cholestasis. *Nat Genet* **18:**219-224.

Bureik M, Lisurek M and Bernhardt R (2002) The human steroid hydroxylases CYP1B1 and CYP11B2. *Biol Chem* **383:**1537-1551.

Burke MD and Mayer RT (1974) Ethoxyresorufin: direct fluorimetric assay of a microsomal O-dealkylation which is preferentially inducible by 3-methylcholanthrene. *Drug Metab Dispos* **2:**583-588.

Carey MC (1984) Bile acids and bile salts: ionization and solubility properties. *Hepatology* **4:**66S-71S.

Cattori V, Eckhardt U and Hagenbuch B (1999) Molecular cloning and functional characterization of two alternatively spliced Ntcp isoforms from mouse liver1. *Biochim Biophys Acta* **1445:**154-159.

Cattori V, Hagenbuch B, Hagenbuch N, Stieger B, Ha R, Winterhalter KE and Meier PJ (2000) Identification of organic anion transporting polypeptide 4 (Oatp4) as a major full-length isoform of the liver-specific transporter-1 (rlst-1) in rat liver. *FEBS Lett* **474:**242-245.

Chang TK, Teixeira J, Gil G and Waxman DJ (1993) The lithocholic acid 6 beta-hydroxylase cytochrome P-450, CYP 3A10, is an active catalyst of steroid-hormone 6 beta-hydroxylation. *Biochem J* **291 (Pt 2):**429-433.

Chang TK, Yu L, Maurel P and Waxman DJ (1997) Enhanced cyclophosphamide and ifosfamide activation in primary human hepatocyte cultures: response to cytochrome P-450 inducers and autoinduction by oxazaphosphorines. *Cancer Res* **57:**1946-1954.

Chen J and Farrell GC (1996) Bile acids produce a generalized reduction of the catalytic activity of cytochromes P450 and other hepatic microsomal enzymes in vitro: relevance to drug metabolism in experimental cholestasis. *J Gastroenterol Hepatol* **11**:870-877.

Chen J, Robertson G, Field J, Liddle C and Farrell GC (1998) Effects of bile duct ligation on hepatic expression of female-specific CYP2C12 in male and female rats. *Hepatology* **28**:624-630.

Chen Y, Ferguson SS, Negishi M and Goldstein JA (2004) Induction of human CYP2C9 by rifampicin, hyperforin, and phenobarbital is mediated by the pregnane X receptor. *J Pharmacol Exp Ther* **308**:495-501.

Cole SP, Bhardwaj G, Gerlach JH, Mackie JE, Grant CE, Almquist KC, Stewart AJ, Kurz EU, Duncan AM and Deeley RG (1992) Overexpression of a transporter gene in a multidrug-resistant human lung cancer cell line. *Science* **258**:1650-1654.

Conney AH (1967) Pharmacological implications of microsomal enzyme induction. *Pharmacol Rev* **19**:317-366.

Cooper KO, Reik LM, Jayyosi Z, Bandiera S, Kelley M, Ryan DE, Daniel R, McCluskey SA, Levin W and Thomas PE (1993) Regulation of two members of the steroid-inducible cytochrome P450 subfamily (3A) in rats. *Arch Biochem Biophys* **301**:345-354.

Costarelli V and Sanders TA (2002) Plasma bile acids and risk of breast cancer. *IARC Sci Publ* **156**:305-306.

Crespi CL, Chang TK and Waxman DJ (1998) Determination of CYP4A11-catalyzed lauric acid 12-hydroxylation by high-performance liquid chromatography with radiometric detection. *Methods Mol Biol* **107**:163-167.

Cui Y, Konig J, Leier I, Buchholz U and Keppler D (2001) Hepatic uptake of bilirubin and its conjugates by the human organic anion transporter SLC21A6. *J Biol Chem* **276**:9626-9630.

Cummings JH, Bingham SA, Heaton KW and Eastwood MA (1992) Fecal weight, colon cancer risk, and dietary intake of nonstarch polysaccharides (dietary fiber). *Gastroenterology* **103**:1783-1789.

De Gottardi A, Touri F, Maurer CA, Perez A, Maurhofer O, Ventre G, Bentzen CL, Niesor EJ and Dufour JF (2004) The bile acid nuclear receptor FXR and the bile acid binding protein IBABP are differently expressed in colon cancer. *Dig Dis Sci* **49**:982-989.

De Maria N, Colantoni A, Fagiuoli S, Liu GJ, Rogers BK, Farinati F, Van Thiel DH and Floyd RA (1996) Association between reactive oxygen species and disease activity in chronic hepatitis C. *Free Radic Biol Med* **21**:291-295.

Diaz MJ, Chinje E, Kentish P, Jarnot B, George M and Gibson GG (1993) Chlorotrifluoroethylene trimer and tetramer are inducers of the CYP4A subfamily. *Biochem Pharmacol* **46**:1076-1080.

Dionne S, Tuchweber B, Plaa GL and Yousef IM (1994) Phase I and phase II metabolism of lithocholic acid in hepatic acinar zone 3 necrosis. Evaluation in rats by combined radiochromatography and gas-liquid chromatography-mass spectrometry. *Biochem Pharmacol* **48**:1187-1197.

Dubuisson C, Cresteil D, Desrochers M, Decimo D, Hadchouel M and Jacquemin E (1996) Ontogenic expression of the Na(+)-independent organic anion transporting polypeptide (oatp) in rat liver and kidney. *J Hepatol* **25**:932-940.

Ekins S, Mirny L and Schuetz EG (2002) A ligand-based approach to understanding selectivity of nuclear hormone receptors PXR, CAR, FXR, LXRalpha, and LXRbeta. *Pharm Res* **19**:1788-1800.

El-Rifai N and Gottrand F (2004) [Role of ursodeoxycholic acid in pediatric cholestatic disease]. *Gastroenterol Clin Biol* **28**:852-859.

Eppens EF, van Mil SW, de Vree JM, Mok KS, Juijn JA, Oude Elferink RP, Berger R, Houwen RH and Klomp LW (2001) FIC1, the protein affected in two forms of hereditary cholestasis, is localized in the cholangiocyte and the canalicular membrane of the hepatocyte. *J Hepatol* **35:**436-443.

Erlinger S (1997) Drug-induced cholestasis. *J Hepatol* **26 Suppl 1:**1-4.

Estabrook R (1999) An introduction to the cytochrome P450s. *Mol Aspects Med* **20:**5-12, 13-137.

Fini A and Roda A (1987) Chemical properties of bile acids. IV. Acidity constants of glycine-conjugated bile acids. *J Lipid Res* **28:**755-759.

Fischer RT, Trzaskos JM, Magolda RL, Ko SS, Brosz CS and Larsen B (1991) Lanosterol 14 alpha-methyl demethylase. Isolation and characterization of the third metabolically generated oxidative demethylation intermediate. *J Biol Chem* **266:**6124-6132.

Fischer S, Beuers U, Spengler U, Zwiebel FM and Koebe HG (1996) Hepatic levels of bile acids in end-stage chronic cholestatic liver disease. *Clin Chim Acta* **251:**173-186.

Fujii-Kuriyama Y, Mizukami Y, Kawajiri K, Sogawa K and Muramatsu M (1982) Primary structure of a cytochrome P-450: coding nucleotide sequence of phenobarbital-inducible cytochrome P-450 cDNA from rat liver. *Proc Natl Acad Sci U S A* **79:**2793-2797.

Furuta T, Suzuki A, Mori C, Shibasaki H, Yokokawa A and Kasuya Y (2003) Evidence for the validity of cortisol 6 beta-hydroxylation clearance as a new index for in vivo cytochrome P450 3A phenotyping in humans. *Drug Metab Dispos* **31:**1283-1287.

Gao B, Hagenbuch B, Kullak-Ublick GA, Benke D, Aguzzi A and Meier PJ (2000) Organic anion-transporting polypeptides mediate transport of opioid peptides across blood-brain barrier. *J Pharmacol Exp Ther* **294:**73-79.

Gerloff T, Stieger B, Hagenbuch B, Madon J, Landmann L, Roth J, Hofmann AF and Meier PJ (1998) The sister of P-glycoprotein represents the canalicular bile salt export pump of mammalian liver. *J Biol Chem* **273:**10046-10050.

Glasova H and Beuers U (2002) Extrahepatic manifestations of cholestasis. *J Gastroenterol Hepatol* **17:**938-948.

Goldstein JA and de Morais SM (1994) Biochemistry and molecular biology of the human CYP2C subfamily. *Pharmacogenetics* **4:**285-299.

Goldstein JA, Faletto MB, Romkes-Sparks M, Sullivan T, Kitareewan S, Raucy JL, Lasker JM and Ghanayem BI (1994) Evidence that CYP2C19 is the major (S)-mephenytoin 4'-hydroxylase in humans. *Biochemistry* **33:**1743-1752.

Gonzalez FJ (1988) The molecular biology of cytochrome P450s. *Pharmacol Rev* **40:**243-288.

Gonzalez FJ (1990) Molecular genetics of the P-450 superfamily. *Pharmacol Ther* **45:**1-38.

Gonzalez FJ, Kimura S, Song BJ, Pastewka J, Gelboin HV and Hardwick JP (1986) Sequence of two related P-450 mRNAs transcriptionally increased during rat development. An R.dre.1 sequence occupies the complete 3' untranslated region of a liver mRNA. *J Biol Chem* **261:**10667-10672.

Gonzalez FJ, Ueno T, Umeno M, Song BJ, Veech RL and Gelboin HV (1991) Microsomal ethanol oxidizing system: transcriptional and posttranscriptional regulation of cytochrome P450, CYP2E1. *Alcohol Alcohol Suppl* **1:**97-101.

Grober J, Zaghini I, Fujii H, Jones SA, Kliewer SA, Willson TM, Ono T and Besnard P (1999) Identification of a bile acid-responsive element in the human ileal bile acid-binding protein gene. Involvement of the farnesoid X receptor/9-cis-retinoic acid receptor heterodimer. *J Biol Chem* **274:**29749-29754.

Guengerich FP (1990) Enzymatic oxidation of xenobiotic chemicals. *Crit Rev Biochem Mol Biol*
25:97-153.

Guengerich FP (1991) *Principles and Methods of Toxicology*. Raven Press Ltd., New York.

Guengerich FP (1995) *Human Cytochrome P450 Enzymes*. Plenum Press, New York.

Guengerich FP (2003) Cytochromes P450, drugs, and diseases. *Mol Interv* **3**:194-204.

Hagenbuch B and Meier PJ (1994) Molecular cloning, chromosomal localization, and functional
characterization of a human liver Na+/bile acid cotransporter. *J Clin Invest* **93**:1326-
1331.

Hagenbuch B, Stieger B, Foguet M, Lubbert H and Meier PJ (1991) Functional expression
cloning and characterization of the hepatocyte Na+/bile acid cotransport system. *Proc
Natl Acad Sci U S A* **88**:10629-10633.

Handschin C and Meyer UA (2003) Induction of drug metabolism: the role of nuclear receptors.
Pharmacol Rev **55**:649-673.

Hardwick JP, Song BJ, Huberman E and Gonzalez FJ (1987) Isolation, complementary DNA
sequence, and regulation of rat hepatic lauric acid omega-hydroxylase (cytochrome P-
450LA omega). Identification of a new cytochrome P-450 gene family. *J Biol Chem*
262:801-810.

Hasegawa T, Hara K, Kenmochi T and Hata S (1994) In vitro metabolism of dorzolamide, a
novel potent carbonic anhydrase inhibitor, in rat liver microsomes. *Drug Metab Dispos*
22:916-921.

Hesse LM, Venkatakrishnan K, Court MH, von Moltke LL, Duan SX, Shader RI and Greenblatt
DJ (2000) CYP2B6 mediates the in vitro hydroxylation of bupropion: potential drug
interactions with other antidepressants. *Drug Metab Dispos* **28**:1176-1183.

Hirohashi T, Suzuki H and Sugiyama Y (1999) Characterization of the transport properties of cloned rat multidrug resistance-associated protein 3 (MRP3). *J Biol Chem* **274**:15181-15185.

Hirohashi T, Suzuki H, Takikawa H and Sugiyama Y (2000) ATP-dependent transport of bile salts by rat multidrug resistance-associated protein 3 (Mrp3). *J Biol Chem* **275**:2905-2910.

Hofmann AF (1999a) Bile Acids: The Good, the Bad, and the Ugly. *News Physiol Sci* **14**:24-29.

Hofmann AF (1999b) The continuing importance of bile acids in liver and intestinal disease. *Arch Intern Med* **159**:2647-2658.

Hofmann AF (2002) Cholestatic liver disease: pathophysiology and therapeutic options. *Liver* **22 Suppl 2**:14-19.

Hofmann AF, Sjovall J, Kurz G, Radominska A, Schteingart CD, Tint GS, Vlahcevic ZR and Setchell KD (1992) A proposed nomenclature for bile acids. *J Lipid Res* **33**:599-604.

Holmberg-Betsholtz I, Lund E, Bjorkhem I and Wikvall K (1993) Sterol 27-hydroxylase in bile acid biosynthesis. Mechanism of oxidation of 5 beta-cholestane-3 alpha,7 alpha,12 alpha,27-tetrol into 3 alpha,7 alpha,12 alpha-trihydroxy-5 beta-cholestanoic acid. *J Biol Chem* **268**:11079-11085.

Honkakoski P, Zelko I, Sueyoshi T and Negishi M (1998) The nuclear orphan receptor CAR-retinoid X receptor heterodimer activates the phenobarbital-responsive enhancer module of the CYP2B gene. *Mol Cell Biol* **18**:5652-5658.

Hooiveld GJ, van Montfoort JE, Meijer DK and Muller M (2001) Function and regulation of ATP-binding cassette transport proteins involved in hepatobiliary transport. *Eur J Pharm Sci* **12**:525-543.

Hori T, Matsumoto K, Sakaitani Y, Sato M and Morotomi M (1998) Effect of dietary deoxycholic acid and cholesterol on fecal steroid concentration and its impact on the colonic crypt cell proliferation in azoxymethane-treated rats. *Cancer Lett* **124:**79-84.

Hrycay EG and Bandiera SM (2003) Spectral interactions of tetrachlorobiphenyls with hepatic microsomal cytochrome p450 enzymes. *Chem Biol Interact* **146:**285-296.

Huynh HT and Teel RW (2002) Effects of plant-derived phenols on rat liver cytochrome P450 2B1 activity. *Anticancer Res* **22:**1699-1703.

Imamura Y, Kimura R, Kozono Y and Otagiri M (1995) Strain- and sex-related differences of acetohexamide reductase activities in liver microsomes and cytosol of rats: the Wistar-Imamichi strain lacks the male-specific microsomal enzyme activity. *Life Sci* **57:**1811-1817.

Imray CH, Radley S, Davis A, Barker G, Hendrickse CW, Donovan IA, Lawson AM, Baker PR and Neoptolemos JP (1992) Faecal unconjugated bile acids in patients with colorectal cancer or polyps. *Gut* **33:**1239-1245.

Jezequel AM, Benedetti A, Bassotti C and Orlandi F (1994) *Drug induced cholestasis*. Elsevier Science BV, Netherlands.

Kanamoto R, Azuma N, Suda H, Saeki T, Tsuchihashi Y and Iwami K (1999) Elimination of Na+-dependent bile acid transporter from small intestine by ileum resection increases [correction of increase] colonic tumorigenesis in the rat fed deoxycholic acid. *Cancer Lett* **145:**115-120.

Karnes HT, Shiu G and Shah VP (1991) Validation of bioanalytical methods. *Pharm Res* **8:**421-426.

Kawajiri K, Gotoh O, Sogawa K, Tagashira Y, Muramatsu M and Fujii-Kuriyama Y (1984) Coding nucleotide sequence of 3-methylcholanthrene-inducible cytochrome P-450d cDNA from rat liver. *Proc Natl Acad Sci U S A* **81:**1649-1653.

Kawashima H, Kusunose E, Kikuta Y, Kinoshita H, Tanaka S, Yamamoto S, Kishimoto T and Kusunose M (1994) Purification and cDNA cloning of human liver CYP4A fatty acid omega-hydroxylase. *J Biochem (Tokyo)* **116:**74-80.

Keppler D and Konig J (2000) Hepatic secretion of conjugated drugs and endogenous substances. *Semin Liver Dis* **20:**265-272.

Kliewer SA, Moore JT, Wade L, Staudinger JL, Watson MA, Jones SA, McKee DD, Oliver BB, Willson TM, Zetterstrom RH, Perlmann T and Lehmann JM (1998) An orphan nuclear receptor activated by pregnanes defines a novel steroid signaling pathway. *Cell* **92:**73-82.

Klingenberg M (1958) Pigments of rat liver microsomes. *Arch Biochem Biophys* **75:**376-386.

Knutson JC and Poland A (1982) Response of murine epidermis to 2,3,7,8-tetrachlorodibenzo-p-dioxin: interaction of the ah and hr loci. *Cell* **30:**225-234.

Kobayashi K, Urashima K, Shimada N and Chiba K (2003) Selectivities of human cytochrome P450 inhibitors toward rat P450 isoforms: study with cDNA-expressed systems of the rat. *Drug Metab Dispos* **31:**833-836.

Kocarek TA, Schuetz EG, Strom SC, Fisher RA and Guzelian PS (1995) Comparative analysis of cytochrome P4503A induction in primary cultures of rat, rabbit, and human hepatocytes. *Drug Metab Dispos* **23:**415-421.

Konig J, Cui Y, Nies AT and Keppler D (2000) Localization and genomic organization of a new hepatocellular organic anion transporting polypeptide. *J Biol Chem* **275:**23161-23168.

Konig J, Nies AT, Cui Y, Leier I and Keppler D (1999) Conjugate export pumps of the multidrug resistance protein (MRP) family: localization, substrate specificity, and MRP2-mediated drug resistance. *Biochim Biophys Acta* **1461:**377-394.

Korzekwa KR, Trager WF, Mancewicz J and Osawa Y (1993) Studies on the mechanism of aromatase and other cytochrome P450 mediated deformylation reactions. *J Steroid Biochem Mol Biol* **44**:367-373.

Kramer W, Stengelin S, Baringhaus KH, Enhsen A, Heuer H, Becker W, Corsiero D, Girbig F, Noll R and Weyland C (1999) Substrate specificity of the ileal and the hepatic Na(+)/bile acid cotransporters of the rabbit. I. Transport studies with membrane vesicles and cell lines expressing the cloned transporters. *J Lipid Res* **40**:1604-1617.

Kullak-Ublick GA, Ismair MG, Stieger B, Landmann L, Huber R, Pizzagalli F, Fattinger K, Meier PJ and Hagenbuch B (2001) Organic anion-transporting polypeptide B (OATP-B) and its functional comparison with three other OATPs of human liver. *Gastroenterology* **120**:525-533.

Kullak-Ublick GA, Stieger B, Hagenbuch B and Meier PJ (2000) Hepatic transport of bile salts. *Semin Liver Dis* **20**:273-292.

Lammert F, Carey MC and Paigen B (2001) Chromosomal organization of candidate genes involved in cholesterol gallstone formation: a murine gallstone map. *Gastroenterology* **120**:221-238.

Lenart J and Pikula S (1999) 10-Undecynoic acid, an inhibitor of cytochrome P450 4A1, inhibits ethanolamine-specific phospholipid base exchange reaction in rat liver microsomes. *Acta Biochim Pol* **46**:203-210.

Lengyel G and Feher J (2004) [Intrahepatic cholestasis of pregnancy]. *Orv Hetil* **145**:2103-2105.

Lieber CS (1997) Cytochrome P-4502E1: its physiological and pathological role. *Physiol Rev* **77**:517-544.

Lin LY, Fujimoto M, Distefano EW, Schmitz DA, Jayasinghe A and Cho AK (1996) Selective mechanism-based inactivation of rat CYP2D by 4-allyloxymethamphetamine. *J Pharmacol Exp Ther* **277**:595-603.

Liu Y, Binz J, Numerick MJ, Dennis S, Luo G, Desai B, MacKenzie KI, Mansfield TA, Kliewer SA, Goodwin B and Jones SA (2003) Hepatoprotection by the farnesoid X receptor agonist GW4064 in rat models of intra- and extrahepatic cholestasis. *J Clin Invest* **112**:1678-1687.

Lu AY, Somogyi A, West S, Kuntzman R and Conney AH (1972) Pregnenolone-16 - carbonitrile: a new type of inducer of drug-metabolizing enzymes. *Arch Biochem Biophys* **152**:457-462.

Ma Q (2001) Induction of CYP1A1. The AhR/DRE paradigm: transcription, receptor regulation, and expanding biological roles. *Curr Drug Metab* **2**:149-164.

MacGeoch C, Morgan ET and Gustafsson JA (1985) Hypothalamo-pituitary regulation of cytochrome P-450(15) beta apoprotein levels in rat liver. *Endocrinology* **117**:2085-2092.

Maglich JM, Parks DJ, Moore LB, Collins JL, Goodwin B, Billin AN, Stoltz CA, Kliewer SA, Lambert MH, Willson TM and Moore JT (2003) Identification of a novel human constitutive androstane receptor (CAR) agonist and its use in the identification of CAR target genes. *J Biol Chem* **278**:17277-17283.

Mahnke A, Strotkamp D, Roos PH, Hanstein WG, Chabot GG and Nef P (1997) Expression and inducibility of cytochrome P450 3A9 (CYP3A9) and other members of the CYP3A subfamily in rat liver. *Arch Biochem Biophys* **337**:62-68.

Makishima M (2005) Nuclear receptors as targets for drug development: regulation of cholesterol and bile acid metabolism by nuclear receptors. *J Pharmacol Sci* **97**:177-183.

Makishima M, Lu TT, Xie W, Whitfield GK, Domoto H, Evans RM, Haussler MR and
 Mangelsdorf DJ (2002) Vitamin D receptor as an intestinal bile acid sensor. *Science*
 296:1313-1316.

Makishima M, Okamoto AY, Repa JJ, Tu H, Learned RM, Luk A, Hull MV, Lustig KD,
 Mangelsdorf DJ and Shan B (1999) Identification of a nuclear receptor for bile acids.
 Science **284:**1362-1365.

Mangelsdorf DJ and Evans RM (1995) The RXR heterodimers and orphan receptors. *Cell*
 83:841-850.

Mason G and Safe S (1986) Synthesis, biologic and toxic effects of the major 2,3,7,8-
 tetrachlorodibenzo-p-dioxin metabolites in the rat. *Toxicology* **41:**153-159.

Mayer R, Kartenbeck J, Buchler M, Jedlitschky G, Leier I and Keppler D (1995) Expression of
 the MRP gene-encoded conjugate export pump in liver and its selective absence from the
 canalicular membrane in transport-deficient mutant hepatocytes. *J Cell Biol* **131:**137-
 150.

Meier PJ and Stieger B (2002) Bile salt transporters. *Annu Rev Physiol* **64:**635-661.

Meng LJ, Reyes H, Palma J, Hernandez I, Ribalta J and Sjovall J (1997) Effects of
 ursodeoxycholic acid on conjugated bile acids and progesterone metabolites in serum
 and urine of patients with intrahepatic cholestasis of pregnancy. *J Hepatol* **27:**1029-
 1040.

Michalets EL (1998) Update: clinically significant cytochrome P-450 drug interactions.
 Pharmacotherapy **18:**84-112.

Moore LB, Parks DJ, Jones SA, Bledsoe RK, Consler TG, Stimmel JB, Goodwin B, Liddle C,
 Blanchard SG, Willson TM, Collins JL and Kliewer SA (2000) Orphan nuclear receptors
 constitutive androstane receptor and pregnane X receptor share xenobiotic and steroid
 ligands. *J Biol Chem* **275:**15122-15127.

Morgan ET, MacGeoch C and Gustafsson JA (1985) Hormonal and developmental regulation of expression of the hepatic microsomal steroid 16 alpha-hydroxylase cytochrome P-450 apoprotein in the rat. *J Biol Chem* **260:**11895-11898.

Nagengast FM, Grubben MJ and van Munster IP (1995) Role of bile acids in colorectal carcinogenesis. *Eur J Cancer* **31A:**1067-1070.

Narimatsu S, Tachibana M, Masubuchi Y, Imaoka S, Funae Y and Suzuki T (1995) Cytochrome P450 isozymes involved in aromatic hydroxylation and side-chain N-desisopropylation of alprenolol in rat liver microsomes. *Biol Pharm Bull* **18:**1060-1065.

Narisawa T, Magadia NE, Weisburger JH and Wynder EL (1974) Promoting effect of bile acids on colon carcinogenesis after intrarectal instillation of N-methyl-N'-nitro-N-nitrosoguanidine in rats. *J Natl Cancer Inst* **53:**1093-1097.

Narisawa T, Reddy BS and Weisburger JH (1978) Effect of bile acids and dietary fat on large bowel carcinogenesis in animal models. *Gastroenterol Jpn* **13:**206-212.

Neat CE, Thomassen MS and Osmundsen H (1981) Effects of high-fat diets on hepatic fatty acid oxidation in the rat. Isolation of rat liver peroxisomes by vertical-rotor centrifugation by using a self-generated, iso-osmotic, Percoll gradient. *Biochem J* **196:**149-159.

Nebert DW (1989) The Ah locus: genetic differences in toxicity, cancer, mutation, and birth defects. *Crit Rev Toxicol* **20:**153-174.

Nebert DW, Adesnik M, Coon MJ, Estabrook RW, Gonzalez FJ, Guengerich FP, Gunsalus IC, Johnson EF, Kemper B, Levin W and et al. (1987) The P450 gene superfamily: recommended nomenclature. *DNA* **6:**1-11.

Nebert DW and Gonzalez FJ (1987) P450 genes: structure, evolution, and regulation. *Annu Rev Biochem* **56:**945-993.

Nelson DR, Kamataki T, Waxman DJ, Guengerich FP, Estabrook RW, Feyereisen R, Gonzalez FJ, Coon MJ, Gunsalus IC, Gotoh O and et al. (1993) The P450 superfamily: update on new sequences, gene mapping, accession numbers, early trivial names of enzymes, and nomenclature. *DNA Cell Biol* **12**:1-51.

Nelson DR, Koymans L, Kamataki T, Stegeman JJ, Feyereisen R, Waxman DJ, Waterman MR, Gotoh O, Coon MJ, Estabrook RW, Gunsalus IC and Nebert DW (1996) P450 superfamily: update on new sequences, gene mapping, accession numbers and nomenclature. *Pharmacogenetics* **6**:1-42.

Noe B, Hagenbuch B, Stieger B and Meier PJ (1997) Isolation of a multispecific organic anion and cardiac glycoside transporter from rat brain. *Proc Natl Acad Sci U S A* **94**:10346-10350.

Norman A (1964) Faecal Excretion Products of Cholic Acid in Man. *Br J Nutr* **18**:173-186.

Norman A and Palmer RH (1964) Metabolites of Lithocholic Acid-24-C-14 in Human Bile and Feces. *J Lab Clin Med* **63**:986-1001.

Oelberg DG, Chari MV, Little JM, Adcock EW and Lester R (1984) Lithocholate glucuronide is a cholestatic agent. *J Clin Invest* **73**:1507-1514.

Oelkers P, Kirby LC, Heubi JE and Dawson PA (1997) Primary bile acid malabsorption caused by mutations in the ileal sodium-dependent bile acid transporter gene (SLC10A2). *J Clin Invest* **99**:1880-1887.

Okey AB (1990) Enzyme induction in the cytochrome P-450 system. *Pharmacol Ther* **45**:241-298.

Omura T and Sato R (1964a) The carbon monoxide binding pigment of liver microsomes I. Evidence for its hemeprotein nature. *Journal of Biological Chemistry* **239**:2370-2378.

Oude Elferink RP and van Berge Henegouwen GP (1998) Cracking the genetic code for benign recurrent and progressive familial intrahepatic cholestasis. *J Hepatol* **29:**317-320.

Pai R, Tarnawski AS and Tran T (2004) Deoxycholic acid activates beta-catenin signaling pathway and increases colon cell cancer growth and invasiveness. *Mol Biol Cell* **15:**2156-2163.

Palut D, Kostka G and Strucinski P (2002) [The role of nuclear receptors in cytochrome P-450 induction by xenochemicals]. *Rocz Panstw Zakl Hig* **53:**321-332.

Panesar SK, Bandiera SM and Abbott FS (1996) Comparative effects of carbamazepine and carbamazepine-10,11-epoxide on hepatic cytochromes P450 in the rat. *Drug Metab Dispos* **24:**619-627.

Parkinson A (1996) *Casarett & Doull's Toxicology: The Basic Science of Poisons.* McGraw Hill, New York.

Perwaiz S, Forrest D, Mignault D, Tuchweber B, Phillip MJ, Wang R, Ling V and Yousef IM (2003) Appearance of atypical 3 alpha,6 beta,7 beta,12 alpha-tetrahydroxy-5 beta-cholan-24-oic acid in spgp knockout mice. *J Lipid Res* **44:**494-502.

Porter TD and Coon MJ (1991) Cytochrome P-450. Multiplicity of isoforms, substrates, and catalytic and regulatory mechanisms. *J Biol Chem* **266:**13469-13472.

Quattrochi LC and Guzelian PS (2001) Cyp3A regulation: from pharmacology to nuclear receptors. *Drug Metab Dispos* **29:**615-622.

Quist RG, Ton-Nu HT, Lillienau J, Hofmann AF and Barrett KE (1991) Activation of mast cells by bile acids. *Gastroenterology* **101:**446-456.

Radominska-Pyrek A, Zimniak P, Irshaid YM, Lester R, Tephly TR and St Pyrek J (1987) Glucuronidation of 6 alpha-hydroxy bile acids by human liver microsomes. *J Clin Invest* **80:**234-241.

Rahman A, Korzekwa KR, Grogan J, Gonzalez FJ and Harris JW (1994) Selective biotransformation of taxol to 6 alpha-hydroxytaxol by human cytochrome P450 2C8. *Cancer Res* **54:**5543-5546.

Rekka E, Ayalogu EO, Lewis DF, Gibson GG and Ioannides C (1994) Induction of hepatic microsomal CYP4A activity and of peroxisomal beta-oxidation by two non-steroidal anti-inflammatory drugs. *Arch Toxicol* **68:**73-78.

Richter T, Schwab M, Eichelbaum M and Zanger UM (2005) Inhibition of human CYP2B6 by N,N',N''-triethylenethiophosphoramide is irreversible and mechanism-based. *Biochem Pharmacol* **69:**517-524.

Roberts LR, Kurosawa H, Bronk SF, Fesmier PJ, Agellon LB, Leung WY, Mao F and Gores GJ (1997) Cathepsin B contributes to bile salt-induced apoptosis of rat hepatocytes. *Gastroenterology* **113:**1714-1726.

Russell DW (1999) Nuclear orphan receptors control cholesterol catabolism. *Cell* **97:**539-542.

Ryan DE, Dixon R, Evans RH, Ramanathan L, Thomas PE, Wood AW and Levin W (1984) Rat hepatic cytochrome P-450 isozyme specificity for the metabolism of the steroid sulfate, 5 alpha-androstane-3 alpha, 17 beta-diol-3,17-disulfate. *Arch Biochem Biophys* **233:**636-642.

Ryan DE and Levin W (1990) Purification and characterization of hepatic microsomal cytochrome P-450. *Pharmacol Ther* **45:**153-239.

Ryan DE and Levin W (1993) *Age- and Gender- Related Expression of Rat Liver Cytochrome P450*. Springer-Verlag, Berlin.

Saeki T, Matoba K, Furukawa H, Kirifuji K, Kanamoto R and Iwami K (1999) Characterization, cDNA cloning, and functional expression of mouse ileal sodium-dependent bile acid transporter. *J Biochem (Tokyo)* **125:**846-851.

Saini SP, Sonoda J, Xu L, Toma D, Uppal H, Mu Y, Ren S, Moore DD, Evans RM and Xie W (2004) A Novel Constitutive Androstane Receptor-Mediated and CYP3A-Independent Pathway of Bile Acid Detoxification. *Mol Pharmacol* **65:**292-300.

Scholmerich J, Becher MS, Schmidt K, Schubert R, Kremer B, Feldhaus S and Gerok W (1984) Influence of hydroxylation and conjugation of bile salts on their membrane-damaging properties--studies on isolated hepatocytes and lipid membrane vesicles. *Hepatology* **4:**661-666.

Selye H (1971) Hormones and resistance. *J Pharm Sci* **60:**1-28.

Setchell KD, Rodrigues CM, Clerici C, Solinas A, Morelli A, Gartung C and Boyer J (1997) Bile acid concentrations in human and rat liver tissue and in hepatocyte nuclei. *Gastroenterology* **112:**226-235.

Sharma R, Lake BG and Gibson GG (1988) Co-induction of microsomal cytochrome P-452 and the peroxisomal fatty acid beta-oxidation pathway in the rat by clofibrate and di-(2-ethylhexyl)phthalate. Dose-response studies. *Biochem Pharmacol* **37:**1203-1206.

Shneider BL, Dawson PA, Christie DM, Hardikar W, Wong MH and Suchy FJ (1995) Cloning and molecular characterization of the ontogeny of a rat ileal sodium-dependent bile acid transporter. *J Clin Invest* **95:**745-754.

Sinal CJ, Tohkin M, Miyata M, Ward JM, Lambert G and Gonzalez FJ (2000) Targeted disruption of the nuclear receptor FXR/BAR impairs bile acid and lipid homeostasis. *Cell* **102:**731-744.

Skene DJ, Papagiannidou E, Hashemi E, Snelling J, Lewis DF, Fernandez M and Ioannides C (2001) Contribution of CYP1A2 in the hepatic metabolism of melatonin: studies with isolated microsomal preparations and liver slices. *J Pineal Res* **31:**333-342.

Sonderfan AJ, Arlotto MP, Dutton DR, McMillen SK and Parkinson A (1987) Regulation of testosterone hydroxylation by rat liver microsomal cytochrome P-450. *Arch Biochem Biophys* **255:**27-41.

Staudinger JL, Goodwin B, Jones SA, Hawkins-Brown D, MacKenzie KI, LaTour A, Liu Y, Klaassen CD, Brown KK, Reinhard J, Willson TM, Koller BH and Kliewer SA (2001) The nuclear receptor PXR is a lithocholic acid sensor that protects against liver toxicity. *Proc Natl Acad Sci U S A* **98:**3369-3374.

Stedman C, Robertson G, Coulter S and Liddle C (2004) Feed-forward regulation of bile acid detoxification by CYP3A4: studies in humanized transgenic mice. *J Biol Chem* **279:**11336-11343.

Stieger B (2001) FIC1: another bile salt carrier within the enterohepatic circulation? *J Hepatol* **35:**522-524.

Sueyoshi T and Negishi M (2001) Phenobarbital response elements of cytochrome P450 genes and nuclear receptors. *Annu Rev Pharmacol Toxicol* **41:**123-143.

Tandon R, Axelson M and Sjovall J (1984) Selective liquid chromatographic isolation and gas chromatographic-mass spectrometric analysis of ketonic bile acids in faeces. *J Chromatogr* **302:**1-14.

Trauner M and Boyer JL (2003) Bile salt transporters: molecular characterization, function, and regulation. *Physiol Rev* **83:**633-671.

Tu YY, Peng R, Chang ZF and Yang CS (1983) Induction of a high affinity nitrosamine demethylase in rat liver microsomes by acetone and isopropanol. *Chem Biol Interact* **44:**247-260.

Ujhazy P, Ortiz D, Misra S, Li S, Moseley J, Jones H and Arias IM (2001) Familial intrahepatic cholestasis 1: studies of localization and function. *Hepatology* **34:**768-775.

van Faassen A, Tangerman A and Bueno-de-Mesquita BH (2004) Serum bile acids and risk factors for colorectal cancer. *Br J Cancer* **90**:632-634.

Vlahcevic ZR, Heuman DM and Hylemon PB (1996) *Physiology and Pathophysiology of Enterohepatic circulation of Bile acids*. Saunders WB, Philadelphia.

Vyvoda OS, Coleman R and Holdsworth G (1977) Effects of different bile salts upon the composition and morphology of a liver plasma membrane preparation. Deoxycholate is more membrane damaging than cholate and its conjugates. *Biochim Biophys Acta* **465**:68-76.

Wang R, Lam P, Liu L, Forrest D, Yousef IM, Mignault D, Phillips MJ and Ling V (2003) Severe cholestasis induced by cholic acid feeding in knockout mice of sister of P-glycoprotein. *Hepatology* **38**:1489-1499.

Wang R, Salem M, Yousef IM, Tuchweber B, Lam P, Childs SJ, Helgason CD, Ackerley C, Phillips MJ and Ling V (2001a) Targeted inactivation of sister of P-glycoprotein gene (spgp) in mice results in nonprogressive but persistent intrahepatic cholestasis. *Proc Natl Acad Sci U S A* **98**:2011-2016.

Wang W, Xue S, Ingles SA, Chen Q, Diep AT, Frankl HD, Stolz A and Haile RW (2001b) An association between genetic polymorphisms in the ileal sodium-dependent bile acid transporter gene and the risk of colorectal adenomas. *Cancer Epidemiol Biomarkers Prev* **10**:931-936.

Waxman DJ (1999) P450 gene induction by structurally diverse xenochemicals: central role of nuclear receptors CAR, PXR, and PPAR. *Arch Biochem Biophys* **369**:11-23.

Waxman DJ and Chang TK (1998) Thin-layer chromatographic analysis of human CYP3A-catalyzed testosterone 6 beta-hydroxylation. *Methods Mol Biol* **107**:153-161.

Waxman DJ, Dannan GA and Guengerich FP (1985) Regulation of rat hepatic cytochrome P-450: age-dependent expression, hormonal imprinting, and xenobiotic inducibility of sex-specific isoenzymes. *Biochemistry* **24:**4409-4417.

Waxman DJ, LeBlanc GA, Morrissey JJ, Staunton J and Lapenson DP (1988) Adult male-specific and neonatally programmed rat hepatic P-450 forms RLM2 and 2a are not dependent on pulsatile plasma growth hormone for expression. *J Biol Chem* **263:**11396-11406.

Wei P, Zhang J, Egan-Hafley M, Liang S and Moore DD (2000) The nuclear receptor CAR mediates specific xenobiotic induction of drug metabolism. *Nature* **407:**920-923.

Westin S, Strom A, Gustafsson JA and Zaphiropoulos PG (1990) Growth hormone regulation of the cytochrome P-450IIC subfamily in the rat: inductive, repressive, and transcriptional effects on P-450f (IIC7) and P-450PB1 (IIC6) gene expression. *Mol Pharmacol* **38:**192-197.

Whitney JO, Ling V, Grunberger J, Thaler MM and Burlingame AL (1983) Identification of hepatic bile acid metabolites in bile by liquid secondary ion mass spectrometry. *Iyo Masu Kenkyukai Koenshu* **8:**47-59.

Williams DA (1999) *Principles of Medicinal Chemistry*. BI Waverly Pvt, Ltd., New Delhi.

Williams RT (1959) *Ditoxication Mechanisms*. J. Wiley & Sons, New York.

Willson TM and Kliewer SA (2002) PXR, CAR and drug metabolism. *Nat Rev Drug Discov* **1:**259-266.

Wong A and Bandiera SM (1996) Inductive effect of Telazol on hepatic expression of cytochrome P450 2B in rats. *Biochem Pharmacol* **52:**735-742.

Wong MH, Oelkers P, Craddock AL and Dawson PA (1994) Expression cloning and characterization of the hamster ileal sodium-dependent bile acid transporter. *J Biol Chem* **269**:1340-1347.

Wong MH, Oelkers P and Dawson PA (1995) Identification of a mutation in the ileal sodium-dependent bile acid transporter gene that abolishes transport activity. *J Biol Chem* **270**:27228-27234.

Wrighton SA and Stevens JC (1992) The human hepatic cytochromes P450 involved in drug metabolism. *Crit Rev Toxicol* **22**:1-21.

Xie W, Barwick JL, Downes M, Blumberg B, Simon CM, Nelson MC, Neuschwander-Tetri BA, Brunt EM, Guzelian PS and Evans RM (2000a) Humanized xenobiotic response in mice expressing nuclear receptor SXR. *Nature* **406**:435-439.

Xie W, Barwick JL, Simon CM, Pierce AM, Safe S, Blumberg B, Guzelian PS and Evans RM (2000b) Reciprocal activation of xenobiotic response genes by nuclear receptors SXR/PXR and CAR. *Genes Dev* **14**:3014-3023.

Xie W and Evans RM (2001) Orphan nuclear receptors: the exotics of xenobiotics. *J Biol Chem* **276**:37739-37742.

Xie W, Radominska-Pandya A, Shi Y, Simon CM, Nelson MC, Ong ES, Waxman DJ and Evans RM (2001) An essential role for nuclear receptors SXR/PXR in detoxification of cholestatic bile acids. *Proc Natl Acad Sci U S A* **98**:3375-3380.

Yabusaki Y, Shimizu M, Murakami H, Nakamura K, Oeda K and Ohkawa H (1984) Nucleotide sequence of a full-length cDNA coding for 3-methylcholanthrene-induced rat liver cytochrome P-450MC. *Nucleic Acids Res* **12**:2929-2938.

Zelko I, Sueyoshi T, Kawamoto T, Moore R and Negishi M (2001) The peptide near the C terminus regulates receptor CAR nuclear translocation induced by xenochemicals in mouse liver. *Mol Cell Biol* **21**:2838-2846.

Zhang J, Huang W, Qatanani M, Evans RM and Moore DD (2004) The constitutive androstane receptor and pregnane X receptor function coordinately to prevent bile acid-induced hepatotoxicity. *J Biol Chem.*

Zimniak P, Holsztynska EJ, Lester R, Waxman DJ and Radominska A (1989) Detoxification of lithocholic acid. Elucidation of the pathways of oxidative metabolism in rat liver microsomes. *J Lipid Res* **30:**907-918.

Zinchuk VS, Okada T, Akimaru K and Seguchi H (2002) Asynchronous expression and colocalization of Bsep and Mrp2 during development of rat liver. *Am J Physiol Gastrointest Liver Physiol* **282:**G540-548.

6. APPENDIX

The role of bile acids in cholestasis has been discussed in the **INTRODUCTION** section. The catalytic activities of CYP enzymes were reported to be altered in cases of chronic cholestasis. *In vitro* studies of CYP enzyme expression in bile duct-ligated male rats, a procedure that induces cholestasis, indicated a dose-dependent decrease in the catalytic activities of CYP2A1, CYP2C11 and CYP3A2 enzymes to about 50-60% of control values (Chen and Farrell, 1996). Unconjugated bile acids such as CDCA, β-muricholic acid, DCA and LCA inhibited CYP-mediated activities, with LCA being the most potent inhibitor. Conjugated bile acids such as taurocholic acid had similar effects (Chen and Farrell, 1996). Bile duct-ligated induced cholestasis decreased CYP reductase activity to 58% of control and decreased CYP reductase protein content to 74% of the control level. However, CYP2C12 protein levels were not altered in female rats and were up-regulated in male rats. A study with bile duct-ligated male rats showed a significant reduction in male specific CYP2C11 and CYP3A2 protein levels (Chen and Farrell, 1996).

In preliminary experiments conducted in our laboratory by E. Hrycay and J. Tai using female and male wild type SPGP knockout mice fed a CA enriched diet, a 1.5- to 2-fold increase in total CYP levels was observed in hepatic microsomes prepared from female and male SPGP knockout mice compared to SPGP knockout mice fed a normal diet. The mechanism for up-regulation involves increased CYP protein synthesis (Dr. Eugene Hrycay, manuscript in preparation).

The results of above mentioned studies suggest that CYP catalytic activities are altered in an induced rat cholestatic model. Thus, a preliminary study to measure CYP activity in an induced cholestatic rat model was carried out. A cholic acid enriched diet was used to induce cholestasis in rats. Rat hepatic microsomes were prepared, total CYP content and protein concentration were measured and compared to control rats. The catalytic activities of several CYP enzymes were measured using the testosterone hydroxylase assay. This work was carried out as a pilot study.

A.1   Hypothesis

1. Treatment with a CA-enriched diet will induce cholestasis in rats and alter hepatic CYP enzyme expression.

A.2   Specific research objectives

1. To prepare a rat model of cholestasis.

2. To measure serum alkaline phosphatase, serum cholesterol, serum triglycerides, and serum total bile acids in rats fed with a cholic acid enriched diet.

3. To study CYP enzyme activities in the rat cholestatic model.

A.3 Materials

BDH Chemicals (Toronto, Ontario, Canada):

Folin and Ciocalteu phenol reagent; magnesium chloride; potassium chloride; sodium chloride; potassium carbonate; sodium hydroxide; sucrose, sulfuric acid.

Boehringer Mannheim Canada Ltd. (Laval, Quebec, Canada):

Nicotinamide adenine dinucleotide phosphate, tetrasodium salt (NADPH).

J.T. Baker Chemical Co. (Phillipsburg, New Jersy, U.S.A):

Sodium dithionite

Praxair (Vancouver, British Columbia, Canada):

Carbon monoxide gas, 99.5% purity; nitrogen gas.

Steraloids Inc. (Wilton, New Hamsphire, USA):

Testosterone; 2α-, 2β-, 6β-, 7α-, 11β-, 16α-, 16β-hydroxytestosterone.

Thermo Trace Ltd. (Louisville, CO, USA):

Infinity^{TM} triglyceride, Infinity^{TM} cholesterol, Infinity^{TM} alkaline phosphatase reagents kits.

Diazyme Laboratories (San Diego, USA):

Total bile acids assay kit.

Dr. Victor Ling (BC Cancer Agency, Vancouver, Canada):

5053 Pico Lab® Rodent Diet 20 supplemented with 0.5% cholic acid as treatment diet (*Richmond, IN, USA*), 5053 Pico Lab® Rodent Diet 20 as normal diet (Richmond, IN, USA).

A.4 Methods

A.4.1 Animals and treatment

Adult male Wistar rats (200-225 g) were purchased from Charles River Canada Inc. (Saint-Constant, Quebec). After arrival, rats were allowed to recover for 3 to 5 days before treatment was initiated. Water was supplied *ad libitum* and the animals were housed in clear, polycarbonated cages containing corncob bedding (Anderson's Maumee, OH) in a room with controlled light (14 hr) and dark (10 hr) cycles and a constant room temperature (23^0C).

Animals were divided in 4 groups with 4 to 5 animals in each group. Control animals were fed a normal 5053 Pico Lab[®] Rodent Diet 20. The three treatment groups were fed a 5053 Pico Lab[®] Rodent Diet 20 supplemented with 0.5% cholic acid for 10, 20 or 30 days. Body weights and amount of food consumed per animal per day were recorded over the treatment period.

A.4.2 Blood collection and serum preparation

Rats were killed by decapitation one day after the end of their treatment periods. Control animals were killed one day after 20 days of treatment with the normal diet. Approximately, 4 ml of trunk blood was collected from each rat immediately after decapitation. Blood was collected in VACUTAINER[®] SST[®] Gel & Clot Activator tubes (Franklin Lakes, NJ, USA) to minimize hemolysis and allowed to clot at 37^0C for 1h. Serum was separated by centrifugation at $1500 \times g$ for 2 min using a benchtop centrifuge. Serum samples were labeled and stored at − 20^oC until analysis.

135

A.4.3   Preparation of hepatic microsomes

Hepatic microsomes were prepared from individual rats. Livers were removed immediately after decapitation, weighed, minced and placed into homogenizer tubes containng ice-cold 0.05 M Tris HCl, 1.15% KCl buffer. Livers were homogenized using a Potter-Elvehjem glass homogenizer and motor driven pestle (Talboys Engineering Corp., Emerson, NJ, USA). The homogenate was centrifuged at 9,000 × g for 20 min at 5^0C using a Beckman J2-21 centrifuge (Beckman Instruments, Palo Alto, CA, USA). The supernatant was filtered through cheesecloth and centrifuged at 105,000 × g for 60 min at 5^0C using a Beckman LE-80 ultracentrifuge. The microsomal pellet was separated from glycogen and resuspended in ice-cold 10 mM EDTA containing 1.15% KCl using a homogenizer. The suspension was centrifuged at 105,000 × g for 60 min at 5^0C using a Beckman LE-80 ultracentrifuge. The resulting pellet was resuspended in 0.25 M sucrose. Aliquots were stored at -80^0C in cryovials (Ingram & Bell, Richmond, BC, Canada).

A.4.4   Determination of protein concentration

Protein concentrations of hepatic microsomal samples were measured using the Lowry protein assay (Lowry et al. 1951). Bovine serum albumin (BSA) was used as the standard. All samples were analyzed in duplicate at an absorbance of 650 nm using a Shimadzu UV-160 UV-visible recording spectrophotometer (Shimadzu Corporation, Kyoto, Japan).

A.4.5   Determination of CYP concentration

Total microsomal CYP concentration was determined by measuring the sodium dithionite reduced carbon monoxide difference spectrum according to the method of Omura and Sato (1964a). Hepatic microsomes were diluted in 0.1 M sodium phosphate buffer (pH 7.4)

containing 20% glycerol, 0.1 mM EDTA. Spectral measurements were performed using a SLM-Aminco DW-2 UV-Vis spectrophotometer equipped with a SLM-Aminco Midan II kinetic processor controller (SLM Instruments Inc. Urbana, IL, USA). Total hepatic CYP content was calculated using a molar extinction of 91 cm^2/mmol (Omura and Sato 1964b).

A.4.6 Determination of CYP enzyme activities

The testosterone hydroxylase assay was carried out as described by Sonderfran *et al.* with slight modifications (Wong and Bandiera, 1996; Ickenstein and Bandiera, 2002; Ickenstein et al., 2004) This HPLC assay is based on regio- and stereospecific hydroxylation of testosterone catalyzed by specific CYP enzymes. The reaction mixture consisted of 0.92 ml of 50 mM potassium phosphate buffer (pH 7.4) containing 3 mM $MgCl_2$, 50 µl of microsomes (diluted in 0.25 M sucrose to a concentration of 6 nmol CYP/ml) and 10 µl of 100 mM NADPH. The mixture was preincubated at room temperature for 10 min. The reaction was initiated at 37^0C by adding 20 µl of 12.5 mM testosterone and was terminated by adding 6 ml of dichloromethane with vigorous mixing. Each sample was then spiked with 50 µl of 50 mM 11β-hydroxytestosterone as internal standard. All testosterone metabolites were extracted in the dichloromethane layer by mixing vigorously for 1 min and shaking for a further 2 min. The organic layer was separated from the aqueous phase by centrifugation at 2,000 × g for 5 min using a Beckman GP centrifuge. The aqueous layer was aspirated and discarded and the remaining organic phase was dried under a gentle stream of nitrogen gas. The reaction products were reconstituted with 200 µl of methanol and filtered into an autosampler vial using a syringe filter (13 mm, pore size 0.45 µm). A 10 µl aliquot of each filtrate was analyzed by reverse phase HPLC at 40^0C at a flow rate of 2 ml/min on a Supelcosil (Supelco, Bellefonte, PA, USA) LC-18 octadecylsilane column (5 µm, 150 × 4.6 mm) connected to a Shimadzu LC-6A binary gradient

HPLC system equipped with a SPD-6A UV detector, a CTO-6A oven and a SIL-6B autosampler (Shimadzu Corporation, Kyoto, Japan). Samples were eluted using the following gradient : 100% solvent A (methanol : water : acetonitrile, 35 :64 :1) from 0-10 min, followed by a linear gradient of solvent B (methanol : water : acetonitrile, 80 :18 :2) from 0 to 100% from 10 to 29 min, 100% solvent B from 29 to 31 min, followed by a linear gradient to 100% solvent A from 31 to 32 min and equilibration with 100% solvent until 34 min. The individual peaks for each metabolite were detected at a wavelength of 254 nm with a Shimadzu SPD-6A UV-spectrophotometric detector. Peaks were integrated by a Shimadzu CR501 chromatopac data processor. Testosterone, 2α-, 2β-, 6β-, 7α-, 16α-, and 16β-hydroxytestosterone, and androstenedione were separated using this assay. The metabolites were identified by co-chromatography using a mixture of authentic metabolite standards. Calibration curves were generated for each testosterone metabolite standard by plotting the peak area ratio (PAR, standard metabolite standard/internal standard) *versus* the amount of metabolite per tube. The amount of each individual metabolite formed was calculated from the slope of the calibration curve for that particular metabolite. Enzymatic activities were calculated by dividing the amounts of metabolites produced (nmol) by the incubation time (min) and the amount of protein (mg) or total CYP (nmol) used in the assay. A zero-time control was included in each assay to account for metabolite impurities within the testosterone substrate solution and to account for non-enzymatic hydroxylation of testosterone. For the zero-time control, a randomly selected microsomal sample was added to the reaction mixture and the reaction was stopped with dichloromethane before the addition of testosterone.

A.4.7 Serum analysis

Levels of serum bile acids, cholesterol, triglycerides, and alkaline phosphatase were measured using commercially available kits to evaluate the development of cholestasis.

Serum triglycerides

Total serum triglyceride levels were analyzed using an Infinity™ triglycerides reagent kit. The kit uses the enzyme lipoprotein lipase, to convert the triglycerides to glycerol and glycerol-3-phosphate at 37^0C. The end product of triglyceride metabolism, glycerol-3-phosphate, is oxidized by glycerol phosphate oxidase, producing hydrogen peroxide, which reacts with 4-aminoantipyrine and 3, 5-dichlorohydroxybenzene dye (DHBS). This produces a red-colored quinine imine dye. The change in absorbance per unit time is measured at 37^0C using a Shimadzu UV-visible spectrophotometer at a wavelength of 520 nm.

Serum cholesterol

Cholesterol levels were analyzed using an Infinity™ cholesterol reagent kit. The kit uses the enzyme cholesterol esterase, to convert cholesterol esters at 37^0C to cholesterol and free fatty acids. Cholesterol is oxidized by cholesterol oxidase to cholest-4-ene-3-one and hydrogen peroxide. The hydrogen peroxide combines with hydroxybenzoic acid and 4-aminopyrine to form a quinone imine dye. The change in absorbance per unit time was measured at 520 nm using a Shimadzu UV-visible photospectrometer.

Serum alkaline phophatase

An alkaline phosphatase Infinity™ reagent kit was used to measure serum levels of alkaline phosphatase. The kit uses 4-nitrophenylphosphate as the substrate. At 37^0C and under optimal conditions of cofactors, alkaline phosphatase catalyzes the conversion of 4-

nitrophenoxide to nitrophenoxide, which has an intense yellow color. The absorbance was measured at 405 nm using a Shimadzu UV-visible spectrophotometer.

Serum total bile acids

Serum bile acids were measured using the Diazyme® colorimetric total bile acids assay kit. The kit consists of 3α-hydroxysteroid dehydrogenase enzyme. In the presence of nicotine adenine diphosphate (NAD), the enzyme 3α-hydroxysteroid dehydrogenase converts the bile acids to 3-keto steroids and NADH. The NADH formed reacts with nitrotetrazolium blue to form a formazan dye in the presence of diaphorase enzyme. Formation of the dye was monitored by measuring absorbance at 540 nm and was directly proportional to the bile acid concentration in the sample.

A.4.8   Statistical analysis

Differences among mean values were analyzed by one way analysis of variance (ANOVA) using GraphPad InStat Ver. 3.0 (GraphPad Software Inc., San Diego, CA) Differences between pairs of mean values were tested by Student Newman-Keuls Test (SNK). Mean differences with a p value < 0.05 were considered to be statistically significant.

A.5 Results

A.5.1 Body and liver weight

The mean body and liver weights of male Wistar rats following treatment are shown in Table 1 and Table 2. The mean body weight of rats in the control group was not significantly different from the mean body weights of rats in the three treatment groups. No significant difference was observed in liver weights between the control and the treatment groups. The mean values were analyzed using ANOVA.

Table 1

Final body weights of male Wistar rats fed a CA-enriched diet

	Treatment Group			
	Normal diet	0.5% CA 10 days	0.5% CA 20 days	0.5% CA 30 days
n	4	4	5	4
Mean body wt. (g)	394.7	344.7	410.0	442.0
SEM	9.9	5.5	8.7	3.6

The data shows the mean body weights of rats in each group along with the standard error of mean (SEM).

Table 2

Mean final liver weights of male Wistar rats fed a CA-enriched diet

	Treatment Group			
	Normal diet	0.5% CA 10 days	0.5% CA 20 days	0.5% CA 30 days
n	4	4	5	4
Mean liver wt. (g)	18.5	17.8	20.6	23.8
SEM	0.8	0.6	0.9	0.8

The data shows the mean liver weights of rats in each group along with the standard error of mean (SEM).

A.5.2 Total CYP content of hepatic microsomes

Total CYP content was measured as described in the **Methods**. There was no significant difference between the treatment groups and the control group with respect to the total CYP content (Table. 3).

Table 3

Total CYP content of hepatic microsomes from male rats fed a CA-enriched diet

	Treatment Group			
	Normal diet	0.5% CA 10 days	0.5% CA 20 days	0.5% CA 30 days
n	4	4	5	4
Mean (nmol/mg)	0.71	0.71	0.74	0.67
SEM	0.05	0.04	0.58	0.05

The data shows mean values of total CYP content of hepatic microsomes of male rats and the standard error of mean (SEM).

A.5.3 Testosterone hydroxylase activities

The rate of formation of 7α-hydroxytestosterone, catalyzed by CYP2A1, was decreased significantly by 45%, 61% and 64%, respectively, in the 10 day, 20 day and 30 day cholic acid treatment groups as compared to the control group. The rate of formation of the other testosterone metabolites was not significantly different among the control and treatment groups. Testosterone hydroxylase activities expressed as nmol/min/mg of protein and nmol/min/nmol of CYP are summarized in Table 4 and Fig. 1, respectively.

Table 4

Hepatic microsomal testosterone hydroxylase activities (nmol/min/mg of protein) of male rats fed a CA-enriched diet

Treatment	Mean activity (nmol metabolite / min / mg of protein)						
	2α	2β	6β	7α	16α	16β	A
Normal diet (n=4)	2.38 ± 0.33	0.34 ± 0.12	1.27 ± 0.15	0.31 ± 0.04	2.78 ± 0.44	0.13 ± 0.03	2.54 ± 0.19
0.5% CA 10 days (n=4)	2.57 ± 0.34	0.51 ± 0.20	1.21 ± 0.11	0.17 ± 0.03*	2.95 ± 0.43	0.24 ± 0.11	2.57 ± 0.17
0.5% CA 20 days (n=5)	3.13 ± 0.37	0.71 ± 0.14	1.54 ± 0.27	0.12 ± 0.03*	3.74 ± 0.43	0.13 ± 0.02	2.78 ± 0.39
0.5% CA 30 days (n=4)	2.03 ± 0.13	0.36 ± 0.11	0.69± 0.07	0.11 ± 0.02*	2.30 ± 0.09	0.11 ± 0.05	2.09 ± 0.15

7α = 7α-hydroxytestosterone, etc, A = androstenedione, CA = cholic acid treatment. * = Mean value of 0.5% CA treated group is statistically different ($p < 0.05$) from the control group. Results show statistical difference obtained using One Way Anova as compared to the normal diet or control group. Paired t tests performed for each individual treatment group *vs.* control also did not show any statistically significant difference except between 6β-hydroxytestosterone formation for 0.5% CA 20 days and 0.5% CA 30 days. The lack of statistical difference could probably be a result of low sample size (n = 5) or high SEM for each group.
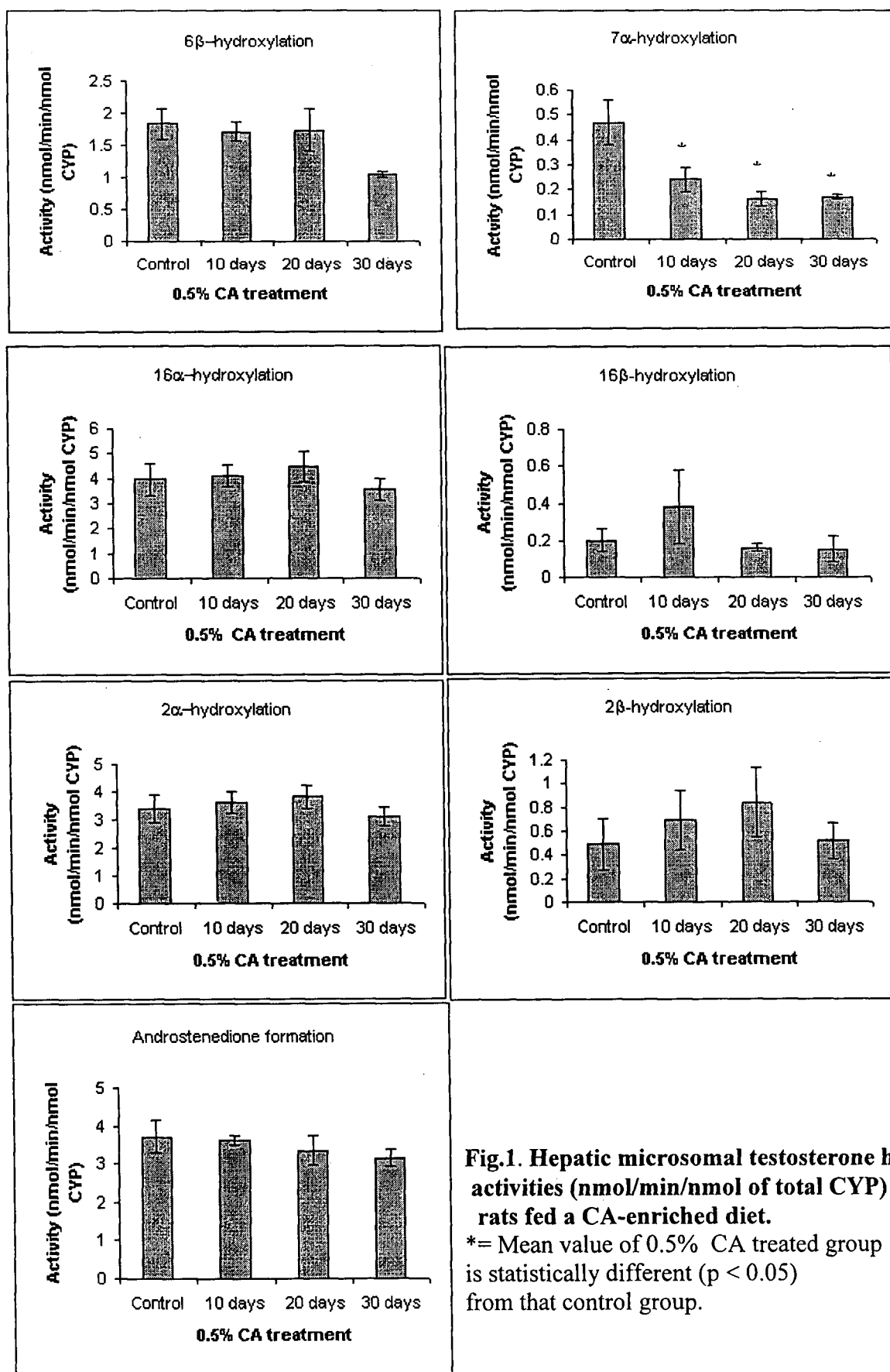
Fig.1. Hepatic microsomal testosterone hydroxylase activities (nmol/min/nmol of total CYP) from male rats fed a CA-enriched diet.

*= Mean value of 0.5% CA treated group is statistically different ($p < 0.05$) from that control group.

A.5.4 Serum analysis

Rat serum was analyzed for various cholestatic parameters as outlined in the **Methods** section previously. The results are summarized in Table 5 and Fig. 2. Serum cholesterol and total bile acid levels were increased by CA treatment, but the increase was not significant (Fig. 2).

Table 5
Serum parameters of rats fed a CA-enriched diet

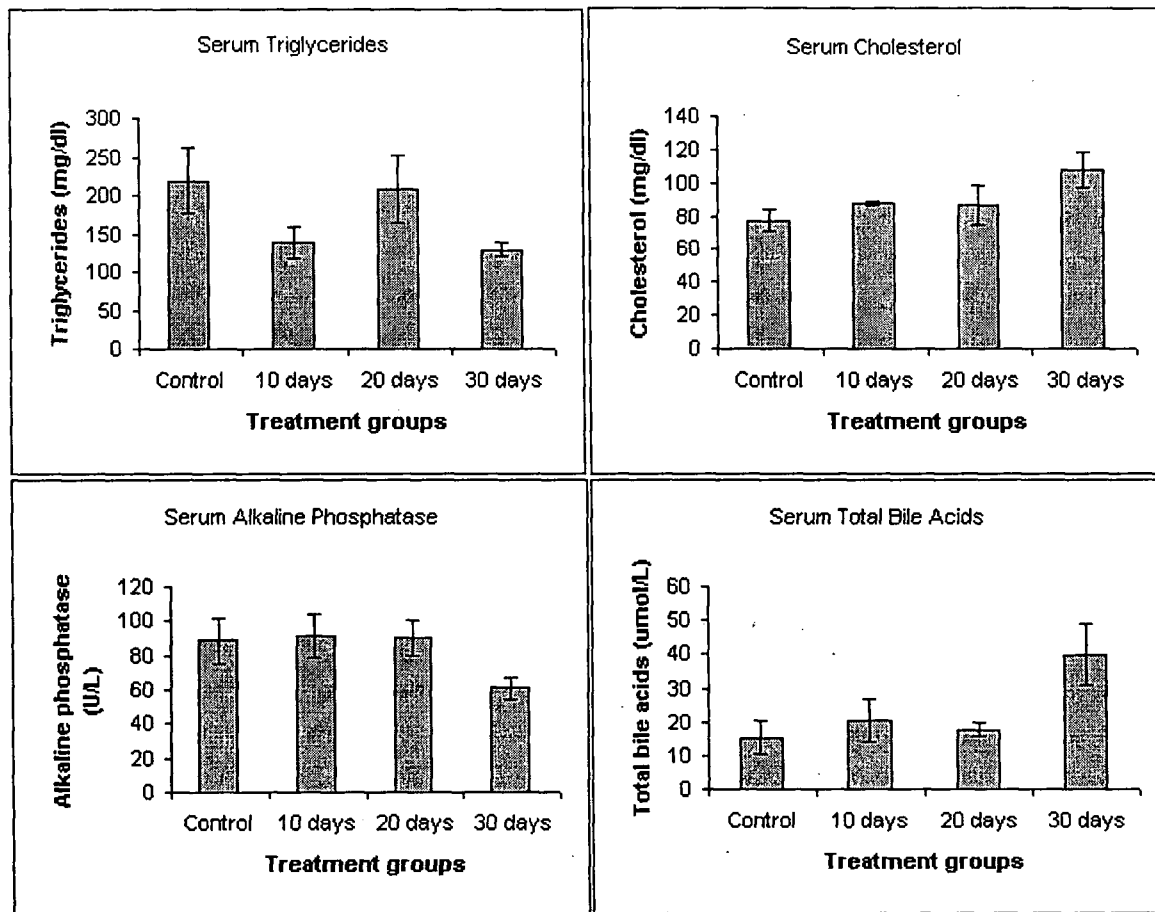| Serum parameter	Normal diet	0.5% CA diet 10 days	0.5% CA diet 20 days	0.5% CA diet 30 days
	n=4	n=4	n=5	n=4
Triglycerides (mg/dl)	219.1	138.9	207.9	128.7
SEM	41.3	20.23	43.7	8.7
Cholesterol (mg/dl)	77.4	88.1	86.7	107.4
SEM	6.5	1.5	11.7	10.7
Alkaline phosphatase (U/L)	88.34	91.4	90.0	60.7
SEM	12.8	12.4	10.1	5.9
Total bile acids (μmol/L)	15.21	20.4	17.7	39.8
SEM	5.0	6.5	1.9	9.1

Fig. 2. Serum parameters of rats fed a CA-enriched diet

A.6 Conclusions

The results indicate there was no difference in body weights, liver weights and total CYP content of rats treated with 0.5% CA as compared to the control group. Serum cholesterol and serum bile acid levels were increased slightly with CA treatment, but the increase was not significant. Formation of 7α-hydroxytestosterone was significantly decreased with CA treatment (Table 4) but there was no significant change in any of the other testosterone hydroxylase activities at any of the time points. The following conclusions can be made –

1. The data shows some indication of altered liver function with CA treatment. The change, however, is not consistent. The methodology used and the data obtained from the study do not suggest induction of cholestasis in rats although it is possible that a mild asymptomatic form of cholestasis was produced. An alternate animal model to study cholestasis needs to be considered. Bile duct ligated rat cholestatic models have been used previously and can be used instead of a cholic acid-fed diet. Alternatively, instead of a CA diet, an LCA diet may be more effective as LCA is a more toxic bile acid.

2. Testosterone 7α-hydroxylation is a characteristic marker assay for CYP2A1. The decrease in the rate of 7α-hydroxytestosterone formation is correlated to a decrease in rat hepatic CYP2A1 levels. However, the catalytic activity of the other CYP enzymes did not decrease significantly. Testosterone 16α- and 2α-hydroxylase activities which are catalyzed by CYP2C11, as well as the rate of formation of 16β-hydroxytestosterone and androstenedione formation, representing CYP2B activity, were slightly increased in the 10 or 20 day treatment groups but were not different in the 30 day CA treated group as compared to the vehicle-treated control group. A similar observation was made in the

case of testosterone 6β- and 2β-hydroxylase activities which serve as catalytic markers of CYP3A enzymes.

3. The current treatment protocol for inducing cholestasis in rats using a diet enriched in CA for up to 30 days did not produce a major change in serum alkaline phosphatase, serum triglycerides, serum cholesterol or serum bile acids levels. The present model was not effective in generating a severe cholestatic rat model. It is possible that a mild form of cholestasis was induced but it was not sufficient to alter assay results. A better methodology should be used to investigate the hypothesis stated earlier.